

**NASA CONTRACTOR
REPORT**



NASA CR-1749

C.1

0060730



TECH LIBRARY KAFB, NM

NASA CR-1749

LOAN COPY: RETURN TO
AFWL (DOGL)
KIRTLAND AFB, N. M.

**THEORETICAL STUDY OF CORRUGATED PLATES:
SHEARING OF A TRAPEZOIDALLY CORRUGATED
PLATE WITH TROUGH LINES HELD STRAIGHT**

by Chuan-jui Lin and Charles Libove

Prepared by
SYRACUSE UNIVERSITY RESEARCH INSTITUTE
Syracuse, N. Y.
for Langley Research Center

NATIONAL AERONAUTICS AND SPACE ADMINISTRATION • WASHINGTON, D. C. • AUGUST 1971



0060730

1. Report No. NASA CR-1749	2. Government Accession No.	3. Recipient's Catalog No.	
4. Title and Subtitle THEORETICAL STUDY OF CORRUGATED PLATES: SHEARING OF A TRAPEZOIDALLY CORRUGATED PLATE WITH TROUGH LINES HELD STRAIGHT		5. Report Date August 1971	
		6. Performing Organization Code	
7. Author(s) Chuan-jui Lin and Charles Libove		8. Performing Organization Report No. MAE 1833 - T1	
		10. Work Unit No. 722-02-10-03	
9. Performing Organization Name and Address Syracuse University Research Institute Department of Mechanical and Aerospace Engineering Syracuse, New York 13210		11. Contract or Grant No. NGR 33-022-115	
		13. Type of Report and Period Covered Contractor Report	
12. Sponsoring Agency Name and Address National Aeronautics and Space Administration Washington, D. C. 20546		14. Sponsoring Agency Code	
15. Supplementary Notes			
16. Abstract <p>A theoretical analysis is presented of the elastic shearing of a trapezoidally corrugated plate with discontinuous attachment at the ends of the corrugations and with trough lines constrained to remain straight. Numerical results on effective shearing stiffness, stresses, and displacements are presented for selected geometries and end-attachment conditions. It is shown that the frame-like deformations of the cross sections, which result from the absence of continuous end attachment, can lead to large transverse bending stresses and large reductions in shearing stiffness. Some suggestions are made for reducing these effects.</p>			
17. Key Words (Suggested by Author(s)) Corrugated plate Shear stress Shear deformation		18. Distribution Statement Unclassified - Unlimited	
19. Security Classif. (of this report) Unclassified	20. Security Classif. (of this page) Unclassified	21. No. of Pages 125	22. Price* \$3.00

THEORETICAL STUDY OF CORRUGATED PLATES:
SHEARING OF A TRAPEZOIDALLY CORRUGATED PLATE WITH
TROUGH LINES HELD STRAIGHT

By Chuan-jui Lin* and Charles Libove**
Syracuse University

SUMMARY

A theoretical analysis is presented of the elastic shearing of a trapezoidally corrugated plate with discontinuous attachment at the ends of the corrugations and with trough lines constrained to remain straight. Numerical results on effective shearing stiffness, stresses, and displacements are presented for selected geometries and end-attachment conditions. It is shown that the frame-like deformations of the cross sections, which result from the absence of continuous end attachment, can lead to large transverse bending stresses and large reductions in shearing stiffness. Some suggestions are made for reducing these effects.

INTRODUCTION

In this report a theoretical study is made of the elastic shearing of a trapezoidally corrugated plate for the purpose of determining the effective shearing stiffness, the deformations and the stresses. The configuration of the plate is shown in figure 1, which also gives some of the notation to be employed.

The trough lines (mn in fig. 1(b)) are assumed to be held straight, and the shearing of the plate is accomplished by shifting them longitudinally with respect to each other so as to produce the same over-all shearing strain in each corrugation. The assumed straightness of the trough lines corresponds to the case in which the corrugated plate is attached to a flat plate or some other structure along the trough lines; the analysis is therefore only approximately applicable to the case of a corrugated plate by itself. In the latter case the trough lines will tend to curve in the horizontal (xz) plane.

*NDEA Fellow

**Professor of Mechanical and Aerospace Engineering

In the analysis two kinds of conditions are assumed along the trough lines: either complete freedom of rotation or complete suppression of rotation, representing two limiting assumptions for the degree of rotational restraint furnished by the medium to which the trough lines might be attached. These two kinds of conditions are shown schematically in figure 2. No other kind of interference is assumed to be present, along the length of the trough lines, between the corrugated plate and the medium to which it is attached.

The analysis encompasses three kinds of conditions at the ends of the plate ($z = \pm b$). These are illustrated in figure 3 and may be described as follows:

- (i) Attachments at the ends of the trough lines only (fig. 3(a)), the attachments being considered as mathematical points, offering restraint against displacement but not against rotation.
- (ii) Attachments at the ends of both the trough lines and the crest lines (fig. 3(b)), the attachments again considered as points.
- (iii) Very wide attachments at the ends of the trough lines only, as shown in figure 3(c). This type of attachment is approximated in the analysis by means of the idealization shown in figure 3(d), i.e. by adding, to the end constraints of figure 3(a), end constraints against vertical displacement (but not against longitudinal displacement) at the junctions of the trough plate element and the adjacent inclined plate elements.

Attachment (iii) also represents an over-estimate of the constraint afforded by interference between the end of the corrugation and the member to which the end of the corrugation is attached. The interference referred to can be seen in the photograph in figure 5 (taken from ref. 1).

Numerical results on shearing stiffness, stresses and deformations for selected geometries are presented and discussed. In the numerical work, only the case of no rotational restraint along the trough lines (fig. 2(a)) is considered. All three of the end conditions shown in figure 3 are considered for the calculations of shearing stiffness, but only the end conditions of figure 3(a) for the calculations of stresses and deformations.

The prediction of the present theory with regard to shearing stiffness is compared with the result of an experiment reported in reference 2, and good agreement is found.

SYMBOLS

A_1, A_2, \dots, A_8	coefficients in equation for $u_1(z)$ (see eq. (C30))
$A_{11}, A_{12}, \text{ etc.}$	defined by equations (A10)
\bar{A}_1, \bar{A}_3	defined by equations (D34); used in equation (D33)
$\bar{\bar{A}}_1, \bar{\bar{A}}_4, \bar{\bar{A}}_5, \bar{\bar{A}}_7$	coefficients in equations (31) to (34) for displacements; obtained by solving equations (C33), (C38) or (C38'), depending on the type of end attachments
$\sim A_1, \sim A_4, \sim A_5, \sim A_7$	defined by equations (50)
$\tilde{A}_{11}, \tilde{A}_{12}, \tilde{A}_{22}$	defined by equations (D8)
A_1^*, A_3^*	defined by equations (E26); used in equations (E25)
a_1, a_2, a_3	defined by equations (62)
a_{11}, a_{12}, a_{22}	coefficients in expression for U_b (see eqs. (14) and (15))
\hat{a}	defined by equation (C7)
\hat{a}_1	defined by equation (C12)
$a_{11}^*, a_{12}^*, a_{22}^*$	defined by equations (C13)
$\tilde{a}_{11}, \tilde{a}_{12}, \tilde{a}_{22}$	defined by equations (D7)
a_{22}'	defined by equation (D15)
\tilde{a}_{22}^*	defined by equation (D24)
\bar{a}_{22}	defined by equation (E7a) or (E7b), depending on the kind of rotational restraint along the trough lines
\bar{a}_{22}^*	defined by equation (E19a) or (E19b), depending on the kind of rotational restraint along the trough lines

$B_j/A_j \quad (j = 1, 2, \dots, 8)$	obtained by solving equations (C24)
b	one-half the length of the corrugations (see fig. 1(b))
b_1, b_2, b_3	defined by equations (62)
b_{11}, b_{12}, b_{22}	coefficients in expression for U_{ext} (see eqs. (3) and (4))
\hat{b}	defined by equation (C7)
\hat{b}_1	defined by equation (C12)
$b_{11}^*, b_{12}^*, b_{22}^*$	defined by equations (C13)
$C_j/A_j \quad (j = 1, 2, \dots, 8)$	obtained by solving equations (C24)
$c_{00}, c_{01}, \text{etc.}$	coefficients in expression for U_{sh} (see eqs. (7) and (8))
c_0, c_1, c_2, \dots	coefficients in series expansion for R (see eqs. (28) and (C21))
\hat{c}	defined by equation (C7)
\hat{c}_1	defined by equation (C12)
$c_{11}^*, c_{12}^*, c_{22}^*$	defined by equations (C13)
$\widehat{cs}, \widehat{cc}$	defined by equations (C35)
$\overline{c}_{00} = Gt/k$	
D	frame flexural stiffness; usually defined by equation (16b)
$D_j/A_j \quad (j = 1, 2, \dots, 8)$	obtained by solving equations (C24)
d_{11}, d_{21}, d_{22}	coefficients in expression for U_{sh} (see eqs. (7) and (8))
$d_{11}^*, d_{21}^*, d_{22}^*$	defined by equations (C13)
$\tilde{d}_{11}, \tilde{d}_{21}$	defined by equation (C37)
E	Young's modulus associated with frame bending of the cross sections
E'	Young's modulus associated with longitudinal extension

e	one-half the width of the trough plate element (see fig. 1(a))
$e_{11}^*, e_{12}^*, e_{22}^*$	coefficients in expression for U_{sh} (see eqs. (7) and (8))
$\bar{e}_{11}, \bar{e}_{12}, \bar{e}_{22}$	coefficients in expression for U_{tw} (see eqs. (12) and (13))
e_{11}, e_{12}, e_{22}	defined by equations (B2)
\hat{e}	defined by equation (C7)
$\hat{e}_1, \hat{e}_2, \hat{e}_3$	defined by equations (C12)
$e_{11}^{**}, e_{12}^{**}, e_{22}^{**}$	defined by equations (C13)
$\bar{e}_{11}^*, \bar{e}_{12}^*, \bar{e}_{22}^*$	defined by equations (C13)
$\tilde{e}_{11}, \tilde{e}_{12}, \tilde{e}_{22}$	defined by equation (C37)
$e_{11}', e_{12}', e_{22}'$	defined by equations (D6)
$\tilde{e}_{11}', \tilde{e}_{12}', \tilde{e}_{22}'$	defined by equations (D10)
e_{22}'	defined by equation (D15)
\tilde{e}_{22}^*	defined by equation (D24)
F	shear force (see fig. 1(b))
F'	shear force associated with γ' (see eq. (38))
F_1, F_2, F_3	cross-sectional shear force resultants in plate elements 01, 12, 23 respectively (see fig. 9(a) and eq. (B15))
f	width of the crest plate element (see fig. 1(a))
$f_{ss}, f_{sc}, f_{cs}, f_{cc}$	functions of z defined by equations (51)
$f_{cX}, f_{cY}, f_{sX}, f_{sY}$	functions of z defined by equations (52)
\hat{f}	defined by equation (C7)
\hat{f}_1	defined by equation (C12)
G	shear modulus associated with middle surface shear of the plate elements
G'	shear modulus associated with torsion of the plate elements
G_{eff}	effective shear modulus of corrugated plate, τ_{av}/γ_{av}
$g_{11}, g_{12}, \text{etc.}$	defined by equations (61)

\hat{g}	defined by equation (C7)
\hat{g}_1, \hat{g}_2	defined by equation (C12)
h	height of corrugation (see fig. 1(a))
\hat{h}	defined by equation (C7)
\hat{h}_1	defined by equation (C12)
$i = \sqrt{-1}$	
J_1, J_2, J_3	torsion constants of plate elements 01, 12, 23 respectively (see eqs. (10))
\hat{j}	defined by equation (C7)
\hat{j}_1	defined by equation (C12)
K	defined by equation (66)
k	width of the inclined plate element (see fig. 1(a))
$k_0, k_2, \text{etc.}$	coefficients of characteristic equation (C8) for r ; defined by equations (C9)
$k_{04}, k_{22}, \text{etc.}$	defined by equations (C11)
\hat{k}	defined by equation (C7)
\hat{k}_1, \hat{k}_2	defined by equations (C12)
$\tilde{k}_{02}, \tilde{k}_{20}, \text{etc.}$	defined by equations (D23)
$\hat{k}_{02}, \hat{k}_{20}, \text{etc.}$	defined by equations (E18)
$L_{11}, L_{12}, \text{etc.}$	defined by equations (C25)
M	frame bending moments per unit length of corrugation
M_{01}, M_{12}, M_{23}	frame bending moments, per unit length of corrugation, at junctions ①, ②, ③ respectively (see fig. 8)
$M_{10} = -M_{12}$	
$M_{21} = -M_{23}$	
\hat{m}	defined by equation (C7)
\hat{m}_1, \hat{m}_2	defined by equations (C12)

N_3, N_4	defined by equations (C34)
$N_{11}, N_{12}, \text{etc.}$	defined by equations (C34)
\bar{N}_4	defined by equation (C39)
$\bar{N}_{31}, \bar{N}_{32}, \bar{N}_{33}, \bar{N}_{34}$	defined by equations (C39)
$\bar{\bar{N}}_{31}, \bar{\bar{N}}_{32}, \bar{\bar{N}}_{33}, \bar{\bar{N}}_{34}$	defined by equations (C39')
p^B, p^C, p^D	real numbers defined by equations (C29) and (C27)
P_2	defined by equations (D35)
$P_{11}, P_{12}, \text{etc.}$	defined by equations (D35)
p	pitch of corrugation (see fig. 1(a))
p'	developed width of one corrugation ($2e + f + 2k$)
p_1, p_3, p_5, \dots	coefficients in series expansion for R (see eqs. (30) and (C20))
$\tilde{p}_1, \tilde{p}_3, \tilde{p}_5, \dots$	coefficients in series expansion for \tilde{X} (see eqs. (D26) and (D28))
$\hat{p}_1, \hat{p}_3, \hat{p}_5, \dots$	coefficients in series expansion for \hat{X} (see eqs. (E21); defined by equations (D28) with all tildes (\sim) replaced by circumflex accents ($\hat{}$))
Q^B, Q^C, Q^D	real numbers defined by equations (C29) and (C27)
Q_2	defined by equations (E27)
$Q_{11}, Q_{12}, \text{etc.}$	defined by equations (E27)
q_0, q_2, q_4, \dots	coefficients in series expansion for R (see eqs. (29) and (C19))
$\tilde{q}_0, \tilde{q}_2, \tilde{q}_4, \dots$	coefficients in series expansion for \tilde{Y} (see eqs. (D26) and (D27))
$\hat{q}_0, \hat{q}_2, \hat{q}_4, \dots$	coefficients in series expansion for \hat{X} (see eq. (E21)); defined by equations (D27) with all tildes (\sim) replaced by circumflex accents ($\hat{}$)
R	variable in characteristic equation (26)
R_1, R_2, \dots, R_8	roots of characteristic equation (26)
$\bar{R}_1, \bar{R}_2, \bar{R}_3$	effective cross-sectional shear force resultants for plate elements 01, 12, 23 respectively (see fig. 9(d) and eq. (B16))
\tilde{R}	variable in characteristic equation (D21)

$\tilde{R}_1, \tilde{R}_2, \tilde{R}_3, \tilde{R}_4$	roots of characteristic equation (D21)
\hat{R}	variable in characteristic equation (E16)
$\hat{R}_1, \hat{R}_2, \hat{R}_3, \hat{R}_4$	roots of characteristic equation (E16)
$r \equiv R/e$	
$r_j \equiv R_j/e$	$(j = 1, 2, \dots, 8)$
$\tilde{r} \equiv \tilde{R}/e$	
$\hat{r} \equiv \hat{R}/k$	
s_1, s_2, s_3	transverse coordinates along the cross-sectional centerline (see fig. 4(a))
$\widehat{ss}, \widehat{sc}$	defined by equations (C35)
S^B, S^C, S^D	real numbers defined by equations (C29) and (C27)
$\widehat{sc} \equiv \cos(Vb/e)$	
s_U, s_X, s_Y	defined by equations (53)
T_1, T_2, T_3	torques carried by plate elements 01, 12, 23 respectively
TPE	total potential energy of a single corrugation (see eq. (18))
T^B, T^C, T^D	real numbers defined by equations (C29) and (C27)
t	thickness of corrugation (see fig. 1(a))
U	strain energy of an entire corrugation (see eq. (17)); also real part of R_1 and R_2 and negative of real part of R_3 and R_4 (see eqs. (27))
U_b	strain energy per unit length of corrugation associated with frame bending of the cross sections
U_{ext}	strain energy per unit length of corrugation associated with longitudinal extension
U_{sh}	strain energy per unit length of corrugation associated with middle surface shear
U_{tw}	strain energy per unit length of corrugation associated with torsion

u	longitudinal displacement
u_0	one-half the relative shearing displacement of two adjacent trough lines (see fig. 4(b))
u_1	longitudinal displacement (function of z) along junction (1) (see fig. 4)
u_2	longitudinal displacement (function of z) along junction (2) (see fig. 4)
V	imaginary part of R_1 and R_3 , negative of imaginary part of R_2 and R_4 (see eqs. (27))
$\tilde{V}'_1, \tilde{V}'_2$	functions of z defined by equations (54) and (55)
v_1, v_2	amplitudes of component modes of displacement in the plane of the cross sections (functions of z) (see fig. 4(c))
W	function of z defined by equation (D43)
\bar{W}	function of z defined by equation (E36)
X	real number equal to R_5 and $-R_6$ (see eqs. (27))
\tilde{X}	real number equal to \tilde{R}_1 and $-\tilde{R}_2$ (see eqs. (D25))
\hat{X}	real number equal to \hat{R}_1 and $-\hat{R}_2$ (see eqs. (E20))
x	transverse coordinate (see fig. 1 (b))
Y	real number equal to R_7 and $-R_8$ (see eqs. (27))
\tilde{Y}	real number equal to \tilde{R}_3 and $-\tilde{R}_4$ (see eqs. (D25))
\hat{Y}	real number equal to \hat{R}_3 and $-\hat{R}_4$ (see eqs. (E20))
z	longitudinal coordinate (see fig. 1(b))
α	numerical constant having the value 0 if the trough lines are free to rotate and 1 if they are prevented from rotating
α_1^B, α_2^B	defined by equations (C36)
β	defined by equation (A8)
$\beta_1^C, \beta_2^C, \beta_1^D, \beta_2^D$	defined by equations (C36)
$\tilde{\beta}$	defined by equation (D8a)
γ	shear strain
$\gamma_1, \gamma_2, \gamma_3$	shear strain in plate elements 01, 12, 23 respectively

$\tilde{\gamma}_1, \tilde{\gamma}_2, \tilde{\gamma}_3, \tilde{\gamma}_4$

γ'

$\gamma_{av} \equiv 2u_0/p$

$\hat{\gamma}_1, \hat{\gamma}_2, \hat{\gamma}_3, \hat{\gamma}_4$

$\left. \begin{aligned} \gamma_j^B &= B_j/A_j \\ \gamma_j^C &= C_j/A_j \\ \gamma_j^D &= D_j/A_j \end{aligned} \right\}$

$\Delta_1, \Delta_2, \Delta_3$

ϵ

$\epsilon_1, \epsilon_2, \epsilon_3$

ζ_1, ζ_2

θ

θ_1, θ_2

ν

σ

$\sigma_1, \sigma_2, \sigma_3$

$\sigma_{(1)}, \sigma_{(2)}$

$\sigma_{(0)}, \sigma_{(1)}, \sigma_{(2)}$

τ

τ_1, τ_2, τ_3

τ_{av}

defined by equations (D31)

uniform shear strain in corrugated sheet corresponding to relative shearing displacement $2u_0$ of adjacent trough lines (see eq. (37))

defined by equations (E24)

computed from equation (C27); representable by equations (C29)

functions of v_1 and v_2 defined in table A1

longitudinal strain

longitudinal strain in plate elements 01, 12, 23 respectively

defined by equations (C2)

angle between sides of corrugation and horizontal (see fig. 1)

angles of rotation of junctions (1) and (2) respectively (see fig. 6)

Poisson's ratio, taken as 0.3 for numerical work

cross-sectional normal stress

cross-sectional normal stress in plate elements 01, 12, 23 respectively

cross-sectional normal stress (functions of z) along junctions (1) and (2) (see fig. 4(a))

extreme-fiber bending stress (functions of z) at junctions (0), (1), (2) respectively, resulting from frame bending of the cross sections (see fig. 18)

middle-surface shear stress

middle-surface shear stress in plate elements 01, 12, 23 respectively

average longitudinal shear stress, $F/2bt$

$\tau'_{01}, \tau'_{12}, \tau'_{23}$	extreme-fiber shear stresses due to twisting of the plate elements 01, 12, 23 respectively (see fig. 18)
$\tau_{01}, \tau_{12}, \tau_{23}$	middle-surface shear stresses in plate elements 01, 12, 23 respectively (see fig. 18)
ϕ	rate of twist
ϕ_1, ϕ_2, ϕ_3	rate of twist of plate elements 01, 12, 23 respectively
ψ	factor in equation (35) for shear stiffness; defined by equation (36)
$\tilde{\psi}$	factor in equation (D37) for shear stiffness; defined by equation (D38)
$\hat{\psi}$	factor in equation (E28) for shear stiffness; defined by equation (E29)
Ω	relative shearing stiffness, i.e. shear stiffness of actual corrugation divided by shear stiffness of an identical corrugation with continuous end attachment producing uniform shearing strain in the sheet
Ω'	another relative shearing stiffness, defined as the shear stiffness of the actual corrugation to that of a uniformly sheared flat plate of the same thickness and length and width equal to p.
$\bar{\Omega}$	defined by equation (69)

ANALYSIS

Since all corrugations are assumed to deform identically, the analysis is based on a single corrugation, i.e. on the portion of the plate between two neighboring trough lines. This corrugation can be regarded as an assemblage of rigidly joined flat-plate elements and can therefore be analyzed by applying flat-plate theory and continuity conditions to these elements. An analysis on this basis, however, can be complicated; therefore in the present paper certain simplifying assumptions are made and a solution effected by means of the method of minimum total potential energy.

Assumption regarding longitudinal displacements. - Figure 4(a) shows a cross section of the middle surface of a single corrugation. The shearing of this corrugation is assumed to be effected by a rigid-body shift of the trough line at station ① through a distance u_0 in the positive-z direction and a rigid-body shift of the trough line at station ⑤ through the same distance in the negative-z direction. Thus the total shearing displacement of one trough line with respect to the other is $2u_0$.

The longitudinal displacements of other points of the cross section are assumed to vary linearly between stations. These longitudinal displacements are shown in the plan view (fig. 4(b)), which also shows their antisymmetrical

nature resulting from the antisymmetrical nature of the imposed displacements of the two trough lines. Thus the longitudinal displacements of all middle-surface points are defined by one prescribed parameter, u_0 , and two unknown functions of z : $u_1(z)$ and $u_2(z)$. If, as is done subsequently, the shearing force F (see fig. 1(b)) is regarded as prescribed, rather than the shearing displacement u_0 , the latter will become an additional unknown.

Assumptions regarding displacements in the plane of the cross section. - The cross sections, especially those near the ends, can be expected to undergo significant flexural deformation in their own planes, somewhat in the manner of a rigid-jointed frame. Figure 5, taken from reference 1, shows such deformations in a particular experiment.*

As is done in frame analysis, the deformation of a cross section in its own plane will be assumed to be inextensional. And the deformed cross section will be assumed to have the same form as a rigid-jointed frame whose joint displacements are the same as the joint displacements of the cross section. With stations ① and ⑤ having no displacements in the plane of the cross section, and considering the required antisymmetry of the deformation, the above assumption leaves only two degrees of freedom for the deformation of the cross section in its own plane. That is, the displacements in the plane of the cross section can be represented as a superposition of the displacements associated with each of two component frame-deformation modes.†

The two frame-deformation modes selected in the present analysis are shown in figure 4(c). The first is obtained by imposing vertical displacements of amount $v_1(z)$ upward at joint ① and downward at joint ④, while joint ② is constrained to slide parallel to line 1-2 and joint ③ is similarly constrained to slide parallel to line 3-4. These sliding displacements must be $v_1 \sin \theta$, as shown in figure 4(c), in order to satisfy the inextensibility assumption. The second component mode of cross-sectional deformation is that obtained by displacing joint ② an amount $v_2(z)$ perpendicular to line 1-2 and joint ③ a like amount perpendicular to line 3-4, while joints ① and ④ are constrained to remain undisplaced. In both component modes the interior joints are permitted complete freedom of rotation, and the edge joints ① and ⑤ are either hinged or clamped, depending on which of the two kinds of external restraint conditions is being considered along the trough lines (see INTRODUCTION).

Thus the displacements in the plane of the cross section are fully defined by two unknown functions of z : $v_1(z)$ and $v_2(z)$.

*The experiment does not correspond exactly to the present analysis because of the interference which is evidently present between the end of the corrugation and the transverse member to which it is attached. However the photograph does serve to show the large magnitude of the flexural deformations that can occur when the ends are not continuously attached.

†The assumptions made here about the deformation of a cross section in its own plane are the same as in reference 2, except that it is evident from figure 10 of reference 2 that the joint displacements are being allowed only one degree of freedom there instead of the two which they naturally possess.

Middle-surface extensional strains. - In consequence of the assumptions discussed above regarding longitudinal displacements, and utilizing the coordinate system of figure 4(a), the z-wise displacements u for all points of the middle surface can be expressed in terms of u_0 , $u_1(z)$ and $u_2(z)$. The results are shown in the column headed "u" of table 1. The corresponding extensional strains ϵ are obtained

TABLE 1. - LONGITUDINAL DISPLACEMENTS AND STRAINS

Plate element	Displacement, u	Strain, ϵ
01	$u_0 + \frac{s_1}{e}(u_1 - u_0)$	$\frac{s_1}{e} \frac{du_1}{dz} \equiv \epsilon_1$
12	$u_1 + \frac{s_2}{k}(u_2 - u_1)$	$\frac{du_1}{dz} + \frac{s_2}{k} \left(\frac{du_2}{dz} - \frac{du_1}{dz} \right) \equiv \epsilon_2$
23	$u_2 \left(1 - \frac{2s_3}{f} \right)$	$\frac{du_2}{dz} \left(1 - \frac{2s_3}{f} \right) \equiv \epsilon_3$

by differentiating these displacements with respect to z . The results are given in the last column of table 1. Because of the antisymmetry of the longitudinal strains with respect to the midpoint of plate element 23, it suffices to consider explicitly only the three plate elements listed in the table.

Middle-surface shear strains. - The shear strains of the middle surface of the plate elements of the corrugation arise from both the longitudinal displacements and the displacements in the plane of the cross section. In view of the assumption that u varies linearly between stations and the assumption of inextensional cross-sectional deformations, for a given z the shear strain will be constant across the width of any plate element. Considering the longitudinal displacements of figure 4(b) and the cross-sectional displacements of figure 4(c), one arrives at the shear strains γ shown in table 2.

TABLE 2. - SHEAR STRAINS

Plate element	Shear strain, γ
01	$\frac{u_1 - u_0}{e} \equiv \gamma_1$
12	$\frac{u_2 - u_1}{k} + \frac{d}{dz}(v_1 \sin \theta) \equiv \gamma_2$
23	$-\frac{2u_2}{f} + \frac{d}{dz}(v_1 \sin \theta \cos \theta) + \frac{d}{dz}(v_2 \sin \theta) \equiv \gamma_2$

Rates of twist of the plate elements. - It is expected that the twisting of the plate elements will make only a minor contribution to the total strain energy, as long as the length of the corrugation is several times the pitch. Therefore, in computing the strain energy due to twisting of a plate element it is considered sufficiently accurate to base this strain energy calculation on an overall rate of twist computed from the displacements of the longitudinal edges of the element rather than on the detailed variation of the rate of twist across the width of the element. For example, the rate of twist of the plate element 01 will be taken as $d(v_1/e)/dz$, in accordance with the edge displacements shown in figure 4(c) for this plate element. The rates of twist ϕ obtained in this way are shown in table 3.

TABLE 3. - RATES OF TWIST

Plate element	Rate of twist, ϕ
01	$\frac{d}{dz}\left(\frac{v_1}{e}\right) \equiv \phi_1$
12	$-\frac{d}{dz}\left(\frac{v_2}{k}\right) - \frac{d}{dz}\left(\frac{v_1 \cos \theta}{k}\right) \equiv \phi_2$
23	$-\frac{d}{dz}\left(\frac{2v_1 \sin^2 \theta}{f}\right) + \frac{d}{dz}\left(\frac{2v_2 \cos \theta}{f}\right) \equiv \phi_3$

Strain energy components. - On the basis of the assumptions discussed above regarding the deformations, it is now possible to write expressions for the following strain-energy components: (a) middle-surface extension, (b) middle-surface shear, (c) twisting of the plate elements, and (d) frame bending of the cross sections. Expressions are developed below for the density (i.e., strain energy per unit length of corrugation) of each of these components.

(a) Middle-surface extension: The strain-energy density of middle-surface extension can be obtained from the expressions for ϵ in table 1 in conjunction with the assumption that the associated longitudinal normal stress σ is related to ϵ by the uniaxial expression

$$\sigma = E' \epsilon \quad (1)$$

where E' is Young's modulus.* The following expression is thus obtained for the extensional strain energy per unit length of corrugation:

$$\begin{aligned} U_{\text{ext}} &= 2 \int_0^e \frac{1}{2} \sigma_1 \epsilon_1 t ds_1 + 2 \int_0^k \frac{1}{2} \sigma_2 \epsilon_2 t ds_2 + \int_0^f \frac{1}{2} \sigma_3 \epsilon_3 t ds_3 \\ &= E' t \left[\int_0^e \epsilon_1^2 ds_1 + \int_0^k \epsilon_2^2 ds_2 + \frac{1}{2} \int_0^f \epsilon_3^2 ds_3 \right] \end{aligned} \quad (2)$$

*The prime on the Young's modulus symbol is merely a tracer to distinguish this Young's modulus, associated with extension, from another Young's modulus associated with flexure, which will be introduced shortly and denoted by E .

where the subscripts 1,2,3 denote the plate elements 01, 12, 23 respectively. Substituting for ϵ_1 , ϵ_2 and ϵ_3 the expressions from table 1, and carrying out the integrations, one obtains

$$U_{\text{ext}} = b_{11} \left(\frac{du_1}{dz} \right)^2 + 2b_{12} \frac{du_1}{dz} \frac{du_2}{dz} + b_{22} \left(\frac{du_2}{dz} \right)^2 \quad (3)$$

where

$$\begin{aligned} b_{11} &= E'te \cdot \frac{1}{3} \left(1 + \frac{k}{e} \right) \\ b_{12} &= \frac{1}{6} E'tk \\ b_{22} &= \frac{1}{6} E't(f + 2k) \end{aligned} \quad (4)$$

(b) Middle-surface shear: Assuming the shear stress τ linearly related to the shear strain γ through the elastic law

$$\tau = G\gamma \quad (5)$$

where G is the shear modulus, one obtains the following expression for the strain energy of middle-surface shear per unit length of corrugation:

$$\begin{aligned} U_{\text{sh}} &= 2 \cdot \frac{1}{2} \tau_1 \gamma_1 t e + 2 \cdot \frac{1}{2} \tau_2 \gamma_2 t k + \frac{1}{2} \tau_3 \gamma_3 t f \\ &= Gt(\gamma_1^2 e + \gamma_2^2 k + \frac{1}{2} \gamma_3^2 f) \end{aligned} \quad (6)$$

Substituting for γ_1 , γ_2 , γ_3 the expressions in table 2, one obtains

$$\begin{aligned} U_{\text{sh}} &= c_{00} u_0^2 + c_{11} u_1^2 + c_{22} u_2^2 + 2 c_{01} u_0 u_1 + 2 c_{12} u_1 u_2 \\ &\quad + d_{11} u_1 \frac{dv_1}{dz} + d_{21} u_2 \frac{dv_1}{dz} + d_{22} u_2 \frac{dv_2}{dz} \\ &\quad + e_{11}^* \left(\frac{dv_1}{dz} \right)^2 + e_{22}^* \left(\frac{dv_2}{dz} \right)^2 + 2e_{12}^* \frac{dv_1}{dz} \frac{dv_2}{dz} \end{aligned} \quad (7)$$

where

$$\left. \begin{aligned} c_{00} &= G \frac{t}{e} & c_{11} &= G \frac{t}{e} \left(1 + \frac{e}{k} \right) \\ c_{22} &= G \left(\frac{t}{k} + 2 \frac{t}{f} \right) \\ c_{01} &= -G \frac{t}{e} & c_{12} &= -G \frac{t}{k} \end{aligned} \right\} \quad (8)$$

(equation continued on next page)

$$\begin{aligned}
d_{11} &= d_{22} = -2 G t \sin \theta \\
d_{21} &= 2 G t \sin \theta (1 - \cos \theta) \\
e_{11}^* &= G t \sin^2 \theta \left(k + \frac{f}{2} \cos^2 \theta \right) \\
e_{22}^* &= \frac{1}{2} G t f \sin^2 \theta \\
e_{12}^* &= \frac{1}{2} G t f \sin^2 \theta \cos \theta
\end{aligned}$$

(c) Twisting of the plate elements: Corresponding to the rates of twist shown in table 3 and regarding each flat-plate element as a bar of narrow rectangular cross section*, the torques carried by the plate elements 01, 12 and 23 are respectively

$$T_1 = G' J_1 \phi_1 \quad T_2 = G' J_2 \phi_2 \quad T_3 = G' J_3 \phi_3 \quad (9)$$

where

$$J_1 = \frac{1}{3} e t^3 \quad J_2 = \frac{1}{3} k t^3 \quad J_3 = \frac{1}{3} f t^3 \quad (10)$$

and G' denotes the shear modulus. (The prime on G is a tracer introduced so that those terms arising from torsion can easily be distinguished from those arising from middle surface shear.) The total strain energy of twisting (per unit length of corrugation) is therefore

$$\begin{aligned}
U_{tw} &= 2 \cdot \frac{1}{2} T_1 \phi_1 + 2 \cdot \frac{1}{2} T_2 \phi_2 + \frac{1}{2} T_3 \phi_3 \\
&= G' (J_1 \phi_1^2 + J_2 \phi_2^2 + \frac{1}{2} J_3 \phi_3^2)
\end{aligned} \quad (11)$$

or, substituting the expressions for ϕ_1, ϕ_2, ϕ_3 from table 3,

$$U_{tw} = \bar{e}_{11} \left(\frac{dv_1}{dz} \right)^2 + \bar{e}_{22} \left(\frac{dv_2}{dz} \right)^2 + 2 \bar{e}_{12} \frac{dv_1}{dz} \frac{dv_2}{dz} \quad (12)$$

where

$$\begin{aligned}
\bar{e}_{11} &= G' \left(\frac{J_1}{e^2} + \frac{J_2}{k^2} \cos^2 \theta + \frac{2J_3}{f^2} \sin^4 \theta \right) \\
\bar{e}_{22} &= G' \left(\frac{J_2}{k^2} + \frac{2J_3}{f^2} \cos^2 \theta \right) \\
\bar{e}_{12} &= G' \left(\frac{J_2}{k^2} \cos \theta - \frac{2J_3}{f^2} \sin^2 \theta \cos \theta \right)
\end{aligned} \quad (13)$$

*The same result (eq. (11)) can be derived using plate theory rather than bar theory.

(d) Frame bending of the cross sections: Considering a unit length of corrugation to be a frame whose joint displacements are a superposition of the two modes shown in figure 4(c), one obtains for the strain energy a quadratic expression in v_1 and v_2 . The derivation of this expression is in appendix A, and the result is

$$U_b = a_{11}v_1^2 + 2a_{12}v_1v_2 + a_{22}v_2^2 \quad (14)$$

where

$$\begin{aligned} a_{11} &= \frac{D}{\beta^2 e^3} \left[A_{11} + A_{22} \left(\frac{e}{k} \right)^2 \cos^2 \theta + 4A_{33} \left(\frac{e}{f} \right)^2 \sin^4 \theta \right. \\ &\quad \left. - A_{12} \frac{e}{k} \cos \theta + 2A_{23} \frac{e}{k} \frac{e}{f} \sin^2 \theta \cos \theta - 2A_{13} \frac{e}{f} \sin^2 \theta \right] \\ a_{12} &= \frac{D}{\beta^2 e^3} \left[A_{22} \left(\frac{e}{k} \right)^2 \cos \theta - 4A_{33} \left(\frac{e}{f} \right)^2 \sin^2 \theta \cos \theta \right. \\ &\quad \left. - \frac{1}{2} A_{12} \frac{e}{k} - A_{23} \frac{e}{k} \frac{e}{f} (\cos^2 \theta - \sin^2 \theta) + A_{13} \frac{e}{f} \cos \theta \right] \\ a_{22} &= \frac{D}{\beta^2 e^3} \left[A_{22} \left(\frac{e}{k} \right)^2 + 4A_{33} \left(\frac{e}{f} \right)^2 \cos^2 \theta - 2A_{23} \frac{e}{k} \frac{e}{f} \cos \theta \right] \end{aligned} \quad (15)$$

The quantities β , A_{11} , A_{22} , A_{33} , A_{12} , A_{23} , A_{13} appearing in equations (15) are dimensionless parameters depending on the geometry of the cross section and the edge conditions regarding rotation along the trough lines. They are defined by equations (A8) and (A10) of appendix A. The symbol α appearing in equations (A8) and (A10) is defined as zero if the corrugation is free to rotate along the trough lines and unity if the corrugation is clamped along the trough lines.

The symbol D appearing in equations (15) stands for the frame flexural stiffness of the corrugation per unit width of frame, i.e. per unit length of corrugation. There is bound to be some ambiguity involved in selecting an appropriate value for D , inasmuch as the frame bending moments are not truly uniquely determined by the curvatures in the plane of the cross section alone (as was assumed in deriving eq. (14)), but depend also on the longitudinal curvatures or longitudinal bending moments in the plate elements making up the corrugation. Only in the following three cases can it be assumed that the frame bending moments and the frame curvatures are uniquely related: (a) when the longitudinal bending moments are zero or negligible, (b) when Poisson's ratio is zero, and (c) when the longitudinal curvatures of the generators of the corrugation are zero or negligible. In cases (a) and (b) an appropriate assumption for D would be the beam flexural stiffness

$$D = \frac{1}{12} Et^3 \quad (16a)$$

where E is Young's modulus. In case (c) the appropriate assumption would be the plate flexural stiffness

$$D = \frac{Et^3}{12(1 - \nu^2)} \quad (16b)$$

where ν is Poisson's ratio. Of these two candidates, the latter (eq. 16(b)) is judged to be appropriate for the present analysis, inasmuch as for corrugation lengths several times the pitch one would expect the longitudinal curvatures of the generators to be small compared to the frame type curvatures of the cross sections*. Therefore the rest of the analysis will be based on equation (16b), but in order to assess the order of magnitude of the uncertainty in the over-all shearing stiffness due to the ambiguity in D a few calculations of shearing stiffness will also be made using equation (16a).

Total strain energy. - Integrating each of the foregoing strain-energy densities over the entire length of a corrugation and summing leads to the following expression for the total strain energy U of a single corrugation:

$$U = \int_{-b}^b (U_{\text{ext}} + U_{\text{sh}} + U_{\text{tw}} + U_b) dz \quad (17)$$

where U_{ext} , U_{sh} , U_{tw} , U_b are defined by equations (3), (7), (12), and (14) respectively.

*In the case of buckling of a plate-column with simply supported loaded edges and free unloaded ends, it is shown in ref. 3 that the effective flexural stiffness is already about five-sixths of the way from the beam value to the plate value when the distance between the free ends is only four times the distance between the supported edges. (The analogous distances in the present case would be the length of the corrugation, $2b$, and (conservatively) the developed width of a corrugation.) In the case of a column with clamped loaded edges the transition from the beam value to the plate value occurs even more rapidly as the ratio of these two distances increases.

Total potential energy. - The prescribed shearing forces F along the sides of a corrugation acquire a potential energy of $-F \cdot 2u_0$ due to the total longitudinal displacement $2u_0$ of one side with respect to the other. Adding this to the above strain energy U gives the following total potential energy (TPE) of a single corrugation:

$$\text{TPE} = -2Fu_0 + U \quad (18)$$

Minimization of the TPE. - The TPE as defined by equation (18) is a functional of $u_0, u_1(z), u_2(z), v_1(z), v_2(z)$. In accordance with the method of minimum total potential energy (ref. 4) the "best" values of these quantities will be those which minimize the TPE. To find these best values, the technique of variational calculus may be used to form the first variation of the TPE with respect to variations in $u_0, u_1(z), \dots, v_2(z)$ and equate it to zero. This will lead to a system of field equations (primarily differential equations) and boundary conditions defining $u_0, u_1(z), \dots, v_2(z)$.

The details of this procedure are given in appendix B. The resulting field equations, equations (B9) and (B8) of appendix B, are given again here for convenience:

$$\left. \begin{aligned} b_{11} \frac{d^2 u_1}{dz^2} + b_{12} \frac{d^2 u_2}{dz^2} - \frac{1}{2} d_{11} \frac{dv_1}{dz} - c_{11} u_1 - c_{12} u_2 &= c_{01} u_0 \\ b_{12} \frac{d^2 u_1}{dz^2} + b_{22} \frac{d^2 u_2}{dz^2} - \frac{1}{2} d_{21} \frac{dv_1}{dz} - \frac{1}{2} d_{22} \frac{dv_2}{dz} - c_{12} u_1 - c_{22} u_2 &= 0 \\ e_{11} \frac{d^2 v_1}{dz^2} + e_{12} \frac{d^2 v_2}{dz^2} + \frac{1}{2} d_{11} \frac{du_1}{dz} + \frac{1}{2} d_{21} \frac{du_2}{dz} - a_{11} v_1 - a_{12} v_2 &= 0 \\ e_{12} \frac{d^2 v_1}{dz^2} + e_{22} \frac{d^2 v_2}{dz^2} + \frac{1}{2} d_{22} \frac{du_2}{dz} - a_{12} v_1 - a_{22} v_2 &= 0 \end{aligned} \right\} \quad (19)$$

and

$$2c_{00}u_0b + c_{01} \int_{-b}^b u_1 dz = F \quad (20)$$

Different sets of boundary conditions are obtained according to the nature of the end attachment. If there are point attachments at the ends of the trough lines only (fig. 3(a)) the boundary conditions at $z = \pm b$ are

$$\frac{du_1}{dz} = 0 \quad , \quad \frac{du_2}{dz} = 0 \quad (21)$$

$$2e_{11} \frac{dv_1}{dz} + 2e_{12} \frac{dv_2}{dz} + d_{11}u_1 + d_{21}u_2 = 0 \quad (22)$$

$$2e_{12} \frac{dv_1}{dz} + 2e_{22} \frac{dv_2}{dz} + d_{22}u_2 = 0$$

If the attachments at the ends of the trough lines are wide as idealized in figure 3c, it is only necessary to replace the first of equations (22) by the condition

$$v_1 = 0 \quad (22')$$

Finally, if the attachments are as shown in figure 3b, namely point attachments at the ends of both the crest lines and the trough lines, the boundary conditions are

$$\frac{du_1}{dz} = 0 \quad , \quad \frac{du_2}{dz} = 0 \quad (23)$$

$$v_1 \cos \theta + v_2 = 0 \quad (24)$$

$$2(e_{11} - e_{12} \cos \theta) \frac{dv_1}{dz} + 2(e_{12} - e_{22} \cos \theta) \frac{dv_2}{dz} + d_{11}u_1 + (d_{21} - d_{22} \cos \theta)u_2 = 0 \quad (25)$$

As discussed in appendix B, these boundary conditions have physical interpretations. The physical interpretation of equation (22') is obvious. Equations (21) and (23) express the vanishing of normal stresses at the ends of the corrugation. Equations (22) express the vanishing of certain effective middle-plane shearing forces at the ends of the inclined plate elements (12 and 34 in fig. 4) and the horizontal plate element (23) forming the crest. Equation (24) expresses the constraint against horizontal displacement furnished by an attachment at the end of the crest line, and equation (25) the vanishing of the resultant equivalent middle-plane shear at the ends of the inclined plate elements (12 and 34).

Solution of the equations. - Fundamentally the solution of the problem consists of solving equations (19) for $u_1(z)$, $u_2(z)$, $v_1(z)$, $v_2(z)$ in terms of u_0 , subject to the appropriate set of boundary conditions. The solution for $u_1(z)$ is then substituted in equation (20), which then gives u_0 in terms of F or F in terms of u_0 .

The equations involved are linear with constant coefficients, so the procedure just described can be carried out in a straight-forward manner. The full details of the solution are in appendix C, and only the main features of the solution (those needed for computational purposes) will be given here.

The numerical realization of the solution requires first that the following characteristic equation be solved for its eight roots $R = R_1, R_2, \dots, R_8$:

$$\begin{aligned} & [k_{80} + k_{82}\left(\frac{t}{e}\right)^2 + k_{84}\left(\frac{t}{e}\right)^4]R^8 + [k_{60} + k_{62}\left(\frac{t}{e}\right)^2 + k_{64}\left(\frac{t}{e}\right)^4]R^6 \\ & + [k_{42}\left(\frac{t}{e}\right)^2 + k_{44}\left(\frac{t}{e}\right)^4]R^4 + [k_{22}\left(\frac{t}{e}\right)^2 + k_{24}\left(\frac{t}{e}\right)^4]R^2 \\ & + [k_{04}\left(\frac{t}{e}\right)^4] = 0 \end{aligned} \quad (26)$$

where k_{80}, k_{82} , etc. are functions of the elastic constants and cross-sectional shape (but not thickness) defined by equations (C11), (C12) and (C13). Calculations show that four of the roots are complex and four real; from this and the fact that only even powers of R appear in equation (26), it follows that the eight roots can be represented in the form

$$\begin{aligned} R_1 &= U + iV & R_5 &= X \\ R_2 &= U - iV & R_6 &= -X \\ R_3 &= -U + iV & R_7 &= Y \\ R_4 &= -U - iV & R_8 &= -Y \end{aligned} \quad (27)$$

where U, V, X and Y are real numbers, and $i = \sqrt{-1}$.

When t/e is small, the values of the eight roots can be computed from the following power series expansions:

$$R = \left(\frac{t}{e}\right)^{1/2} [c_0 + c_1 \frac{t}{e} + c_2 \left(\frac{t}{e}\right)^2 + \dots] \quad (28)$$

$$R = q_0 + q_2 \left(\frac{t}{e}\right)^2 + q_4 \left(\frac{t}{e}\right)^4 + \dots \quad (29)$$

$$R = p_1 \frac{t}{e} + p_3 \left(\frac{t}{e}\right)^3 + p_5 \left(\frac{t}{e}\right)^5 + \dots \quad (30)$$

where the coefficients $c_0, c_1, \dots, q_0, q_2, \dots, p_1, p_3, \dots$ are defined by equations (C21), (C19) and (C20). Equations (C21) give four sets of complex values for c_0, c_1, \dots , and therefore equation (28) generates the four complex roots R_1, R_2, R_3, R_4 . Equation (C19) gives two sets of real values of q_0, q_2, \dots ; the two real roots thus resulting from equation (29) will be identified with R_5 and R_6 . Similarly equations (C20) yield two sets of real values for p_1, p_3, \dots ; thus equation (30) yields two real roots, which will be identified with R_7 and R_8 .

With U, V, X and Y known, the displacements can be computed in terms of u_0 from the following equations:

$$\begin{aligned} \frac{u_1(z)}{u_0} = & \zeta_1 + \left(\frac{\bar{A}_1}{u_0} \right) \cosh \frac{Uz}{e} \cos \frac{Vz}{e} + \left(\frac{\bar{A}_4}{u_0} \right) \sinh \frac{Uz}{e} \sin \frac{Vz}{e} \\ & + \left(\frac{\bar{A}_5}{u_0} \right) \cosh \frac{Xz}{e} + \left(\frac{\bar{A}_7}{u_0} \right) \cosh \frac{Yz}{e} \end{aligned} \quad (31)$$

$$\begin{aligned} \frac{u_2(z)}{u_0} = & \zeta_2 + \left[\left(\frac{\bar{A}_1}{u_0} \right) P^B + \left(\frac{\bar{A}_4}{u_0} \right) Q^B \right] \cosh \frac{Uz}{e} \cos \frac{Vz}{e} \\ & + \left[\left(\frac{\bar{A}_4}{u_0} \right) P^B - \left(\frac{\bar{A}_1}{u_0} \right) Q^B \right] \sinh \frac{Uz}{e} \sin \frac{Vz}{e} \\ & + \left(\frac{\bar{A}_5}{u_0} \right) S^B \cosh \frac{Xz}{e} + \left(\frac{\bar{A}_7}{u_0} \right) T^B \cosh \frac{Yz}{e} \end{aligned} \quad (32)$$

$$\begin{aligned} \frac{v_1(z)}{u_0} = & \left[\left(\frac{\bar{A}_4}{u_0} \right) P^C - \left(\frac{\bar{A}_1}{u_0} \right) Q^C \right] \cosh \frac{Uz}{e} \sin \frac{Vz}{e} \\ & + \left[\left(\frac{\bar{A}_1}{u_0} \right) P^C + \left(\frac{\bar{A}_4}{u_0} \right) Q^C \right] \sinh \frac{Uz}{e} \cos \frac{Vz}{e} \\ & + \left(\frac{\bar{A}_5}{u_0} \right) S^C \sinh \frac{Xz}{e} + \left(\frac{\bar{A}_7}{u_0} \right) T^C \sinh \frac{Yz}{e} \end{aligned} \quad (33)$$

$$\begin{aligned}
\frac{v_2(z)}{u_0} = & \left[\left(\frac{\bar{A}_4}{u_0} \right) P^D - \left(\frac{\bar{A}_1}{u_0} \right) Q^D \right] \cosh \frac{Uz}{e} \sin \frac{Vz}{e} \\
& + \left[\left(\frac{\bar{A}_1}{u_0} \right) P^D + \left(\frac{\bar{A}_4}{u_0} \right) Q^D \right] \sinh \frac{Uz}{e} \cos \frac{Vz}{e} \\
& + \left(\frac{\bar{A}_5}{u_0} \right) S^D \sinh \frac{Xz}{e} + \left(\frac{\bar{A}_7}{u_0} \right) T^D \sinh \frac{Yz}{e}
\end{aligned} \tag{34}$$

where ζ_1 and ζ_2 are defined by equations (C2); $P^{B,C,D}$, $Q^{B,C,D}$, $S^{B,C,D}$, and $T^{B,C,D}$ are obtained by solving equations (C27) for $j = 1, 5$ and 7 and noting equations (C29); and $\frac{\bar{A}_1}{u_0}$, $\frac{\bar{A}_4}{u_0}$, $\frac{\bar{A}_5}{u_0}$, $\frac{\bar{A}_7}{u_0}$ are obtained by solving equations (C33) if there are point attachments at the ends of the trough lines only, (C38) if there are point attachments at the ends of the trough lines and the crest lines, or (C38') if there are wide attachments at the ends of the trough lines only.

Relationship between F and u_0 . - The above results give the displacements in terms of u_0 , which is one half of the relative shearing displacement of the two sides of the corrugation. In order to determine the displacements resulting from prescribed shearing forces F rather than prescribed shearing displacement, it is necessary to know the relationship between F and u_0 . This relationship is given by the following equation:

$$\frac{F}{2u_0} = \frac{Gtb}{e} \psi \tag{35}$$

where

$$\begin{aligned}
\psi = & 1 - \zeta_1 - \frac{e}{b} \left[\left(\frac{\bar{A}_1}{u_0} \sinh \frac{Ub}{e} \right) \frac{U\widehat{sc} + V\widehat{cs}}{U^2 + V^2} + \left(\frac{\bar{A}_4}{u_0} \sinh \frac{Ub}{e} \right) \frac{U\widehat{cs} - V\widehat{sc}}{U^2 + V^2} \right. \\
& \left. + \left(\frac{\bar{A}_5}{u_0} \sinh \frac{bX}{e} \right) \frac{1}{X} + \left(\frac{\bar{A}_7}{u_0} \sinh \frac{bY}{e} \right) \frac{1}{Y} \right]
\end{aligned} \tag{36}$$

with \widehat{sc} and \widehat{cs} defined by equations (C35).

Equation (35) gives the overall shearing stiffness of the corrugation. It is of interest to compare this shearing stiffness with certain other shearing stiffnesses. For example, if there were continuous attachment at the corrugation ends capable of producing uniform middle surface shear strain throughout the corrugation, that shear strain would be

$$\gamma' = \frac{2u_0}{2e + 2k + f} \tag{37}$$

where $2e + 2k + f$ is the developed width of the corrugation. The corresponding shear force would be

$$F' = Gt \cdot 2b\gamma' \quad (38)$$

and the corresponding overall shear stiffness would be

$$\frac{F'}{2u_0} = \frac{2Gtby'}{2u_0} = \frac{Gtb}{e + k + \frac{1}{2}f} \quad (39)$$

The ratio Ω of the shear stiffness $F/2u_0$ of the actual corrugation (eq. (35)) to the shear stiffness $F'/2u_0$ of the hypothetical continuously attached corrugation (eq. (39)) is thus given by

$$\Omega = (1 + \frac{k}{e} + \frac{1}{2}\frac{f}{e})\psi \quad (40)$$

A second kind of relative shearing stiffness can be obtained by comparing the stiffness of the actual corrugation (eq. (35)) with that of a uniformly sheared flat plate having the same thickness t , the same width p , and the same length $2b$. Such a flat plate with a relative shearing displacement of $2u_0$ between its edges would require a shearing force of

$$F'' = Gt \cdot 2b \cdot \frac{2u_0}{p} \quad (41)$$

whence its overall shearing stiffness would be

$$\frac{F''}{2u_0} = \frac{2Gtb}{p} \quad (42)$$

Thus, the ratio Ω' of the stiffness of the actual corrugation to that of the hypothetical flat plate is

$$\begin{aligned} \Omega' &= \frac{p}{2e} \cdot \psi \\ &= (1 + \frac{k}{e} \cos\theta + \frac{1}{2}\frac{f}{e})\psi \end{aligned} \quad (43)$$

Finally, the shearing stiffness of the corrugated plate can also be described in terms of an effective shear modulus in the following way: The average shear stress τ_{av} along an edge of the corrugation is

$$\tau_{av} = \frac{F}{2bt} \quad (44)$$

and the overall shear strain of the corrugation will be taken as

$$\gamma_{av} = \frac{2u_0}{p} \quad (45)$$

Defining an effective shear modulus G_{eff} as τ_{av}/γ_{av} , it follows that

$$\begin{aligned} G_{eff} &= \frac{F}{2bt} \frac{p}{2u_0} = \frac{p}{2bt} \frac{F}{2u_0} \\ &= \frac{p}{2bt} \cdot \frac{Gtb}{e} \psi \\ &= G \cdot \frac{p}{2e} \psi \\ &= G\Omega' \end{aligned} \quad (46)$$

Stresses. - The displacements $u_1(z)$, $u_2(z)$, $v_1(z)$, $v_2(z)$ are the key to the computation of the stresses in the corrugation. The equations for computing the stresses will now be given. In order to avoid lengthy expressions, the following short-hand notation will be employed:

$$\begin{aligned} \tilde{A}_1 &\equiv \frac{\bar{A}_1}{u_0} \sinh \frac{U_b}{e} \\ \tilde{A}_4 &\equiv \frac{\bar{A}_4}{u_0} \sinh \frac{U_b}{e} \\ \tilde{A}_5 &\equiv \frac{\bar{A}_5}{u_0} \sinh \frac{X_b}{e} \\ \tilde{A}_7 &\equiv \frac{\bar{A}_7}{u_0} \sinh \frac{Y_b}{e} \end{aligned} \quad (47)$$

$$\begin{aligned} f_{ss}(z) &\equiv \sinh \frac{Uz}{e} \sin \frac{Vz}{e} \\ f_{sc}(z) &\equiv \sinh \frac{Uz}{e} \cos \frac{Vz}{e} \\ f_{cs}(z) &\equiv \cosh \frac{Uz}{e} \sin \frac{Vz}{e} \\ f_{cc}(z) &\equiv \cosh \frac{Uz}{e} \cos \frac{Vz}{e} \end{aligned} \quad (48)$$

$$\begin{aligned}
f_{sX}(z) &\equiv \sinh \frac{Xz}{e} \\
f_{sY}(z) &\equiv \sinh \frac{Yz}{e} \\
f_{cX}(z) &\equiv \cosh \frac{Xz}{e} \\
f_{cY}(z) &\equiv \cosh \frac{Yz}{e}
\end{aligned} \tag{49}$$

$$\begin{aligned}
s_U &\equiv \sinh \frac{Ub}{e} \\
s_X &\equiv \sinh \frac{Xb}{e} \\
s_Y &\equiv \sinh \frac{Yb}{e}
\end{aligned} \tag{50}$$

$$\begin{aligned}
\tilde{v}_1'(z) &\equiv (\tilde{A}_4 P^C - \tilde{A}_1 Q^C) \frac{Uf_{ss} + Vf_{cc}}{s_U} + (\tilde{A}_1 P^C + \tilde{A}_4 Q^C) \frac{Uf_{cc} - Vf_{ss}}{s_U} \\
&+ \tilde{A}_5 S^C X \frac{f_{cX}}{s_X} + \tilde{A}_7 T^C Y \frac{f_{cY}}{s_Y}
\end{aligned} \tag{51}$$

$$\begin{aligned}
\tilde{v}_2'(z) &\equiv (\tilde{A}_4 P^D - \tilde{A}_1 Q^D) \frac{Uf_{ss} + Vf_{cc}}{s_U} + (\tilde{A}_1 P^D + \tilde{A}_4 Q^D) \frac{Uf_{cc} - Vf_{ss}}{s_U} \\
&+ \tilde{A}_5 S^D X \frac{f_{cX}}{s_X} + \tilde{A}_7 T^D Y \frac{f_{cY}}{s_Y}
\end{aligned} \tag{52}$$

The longitudinal normal stress $\sigma_{(1)}$ along junction (1) (see fig. 4(a)) is then given by

$$\sigma_{(1)} = E' \frac{du_1}{dz} \tag{53}$$

whence

$$\frac{\sigma_{(1)} e}{E' u_0} = \tilde{A}_1 \frac{Uf_{sc} - Vf_{cs}}{s_U} + \tilde{A}_4 \frac{Uf_{cs} + Vf_{sc}}{s_U} + \tilde{A}_5 \frac{Xf_{sX}}{s_X} + \tilde{A}_7 \frac{Yf_{sY}}{s_Y} \tag{53a}$$

Similarly the longitudinal normal stress $\sigma_{(2)}$ along junction (2) is given in non-dimensional form by

$$\begin{aligned} \frac{\sigma_{(2)}^e}{E' u_0} = & (\tilde{A}_1 P^B + \tilde{A}_4 Q^B) \frac{U f_{sc} - V f_{cs}}{s_U} + (\tilde{A}_4 P^B - \tilde{A}_1 Q^B) \frac{U f_{cs} + V f_{sc}}{s_U} \\ & + \tilde{A}_5 \frac{S^B_X f_{sX}}{s_X} + \tilde{A}_7 \frac{T^B_Y f_{sY}}{s_Y} \end{aligned} \quad (53b)$$

The middle-surface shear stresses in the plate elements making up the corrugation can be obtained with the aid of table 2. These stresses are denoted by τ_{01} , τ_{12} , and τ_{23} for the plate elements 01, 12, and 23 respectively, and the following non-dimensional measures are obtained for them:

$$\frac{\tau_{01}^e}{G u_0} = \zeta_1 - 1 + \tilde{A}_1 \frac{f_{cc}}{s_U} + \tilde{A}_4 \frac{f_{ss}}{s_U} + \tilde{A}_5 \frac{f_{cX}}{s_X} + \tilde{A}_7 \frac{f_{cY}}{s_Y} \quad (54a)$$

$$\begin{aligned} \frac{\tau_{12}^e}{G u_0} = & \frac{e}{k} [\zeta_2 - \zeta_1 + [\tilde{A}_1 (P^B - 1) + \tilde{A}_4 Q^B] \frac{f_{cc}}{s_U} \\ & + [\tilde{A}_4 (P^B - 1) - \tilde{A}_1 Q^B] \frac{f_{ss}}{s_U} \\ & + \tilde{A}_5 (S^B - 1) \frac{f_{cX}}{s_X} + \tilde{A}_7 (T^B - 1) \frac{f_{cY}}{s_Y}] + \tilde{V}_1' \sin \theta \end{aligned} \quad (54b)$$

$$\begin{aligned} \frac{\tau_{23}^e}{G u_0} = & -2 \frac{e}{f} \left[\zeta_2 + (\tilde{A}_1 P^B + \tilde{A}_4 Q^B) \frac{f_{cc}}{s_U} + (\tilde{A}_4 P^B - \tilde{A}_1 Q^B) \frac{f_{ss}}{s_U} \right. \\ & \left. + \tilde{A}_5 S^B \frac{f_{cX}}{s_X} + \tilde{A}_7 T^B \frac{f_{cY}}{s_Y} \right] + \tilde{V}_1' \sin \theta \cos \theta + \tilde{V}_2' \sin \theta \end{aligned} \quad (54c)$$

The rates of twist of the plate elements are given in table 3. The extreme-fiber shearing stresses due to these rates of twist will be denoted by $\tau'_{01}, \tau'_{12}, \tau'_{23}$ for plate elements 01, 12 and 23 respectively. They can be obtained by multiplying the corresponding rate of twist in table 3 by $G't$ (ref. 5). The resulting expressions are

$$\frac{\tau'_{01}e}{G'u_0} = \frac{t}{e} \tilde{v}_1' \quad (55a)$$

$$\frac{\tau'_{12}e}{G'u_0} = -\frac{t}{k}(\tilde{v}_2' + \tilde{v}_1' \cos \theta) \quad (55b)$$

$$\frac{\tau'_{23}e}{G'u_0} = -2 \frac{t}{f}(\tilde{v}_1' \sin^2 \theta - \tilde{v}_2' \cos \theta) \quad (55c)$$

The bending moments and stresses associated with frame-like deformations of the cross sections are now considered. At a given cross section these bending moments vary linearly between junction points, in consequence of the assumptions made at the outset, and therefore only the bending moments at the junctions need be evaluated. Referring to figure 8, the bending moments of interest are seen to be M_{01}, M_{12} and M_{23} at junctions 0, 1 and 2 respectively. These bending moments are given by equations (A1), with θ_1 and θ_2 defined by equations (A7) and $\Delta_1, \Delta_2, \Delta_3$ defined in table A1. Multiplying the bending moments by $6/t^2$, one obtains the corresponding extreme-fiber bending stresses, which will be denoted by $\sigma'_{(0)}, \sigma'_{(1)}$ and $\sigma'_{(2)}$ respectively and will be positive for compression in the upper fibers. The resulting equations for these stresses, in dimensionless form, are

$$\begin{bmatrix} \frac{\sigma'_{(0)}e}{Eu_0} \\ \frac{\sigma'_{(1)}e}{Eu_0} \\ \frac{\sigma'_{(2)}e}{Eu_0} \end{bmatrix} = \left(\frac{1}{1 - \nu^2} \right) \frac{t}{e} \begin{bmatrix} g_{11} & g_{12} \\ g_{21} & g_{22} \\ g_{31} & g_{32} \end{bmatrix} \begin{bmatrix} v_1/u_0 \\ v_2/u_0 \end{bmatrix} \quad (56)$$

where v_1/u_0 and v_2/u_0 are given by equations (33) and (34), and the g_{ij} matrix elements are defined as follows:

$$\begin{aligned}
g_{11} &= \frac{\alpha}{\beta} (a_1 - a_2 \frac{e}{k} \cos \theta - 2a_3 \frac{e}{f} \sin^2 \theta) + 3\alpha \\
g_{12} &= \frac{\alpha}{\beta} (-a_2 \frac{e}{k} + 2a_3 \frac{e}{f} \cos \theta) \\
g_{21} &= \frac{1}{\beta} \frac{e}{k} [2a_1 + b_1 - (2a_2 + b_2) \frac{e}{k} \cos \theta - (4a_3 + 2b_3) \frac{e}{f} \sin^2 \theta] \\
&\quad - 3(\frac{e}{k})^2 \cos \theta \\
g_{22} &= \frac{1}{\beta} \frac{e}{k} [-(2a_2 + b_2) \frac{e}{k} + (4a_3 + 2b_3) \frac{e}{f} \cos \theta] - 3(\frac{e}{k})^2 \\
g_{31} &= \frac{3}{\beta} \frac{e}{f} (b_1 - b_2 \frac{e}{k} \cos \theta - 2b_3 \frac{e}{f} \sin^2 \theta) - 6(\frac{e}{f})^2 \sin^2 \theta \\
g_{32} &= \frac{3}{\beta} \frac{e}{f} (-b_2 \frac{e}{k} + 2b_3 \frac{e}{f} \cos \theta) + 6(\frac{e}{f})^2 \cos \theta
\end{aligned} \tag{57}$$

with

$$\begin{aligned}
a_1 &\equiv -6(1 + \alpha) (2 \frac{e}{k} + 3 \frac{e}{f}) \\
a_2 &\equiv -12 \frac{e}{k} (\frac{e}{k} + 3 \frac{e}{f}) \\
a_3 &\equiv 12 \frac{e}{k} \frac{e}{f} \\
b_1 &\equiv 6(1 + \alpha) \frac{e}{k} \\
b_2 &\equiv -6 \frac{e}{k} (2 \frac{e}{k} + 3 + \alpha) \\
b_3 &\equiv -6 \frac{e}{f} (4 \frac{e}{k} + 3 + \alpha)
\end{aligned} \tag{58}$$

Special cases. - The above results apply to the general case in which none of the dimensions e , f and k is zero (fig. 10a). Two special cases are of interest because they represent limiting geometries obtainable or nearly obtainable in practice. These are the cases $f = 0$ and $e = 0$ shown in figures 10b and 10c.

The analyses for these two cases are contained in appendixes D and E respectively, and only the main results of these analyses will be cited here. In appendixes D and E only the end conditions of figure 3(a) are considered. With e or f approaching zero, the end conditions of figure 3(b) are equivalent to continuous attachment since the deformation of the end cross section in its own plane is then completely suppressed. Similarly with f approaching zero, the end conditions of figure 3(d) are also

equivalent to continuous attachment. With e approaching zero, the end conditions of figure 3(d) are equivalent to those of figure 3(a).

The case $f = 0$ leads to a fourth degree (rather than an eighth degree) characteristic equation, (D21), whose four roots (all real) have the form (D25). The numerical evaluation of these roots can be done exactly by means of the quadratic formula or approximately by means of the series expansions (D26). With the roots known, equations (D31) give the values of certain constants $\tilde{\gamma}_1$ and $\tilde{\gamma}_3$. Equations (D33), with \bar{A}_1 , \bar{A}_3 defined by (D34), then give the displacements $u_1(z)$ and $v_2(z)$. Equation (D37) is the basic form of the result for shear stiffness, and equations (D40) through (D44) give the stresses.

For the case $e = 0$ the characteristic equation, (E16), is also of fourth degree with real roots in the form (E20) having series expansions (E21). A knowledge of the roots permits certain quantities $\hat{\gamma}_1$ and $\hat{\gamma}_3$ to be evaluated (eq. (E24)). Then the displacements $u_2(z)$ and $v_2(z)$ can be obtained from equation (E25) with A_1^* and A_3^* defined by (E26). Equation (E28) gives the basic shearing stiffness result, and equations (E33) through (E38) give the stresses.

NUMERICAL RESULTS AND DISCUSSION

The foregoing analysis was used to obtain numerical results on shear stiffness, stresses and deformations for selected geometries and end-attachment conditions. Poisson's ratio ν was taken as 0.3, G was taken as $E/[2(1 + \nu)]$, and no distinction was made between E and E' or G and G' , except for a special numerical investigation of the effect of torsional stiffness, in which G' was set equal to zero.

For the numerical studies, only the case of trough lines free to rotate ($\alpha = 0$) was considered, and the cross sections were limited to the case $f = 2e$, that is equal width for the trough and crest plate elements. In varying the cross sections h/p and f/p were taken as independent parameters and assigned the following values:

$$h/p = .2, .4$$

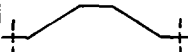
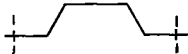




$$f/p = .2, .4, .5$$

Table 4 shows for each combination of h/p and f/p the resulting values of θ , k/p , k/f , and p'/p (ratio of developed width to projected width), and a diagram of the cross section.

Shear stiffness. - Figures 11 through 13 give the basic numerical results for shear stiffness. The results are given in terms of the relative shear stiffness parameter Ω , defined as the ratio of the absolute shear stiffness $F/2u_0$ of the actual corrugation to that of an identical corrugation with continuous end attachment producing a state of uniform shear (eq. (39)). To convert the relative shear stiffness Ω into absolute shear stiffness $F/2u_0$, it is only necessary to multiply Ω by $Gt_b/(e + k + 1/2 f)$, in accordance with equation (39). That is,

TABLE 4

CROSS-SECTIONAL GEOMETRIES CONSIDERED IN CALCULATIONS

$\frac{h}{p}$	$\frac{f}{p} = \frac{2e}{p}$	θ (degrees)	$\frac{k}{p}$	$\frac{k}{f}$	$\frac{p'}{p}$	Diagram
.2	.2	33.7	.361	1.85	1.121	
	.4	63.5	.224	.56	1.247	
	.5	90	.200	.400	1.400	
.4	.2	53.1	.500	2.50	1.400	
	.4	76	.412	1.03	1.625	
	.5	90	.400	.800	1.800	

$$\frac{F}{2u_0} = \frac{Gtb}{e + k + \frac{1}{2}f} \Omega = \frac{Gt \cdot 2b}{p'} \Omega \quad (59)$$

In these figures Ω is given as a function of bt/p^2 for selected values of h/p and f/p ($= 2e/p$) and two values of t/p . Figure 11 is for the case of point attachment at the ends of the trough lines only (fig. 3(a)), figure 12 for the case of point attachment at the ends of both the crest lines and the trough lines (fig. 3(b)), and figure 13 for the case of wide attachments at the ends of the trough lines only (fig. 3(d)).

Figures 14, 15 and 16 present the same data as figures 11, 12 and 13, but re-plotted on log-log scales in order to show more clearly the relationship between Ω and bt/p^2 in the region of very low Ω and very high Ω . Each curve has a kink at $\Omega = .5$. To the left of this kink the curve gives Ω as a function of bt/p^2 ; to the right of the kink it gives $1 - \Omega$ as a function of bt/p^2 .

By comparing the dotted and solid curves in each figure, it is seen that Ω is mainly a function of bt/p^2 , i.e. relatively insensitive to t/p , with the maximum sensitivity occurring for the case of wide attachments at the ends of the trough lines. The fact that Ω is mainly a function of bt/p^2 means that the length ($2b$) and the thickness (t) have approximately equivalent effects in altering the shear stiffness. More precisely, it can be said that a given percentage change in t or the same percentage change in b will produce approximately equal relative changes in the shear stiffness. Observing that the product bt also appears explicitly in the right side of equation (59), it can also be said that the percentage change in the absolute shear stiffness ($F/2u_0$) will be greater than the percentage change in the relative shear stiffness (Ω).

Comparison of figures 11 and 12 (or 14 and 15) shows that, except in the region of very low Ω , there is negligible increase of stiffness by having point attachments at the ends of the crest lines in addition to point attachments at the ends of the trough lines. However, comparison of figures 11 and 13 (or 14 and 16) shows that an appreciable increase of shear stiffness is obtained by changing from point attachments to wide attachments at the ends of the trough lines. This increase is also an upper limit to the increase that can be expected as a result of interference, like that shown in figure 5, between the troughs and the end member to which they are attached.

As is to be expected, figures 11 to 13 (or 14 to 16) show that an increase of h or f will lead to a reduction of the relative shear stiffness Ω . Since increasing h or f also increases the developed width p' , equation (59) shows that the absolute shear stiffness $F/2u_0$ will experience an even greater reduction, percentage-wise, than the relative shear stiffness Ω .

Displacements and stresses. - Detailed displacement and stress patterns along the length of the corrugation were computed only for one type of end attachment, namely point attachments at the ends of the trough lines (fig. 3(a)). Table 5 shows the geometries considered, as defined by h/p , f/p , bt/p^2 and t/p . As a matter of interest, the length-pitch ratio $2b/p$ and the relative shear stiffness Ω of each geometry are also given. The last column of table 5 tells the figure in which the results are plotted.

TABLE 5. - GEOMETRIES CONSIDERED FOR DISPLACEMENT AND STRESS CALCULATIONS

h/p	f/p	bt/p^2	t/p	$2b/p$	Ω	Figure
.2	.2	.02	.005	8	.2155	17(a)
			.02	2	.2201	17(b)
		.2	.005	80	.8928	17(c)
			.02	20	.8933	17(d)
.4	.4	.02	.005	8	.0194	17(e)
			.02	2	.0211	17(f)
		.2	.005	80	.5954	17(g)
			.02	20	.5960	17(h)

The displacements selected for plotting, and shown as functions of z/b in the lower parts of the figures, are the longitudinal displacements u_1 and u_2 along junctions ① and ② (see fig. 4(b)) and the amplitudes v_1 and v_2 of the lateral displacement modes of the cross section (see fig. 4(c)). These displacements are given through the dimensionless parameters u_1/u_0 , u_2/u_0 , v_1/u_0 and v_2/u_0 .

It is seen from these figures that for the smaller length-to-pitch ratios (8 and 2), the longitudinal displacements u_1 and u_2 are approximately constant along the length and the lateral displacements v_1 and v_2 are very nearly linear in z . However it is seen that this behavior does not hold true for the larger length-to-pitch ratios (80 and 20). For those, u_1 and u_2 may be approximately constant in the central region but vary sharply near the ends, as in figures 17(c) and (d), or they may vary markedly over the entire length as in figures 17(g) and (h). These same figures show that v_1 and v_2 may be noticeably non-linear in z , sometimes being very small in a central region and very large near the ends as in figures 17(c) and (d).

It has been the custom in previous analyses of the shearing of corrugated plates with discrete end attachments to assume inextensional deformation for the middle surface of the sheet. This leads to the straight-line generators of the corrugation remaining straight lines, and as a result the longitudinal displacements become independent of z while the lateral displacements vary linearly with z . The present results suggest that this assumption can sometimes seriously misrepresent the actual displacement patterns.

Comparing any set of curves for $t/p = .005$ with the corresponding set of curves for $t/p = .02$, one is led to the following simple conclusion regarding the dependence of v_1/u_0 and v_2/u_0 on t/p : All other things (h/p , f/p , bt/p^2) remaining constant, v_1/u_0 and v_2/u_0 vary inversely as t/p . It should be kept in mind, of course, that bt/p^2 remaining constant implies that b/p must vary inversely with t/p as t/p changes.

The stresses which are plotted in the upper parts of the figures are: the mid-plane shearing stresses τ_{01} , τ_{12} and τ_{23} in the plate elements 01, 12 and 23 respectively; the extreme-fiber transverse bending stresses $\sigma_{(1)}$ and $\sigma_{(2)}$ at junctions (1) and (2) respectively; the extreme-fiber shearing stresses τ'_{01} , τ'_{12} and τ'_{23} , due to torsion only, in the plate elements 01, 12 and 23 respectively; and the longitudinal normal stresses $\sigma_{(1)}$ and $\sigma_{(2)}$ at junctions (1) and (2) respectively.

The stresses $\sigma_{(1)}$ and $\sigma_{(2)}$ are positive for tension. The sign conventions for τ_{01} , τ'_{01} and $\sigma_{(1)}$ are shown in figure 18, and the sign conventions for the corresponding stresses in the other plate elements are analogous to those shown in figure 18.

The stresses in figure 17 are given through the dimensionless parameters $\tau_{01}p/Eu_0$, etc. These are best suited to the situation in which one wishes to determine the stresses resulting from a prescribed relative shearing displacement $2u_0$. If one wishes instead to determine the stresses resulting from a prescribed shearing force F it would be more convenient to have the stresses given via the dimensionless parameters

$$\frac{\tau_{01}}{\left(\frac{F}{2bt}\right)}, \quad \frac{\tau_{02}}{\left(\frac{F}{2bt}\right)}, \quad \text{etc.}$$

which represent the ratio of the stress in question to the average applied shearing stress. Equation (59) can be used to effect the conversion from one dimensionless stress parameter to the other, as in the following typical example:

$$\frac{\tau_{01}}{\left(\frac{F}{2bt}\right)} = \frac{\tau_{01}}{\left(\frac{2u_0 G \Omega}{p'}\right)} = \left(\frac{\tau_{01} p}{Eu_0}\right) \cdot \left(\frac{E}{2G} \frac{p'}{p} \frac{1}{\Omega}\right) \quad (60)$$

This shows that to convert any numerical value of $\tau_{01}p/Eu_0$ into a corresponding numerical value of $\tau_{01}/(F/2bt)$ it is only necessary to multiply the former by the factor

$$\frac{E}{2G} \frac{p'}{p} \frac{1}{\Omega}$$

The conversion equation (60) applies with τ_{01} replaced by any of the other stresses.

Turning now to the stresses themselves and examining their magnitudes, it is seen that in all the cases investigated the predominant stress is the end value of the extreme-fiber stress σ_1' due to frame bending of the cross sections. The next largest stresses are the middle ($z = 0$) values of the middle-surface shear stresses τ_{01} , τ_{12} and τ_{23} , except in the case of the very short corrugations (figs. 17(b), (e), (f)), when the torsional shear stresses at $z = b$ may be higher than the middle-surface shear stresses at $z = 0$. In these exceptional cases, however, both shear stress maximums are much smaller than the maximum magnitude of σ_1' . The maximum value of σ_2' is generally much smaller than the maximum σ_1' .

In all cases the longitudinal normal stresses σ_1 and σ_2 are seen to be of negligible magnitude compared to the maximum value of the transverse bending stress σ_1' . This suggests that the assumption of inextensibility of the generators (rather than inextensionality of the entire middle surface) may be a legitimate simplifying assumption for purposes of analysis.

Examining the variation of the stresses across the corrugation, it is seen that the middle-surface shear stresses τ_{01} , τ_{12} and τ_{23} are only slightly different from each other (except near the ends), while the other kinds of stresses do show significant variation across the corrugation.

The variation of the significant stresses along the length of the corrugation seems to correlate with the nature of $v_1(z)$ and $v_2(z)$. When these lateral displacement components are nearly linear in z (as in figs. 17(a), (b), (e), (f)), the frame bending stresses σ_1' and σ_2' are also nearly linear in z , and the middle-surface shearing stresses τ_{01} , τ_{12} , τ_{23} are approximately parabolic in z . When $v_1(z)$ and $v_2(z)$ are small in the central region and large near the ends (as in figs. 17(c) and (d)), the frame bending stresses exhibit a similar behavior, and the middle-surface shearing stresses are nearly constant along the central region, dipping towards zero near the ends.

Comparing any set of curves for $t/p = .005$ with the corresponding set of curves for $t/p = .02$, one can investigate the effect of t/p on the major stresses, i.e. on the mid-plane shear stress τ_{23} , the torsional shear stress τ_{01} and the frame bending stress σ_1' . The following behavior is apparent: All other things (h/p , f/p , bt/p^2) remaining constant, τ_{23} and σ_1' remain virtually unchanged as t/p varies, while τ_{01} varies directly with t/p . (As noted previously, however, b/p must vary inversely as t/p if bt/p^2 is to remain constant.)

Effect of torsional stiffness. - In the analysis it was assumed that the strain energy of torsion of the plate elements would account for only a small portion of the total, and that therefore this strain energy could be computed approximately by assuming a constant rate of twist across the width of each plate element, this constant rate of twist being based on the lateral displacements of the edges of the plate element.

The smallness of the computed values of the extreme-fiber shear stress due to torsion compared to the extreme-fiber normal stress due to frame bending tends to confirm this assumption, or at least is consistent with it. Only in the case of the very shortest corrugations ($2b/p = 2$) does the largest torsional stress τ_{01} , start to look significant compared to the larger frame bending stress σ_1 .

The unimportance of the torsional stiffness is demonstrated further by figure 19 which, for four selected cross-sectional geometries, compares the Ω versus bt/p^2 relationship obtained by neglecting torsional strain energy ($G' = 0$) with that obtained by considering it ($G' = G$). In figure 19(a) the curves for $G' = 0$ and $G' = G$ are indistinguishable from each other; in figure 19(b) they are only slightly distinguishable from each other at their lower ends.

In figures 17(d) and 17(e) the dotted curves show the effect on the stresses and displacements resulting from complete neglect of the torsional strain energy in the derivation of the differential equations. It is seen that there is no noticeable effect on the major stresses and displacements and only a small effect on the others.

Effect of frame flexural stiffness. - In the analysis it was pointed out that there is bound to be some ambiguity in defining an appropriate value for the frame flexural stiffness D , and two possible values were mentioned: the beam flexural stiffness $Et^3/12$ and the plate flexural stiffness $Et^3/[12(1 - \nu^2)]$ (eqs. (16a) and (16b)).

The calculated results thus far presented are based on the latter value of D . In order to determine the possible effect that the uncertainty in D might have on the overall shearing stiffness, some computations of Ω were also made using the former value. The results are also shown in figure 19, where the curves now to be compared are the solid and the dot-dash curves. It is seen that the change in Ω due to using one value of D instead of the other is negligible. The effect on the frame bending stresses can of course be expected to be more significant, amounting to perhaps ten percent when $\nu = .3$. For reasons discussed in the analysis section, it is felt that the value of D used in the analysis (eq. (16b)) is the most appropriate one.

COMPARISON WITH EXPERIMENT

Bryan and Jackson in reference 2 give experimental data on shearing force versus shearing deformation for a single corrugation. The geometry of the test specimen and the experimental results are shown in figure 20. The Young's modulus and Poisson's ratio of the material are given as 10^7 psi and 0.25 respectively in reference 2.

The solid lines in figure 20 show the results computed for this geometry from the present theory, using four different assumptions regarding the restraint conditions along the sides and ends. Considering the thinness of the sheet, the smallness of e , and the probable size of the bolt heads used in the attachments, it is felt that the uppermost theoretical solid line is the most appropriate one to use for comparison with the experimental results. From figure 20 it appears that this line agrees fairly well with the initial slope of the experimental curve.

Since the present theory is a linear one, no comparison except with the initial slope is valid. Figure 20 does point up, however, the non-linear behavior possible with extremely flexible corrugations like the one tested. (This non-linearity is probably due to the membrane action associated with large twisting of the plate elements, as suggested in reference 2.)

It should be noted that the bt/p^2 parameter for this specimen has the following value:

$$\frac{bt}{p^2} = \frac{(6.25)(.0057)}{(5.00)^2} = .001425$$

which is probably outside the range of most practical applications and below the smallest value (.005) considered in the bulk of the present calculations. For larger values of bt/p^2 , i.e. geometries of larger relative stiffness, the behavior should be more nearly linear.

CONCLUDING REMARKS

A theoretical analysis has been presented of the shearing of a trapezoidally corrugated plate with discontinuous attachments at the ends of the corrugations and with the trough lines constrained to remain straight. The last condition means that the analysis is applicable primarily to the case in which the corrugated plate is attached a flat plate or some other structure along its trough lines to prevent these lines from curving in the plane of the plate, and it will over-estimate somewhat the shearing stiffness of a corrugated plate without such constraint. By adding one degree of freedom to the displacements in the plane of the cross section, the analysis can be extended to the case in which the trough lines are permitted to curve in the plane of the plate, and it will then be more precisely applicable to the case of a corrugated plate alone.

The present analysis is considered to be more accurate than previous shearing analyses of corrugated plates (e.g., ref.2) in the following two respects: (a) it permits more degrees of freedom for displacements in the plane of the cross section, and (b) it does not assume that the straight line generators of the corrugation remain straight lines. It should be noted that the presence of the last assumption in an analysis prevents that analysis from distinguishing between the case of trough lines held straight and trough lines permitted to curve.

Numerical results on over-all shearing stiffness, stresses and displacements have been presented for selected geometries for the case of no external rotational restraint along the trough lines. The results for shearing stiffness are for three kinds of attachment at the ends of the corrugations: (a) point attachments at the ends of the trough lines only, (b) point attachments at the ends of both the crest lines and the trough lines, and (c) wide attachments at the ends of the trough lines only. The stress and displacement numerical results are only for type (a) end attachments.

From a study of the numerical results it is evident that $2bt/p^2$ (length times thickness divided by the square of the pitch) is a very significant parameter. The relative shearing stiffness (i.e. the ratio of the actual shearing stiffness to that corresponding to uniform shear) is primarily a function of this parameter and only secondarily a function of t/p (thickness divided by pitch). And the major stresses and displacements vary in a simple way with t/p if $2bt/p^2$ is kept constant.

For the range of geometries studied numerically the following main features were observed for the stresses in the case of no external rotational restraint along the trough lines and type (a) end attachments: The largest stress in each case was the transverse extreme-fiber bending stress associated with frame-like bending of the end cross sections. The next largest stress was a middle-surface shear stress at the middle cross section, except in the case of the very short corrugations, for which case an extreme-fiber torsional shear stress could exceed the middle-surface shear stress. In that case, however, both shear stresses were small compared to the maximum frame bending stress. In all cases the longitudinal normal stresses were negligibly small compared to the other stresses.

This last result suggests that in future work it may sometimes be possible to simplify the analyses by assuming that the straight-line generators of the corrugation are inextensible.

The numerical studies of over-all shearing stiffness showed that the discontinuous nature of the end attachments can reduce the stiffness to a value considerably below that corresponding to uniform shear, sometimes (in the case of very short or very thin corrugations) to a minute fraction of that value.

Very little increase in stiffness was obtained in going from type (a) to type (b) attachment -- i.e., by adding point attachments at the ends of the crest lines to point attachments at the ends of the trough lines. However a considerable increase in stiffness was obtained by going from type (a) to type (c) attachments -- i.e., changing from point attachments to wide attachments at the ends of the trough lines.

This suggests that considerable increase in stiffness, in the case of point attachments at the ends of the trough lines only, can also arise from interference between the end of the deforming corrugation and the member to which the attachment is made. (The importance of this interference was noted in ref. 7.) This kind of interference, being one-sided, destroys the anti-symmetry of the deformation pattern that would otherwise exist. It can be taken into account in the analysis by adding two more degrees of freedom to the displacements in the plane of the cross section and three to the longitudinal displacements. Additional complexity due to these additional degrees of freedom can be minimized through judicious use of the method of superposition.

We close with the following perhaps obvious practical observation: If, for a given geometry, the objective is to maximize over-all shearing stiffness and minimize frame bending stresses (which, as noted above, can be the largest), this can be achieved by designing the end attachments so

as to reduce as much as possible the frame-like bending of the end cross sections. For the trapezoidal corrugation, this can be accomplished by having, for example, attachments at the ends of both the trough lines and the crest lines, with at least one of these sets of attachments being the full width of the trough or crest. It can also be accomplished with only point attachments at the ends of the crest lines and the trough lines provided that there is interference with fairly rigid members at both these places. The frame bending of the end cross sections can of course also be suppressed by specially machined end fittings or by continuous-weld end attachments.

APPENDIX A

STRAIN ENERGY OF FRAME BENDING

A unit length of corrugation will herein be analyzed as a frame whose joint displacements are made up of the two components shown in figure 4(c). The slope-deflection method will first be used to determine the frame bending moments in terms of v_1 , v_2 and the unknown rotation θ_1 of joints 1 and 4 and θ_2 of joints 2 and 3. The rotations θ_1 and θ_2 are taken positive when clockwise as viewed from the positive end of the z-axis (see fig. 6). From these bending moments the strain energy of frame bending can be determined in terms of v_1 , v_2 , θ_1 , and θ_2 . Using the condition of moment equilibrium for the joints, one can evaluate θ_1 and θ_2 in terms of v_1 and v_2 and thus eliminate the joint rotations from the strain energy expression.

In order to carry out the analysis proposed above, the basic beam end-moment formulas shown in figure 7 will be helpful. In applying these formulas to each member of the frame, the appropriate θ quantities can be obtained from the joint rotations of figure 6, and the appropriate Δ can be computed from the v_1 and v_2 joint displacements shown in figure 4(c). The Δ expressions are tabulated below.

TABLE A1

Member	Δ		
01	v_1	\equiv	Δ_1
12	$-v_1 \cos \theta - v_2$	\equiv	Δ_2
23	$-2 v_1 \sin^2 \theta + 2 v_2 \cos \theta$	\equiv	Δ_3

Using figure 7, the notation Δ_1 , Δ_2 , Δ_3 defined in Table A1, and the notation shown in figure 8, one can write the following expressions for the frame-element end moments per unit width of frame (i.e., per unit length of corrugation):

$$\begin{aligned}
M_{01} &= \alpha \cdot \left(\frac{2D}{e} \theta_1 + \frac{6D}{e} \frac{\Delta_1}{e} \right) \\
M_{10} &= \frac{(3+\alpha)D}{e} \theta_1 + \frac{3(1+\alpha)D}{e} \frac{\Delta_1}{e} \\
M_{12} &= \frac{4D}{k} \theta_1 + \frac{2D}{k} \theta_2 + \frac{6D}{k} \frac{\Delta_2}{k} \\
M_{21} &= \frac{2D}{k} \theta_1 + \frac{4D}{k} \theta_2 + \frac{6D}{k} \frac{\Delta_2}{k} \\
M_{23} &= \frac{6D}{f} \theta_2 + \frac{6D}{f} \frac{\Delta_3}{f}
\end{aligned} \tag{A1}$$

where α is defined as zero if joints 0 and 5 are hinged, or unity if these joints are clamped, and D is the flexural stiffness per unit width of frame (i.e., per unit length of corrugation).

The bending moments vary linearly between joints in a frame with imposed displacements and rotations at the joints. Thus the bending moments per unit width of frame are given by the following expressions, in which bending moment which puts compression in the upper fibers is considered positive:

$$\begin{aligned}
M &= M_{01} + \frac{s_1}{e} (-M_{10} - M_{01}) && \text{for member 01} \\
M &= M_{12} + \frac{s_2}{k} (-M_{21} - M_{12}) && \text{for member 12} \\
M &= M_{23} \left(1 - \frac{2s_3}{f} \right) && \text{for member 23}
\end{aligned} \tag{A2}$$

The strain energy per unit width of frame (unit length of corrugation) can be obtained by integrating $M^2/(2D)$ along the entire profile of the corrugation. Thus the strain energy of frame bending is

$$\begin{aligned}
U_b &\equiv \frac{1}{2D} \left[2 \cdot \int_0^e \left[M_{01} + \frac{s_1}{e} (-M_{10} - M_{01}) \right]^2 ds_1 \right. \\
&\quad \left. + 2 \cdot \int_0^k \left[M_{12} + \frac{s_2}{k} (-M_{21} - M_{12}) \right]^2 ds_2 + \int_0^f \left[M_{23} \left(1 - \frac{2s_3}{f} \right) \right]^2 ds_3 \right]
\end{aligned}$$

or

$$U_b = \frac{e}{3D} (M_{01}^2 - M_{01} M_{10} + M_{10}^2) + \frac{k}{3D} (M_{12}^2 - M_{12} M_{21} + M_{21}^2) + \frac{f}{6D} (M_{23}^2) \quad (A3)$$

With the joint moments eliminated through equations (A1),

$$\begin{aligned} U_b = & \theta_1^2 \frac{D}{e} (\alpha^2 + 3) + \theta_1 \frac{\Delta_1}{e} \frac{6D}{e} (\alpha^2 + 1) + \left(\frac{\Delta_1}{e}\right)^2 \frac{3D}{e} (3\alpha^2 + 1) \\ & + 4 \frac{D}{k} (\theta_1^2 + \theta_1 \theta_2 + \theta_2^2) + \frac{12D}{k} \left[\theta_1 \frac{\Delta_2}{k} + \theta_2 \frac{\Delta_2}{k} + \left(\frac{\Delta_2}{k}\right)^2 \right] \\ & + 6 \frac{D}{f} \left[\theta_2^2 + 2\theta_2 \frac{\Delta_3}{f} + \left(\frac{\Delta_3}{f}\right)^2 \right] \end{aligned} \quad (A4)$$

This equation expresses the strain energy of frame bending in terms of the joint rotations θ_1 and θ_2 and the quantities Δ_1 , Δ_2 , Δ_3 , the latter being functions of v_1 and v_2 defined in table A1. The rotations can be eliminated from this expression by means of the moment-equilibrium conditions for the joints, namely

$$M_{10} + M_{12} = 0 \quad \text{and} \quad M_{21} + M_{23} = 0. \quad (A5)$$

By virtue of equations (A1) these conditions become

$$\begin{bmatrix} \frac{(3+\alpha)D}{e} + \frac{4D}{k} & \frac{2D}{k} \\ \frac{2D}{k} & \frac{4D}{k} + \frac{6D}{f} \end{bmatrix} \begin{bmatrix} \theta_1 \\ \theta_2 \end{bmatrix} = \begin{bmatrix} -\frac{3(1+\alpha)D}{e} \frac{\Delta_1}{e} - \frac{6D}{k} \frac{\Delta_2}{k} \\ -\frac{6D}{k} \frac{\Delta_2}{k} - \frac{6D}{f} \frac{\Delta_3}{f} \end{bmatrix} \quad (A6)$$

The solution of these equations is

$$\begin{aligned} \theta_1 &= \frac{1}{\beta} \left[-6(1+\alpha) \left(2 \frac{e}{k} + 3 \frac{e}{f} \right) \left(\frac{\Delta_1}{e} \right) - 12 \frac{e}{k} \left(\frac{e}{k} + 3 \frac{e}{f} \right) \left(\frac{\Delta_2}{k} \right) + 12 \frac{e}{k} \frac{e}{f} \left(\frac{\Delta_3}{f} \right) \right] \\ \theta_2 &= \frac{1}{\beta} \left[6(1+\alpha) \frac{e}{k} \left(\frac{\Delta_1}{e} \right) - 6 \frac{e}{k} \left(2 \frac{e}{k} + 3+\alpha \right) \left(\frac{\Delta_2}{k} \right) - 6 \frac{e}{f} \left(4 \frac{e}{k} + 3+\alpha \right) \left(\frac{\Delta_3}{f} \right) \right] \end{aligned} \quad (A7)$$

where

$$\beta \equiv 4(3+\alpha) \frac{e}{k} + 12 \left(\frac{e}{k}\right)^2 + 6(3+\alpha) \frac{e}{f} + 24 \frac{e}{k} \frac{e}{f} \quad (A8)$$

With equations (A7) used to eliminate the rotations in (A4), the latter becomes

$$\beta \frac{2e}{D} U_b = A_{11} \left(\frac{\Delta_1}{e}\right)^2 + A_{22} \left(\frac{\Delta_2}{k}\right)^2 + A_{33} \left(\frac{\Delta_3}{f}\right)^2 + A_{12} \frac{\Delta_1}{e} \frac{\Delta_2}{k} + A_{23} \frac{\Delta_2}{k} \frac{\Delta_3}{f} + A_{13} \frac{\Delta_1}{e} \frac{\Delta_3}{f} \quad (A9)$$

where

$$\begin{aligned} A_{11} = & 192 \alpha^2 \left(2 \frac{e}{k} + 3 \frac{e}{f}\right)^2 + 72(15\alpha^2 + 2\alpha + 3) \left[\frac{e}{k} \left(\frac{e}{k} + 2 \frac{e}{f}\right)\right] \left(2 \frac{e}{k} + 3 \frac{e}{f}\right) \\ & + 432(3\alpha^2 + 1) \left[\left(\frac{e}{k}\right) \left(\frac{e}{k} + 2 \frac{e}{f}\right)\right]^2 \end{aligned} \quad (A10a)$$

$$\begin{aligned} A_{22} = & 24(\alpha + 3) \frac{e}{k} \left(\frac{e}{k} + 6 \frac{e}{f}\right) \left(2 \frac{e}{k} + 3 \frac{e}{f}\right) \\ & + 144 \left(\frac{e}{k}\right)^2 \left[(\alpha^2 + 3) \left(\frac{e}{k}\right)^2 + 2(3\alpha^2 + 2\alpha + 15) \frac{e}{k} \frac{e}{f} + 3(3\alpha^2 + 2\alpha + 15) \left(\frac{e}{f}\right)^2\right] \\ & + 864 \left(\frac{e}{k}\right)^3 \frac{e}{f} \left(\frac{e}{k} + 2 \frac{e}{f}\right) \end{aligned} \quad (A10b)$$

$$\begin{aligned} A_{33} = & 48(\alpha + 3) \frac{e}{k} \frac{e}{f} \left(2 \frac{e}{k} + 3 \frac{e}{f}\right) \\ & + 144 \left(\frac{e}{k}\right)^2 \frac{e}{f} \left[4(\alpha + 3) \frac{e}{k} + (\alpha^2 + 6\alpha + 21) \frac{e}{f}\right] \\ & + 864 \left(\frac{e}{k}\right)^3 \frac{e}{f} \left(\frac{e}{k} + 2 \frac{e}{f}\right) \end{aligned} \quad (A10c)$$

$$\begin{aligned} A_{12} = & -144(3\alpha^2 + 2\alpha + 3) \frac{e}{k} \left(\frac{e}{k} + 3 \frac{e}{f}\right) \left(2 \frac{e}{k} + 3 \frac{e}{f}\right) \\ & - 864(\alpha^2 + 1) \left(\frac{e}{k}\right)^2 \left(\frac{e}{k} + 3 \frac{e}{f}\right) \left(\frac{e}{k} + 2 \frac{e}{f}\right) \end{aligned} \quad (A10d)$$

$$A_{13} = 144(3\alpha^2 + 2\alpha + 3) \frac{e}{k} \frac{e}{f} \left(2 \frac{e}{k} + 3 \frac{e}{f}\right) + 864(\alpha^2 + 1) \left(\frac{e}{k}\right)^2 \frac{e}{f} \left(\frac{e}{k} + 2 \frac{e}{f}\right) \quad (A10e)$$

$$\begin{aligned}
A_{23} = & - 144(\alpha + 3)^2 \frac{e}{k} \frac{e}{f} (2 \frac{e}{k} + 3 \frac{e}{f}) \\
& - 288(\frac{e}{k})^2 \frac{e}{f} [(\alpha^2 + 4\alpha + 15) \frac{e}{k} + 3(\alpha^2 + 2\alpha + 9) \frac{e}{f}] \\
& - 1728(\frac{e}{k})^3 \frac{e}{f} (\frac{e}{k} + 2 \frac{e}{f})
\end{aligned} \tag{A10f}$$

(Inasmuch as α takes on only the values zero and one, the above equation and subsequent equations involving α could be simplified by replacing α^2 by α .)

Substituting for Δ_1 , Δ_2 and Δ_3 the expressions from table A1, one finally obtains U_b in terms of v_1 and v_2 :

$$U_b = a_{11} v_1^2 + 2a_{12} v_1 v_2 + a_{22} v_2^2 \tag{A11}$$

where

$$\begin{aligned}
a_{11} &= \frac{D}{\beta^2 e^3} [A_{11} + A_{22} (\frac{e}{k})^2 \cos^2 \theta + 4A_{33} (\frac{e}{f})^2 \sin^4 \theta - A_{12} \frac{e}{k} \cos \theta \\
&\quad + 2A_{23} \frac{e}{k} \frac{e}{f} \sin^2 \theta \cos \theta - 2A_{13} \frac{e}{f} \sin^2 \theta] \\
a_{12} &= \frac{D}{\beta^2 e^3} [A_{22} (\frac{e}{k})^2 \cos \theta - 4A_{33} (\frac{e}{f})^2 \sin^2 \theta \cos \theta - \frac{1}{2} A_{12} \frac{e}{k} \\
&\quad - A_{23} \frac{e}{k} \frac{e}{f} (\cos^2 \theta - \sin^2 \theta) + A_{13} \frac{e}{f} \cos \theta] \\
a_{22} &= \frac{D}{\beta^2 e^3} [A_{22} (\frac{e}{k})^2 + 4A_{33} (\frac{e}{f})^2 \cos^2 \theta - 2A_{23} \frac{e}{k} \frac{e}{f} \cos \theta]
\end{aligned} \tag{A12}$$

APPENDIX B

VARIATION OF THE TPE

Equation (18) in expanded form is

$$\begin{aligned}
 \text{TPE} = & \int_{-b}^b \left[b_{11} \left(\frac{du_1}{dz} \right)^2 + 2b_{12} \frac{du_1}{dz} \frac{du_2}{dz} + b_{22} \left(\frac{du_2}{dz} \right)^2 \right] dz \\
 & + \int_{-b}^b (c_{00} u_0^2 + c_{11} u_1^2 + c_{22} u_2^2 + 2c_{01} u_0 u_1 + 2c_{12} u_1 u_2) dz \\
 & + \int_{-b}^b (d_{11} u_1 \frac{dv_1}{dz} + d_{21} u_2 \frac{dv_1}{dz} + d_{22} u_2 \frac{dv_2}{dz}) dz \\
 & + \int_{-b}^b \left[e_{11} \left(\frac{dv_1}{dz} \right)^2 + e_{22} \left(\frac{dv_2}{dz} \right)^2 + 2e_{12} \frac{dv_1}{dz} \frac{dv_2}{dz} \right] dz \\
 & + \int_{-b}^b (a_{11} v_1^2 + 2a_{12} v_1 v_2 + a_{22} v_2^2) dz \\
 & - 2Fu_0
 \end{aligned} \tag{B1}$$

where

$$\begin{aligned}
 e_{11} & \equiv e_{11}^* + \bar{e}_{11} \\
 e_{22} & \equiv e_{22}^* + \bar{e}_{22} \\
 e_{12} & \equiv e_{12}^* + \bar{e}_{12}
 \end{aligned} \tag{B2}$$

The first variation of the TPE due to the variations δu_0 , $\delta u_1(z)$, $\delta u_2(z)$, $\delta v_1(z)$, $\delta v_2(z)$ is

$$\delta(\text{TPE}) = 2 \int_{-b}^b \left[b_{11} \frac{du_1}{dz} \frac{d(\delta u_1)}{dz} + b_{12} \left[\frac{du_1}{dz} \frac{d(\delta u_2)}{dz} + \frac{du_2}{dz} \frac{d(\delta u_1)}{dz} \right] + b_{22} \frac{du_2}{dz} \frac{d(\delta u_2)}{dz} \right] dz$$

(equation continued on next page)

$$\begin{aligned}
& + 2 \int_{-b}^b \left[c_{00} u_0 \delta u_0 + c_{11} u_1 \delta u_1 + c_{22} u_2 \delta u_2 + c_{01} (u_0 \delta u_1 + u_1 \delta u_0) + c_{12} (u_1 \delta u_2 + u_2 \delta u_1) \right] dz \\
& + \int_{-b}^b \left[d_{11} \left[u_1 \frac{d(\delta v_1)}{dz} + \frac{dv_1}{dz} \delta u_1 \right] + d_{21} \left[u_2 \frac{d(\delta v_1)}{dz} + \frac{dv_1}{dz} \delta u_2 \right] + d_{22} \left[u_2 \frac{d(\delta v_2)}{dz} + \frac{dv_2}{dz} \delta u_2 \right] \right] dz \\
& + 2 \int_{-b}^b \left[e_{11} \frac{dv_1}{dz} \frac{d(\delta v_1)}{dz} + e_{22} \frac{dv_2}{dz} \frac{d(\delta v_2)}{dz} + e_{12} \left[\frac{dv_1}{dz} \frac{d(\delta v_2)}{dz} + \frac{dv_2}{dz} \frac{d(\delta v_1)}{dz} \right] \right] dz \\
& + 2 \int_{-b}^b \left[a_{11} v_1 \delta v_1 + a_{12} (v_1 \delta v_2 + v_2 \delta v_1) + a_{22} v_2 \delta v_2 \right] dz \\
& - 2F \cdot \delta u_0
\end{aligned} \tag{B3}$$

Where the derivative of a variation appears in the integrand of equation (B3), integration by parts will transform such a term so that the integrand involves the variation itself, rather than its derivative, and will also introduce boundary terms. For example,

$$\int_{-b}^b \frac{du_1}{dz} \frac{d(\delta u_1)}{dz} dz = \left(\frac{du_1}{dz} \delta u_1 \right) \Big|_{-b}^b - \int_{-b}^b \frac{d^2 u_1}{dz^2} \delta u_1 dz$$

Reducing all integrands in this manner wherever possible, and rearranging terms, one obtains:

$$\begin{aligned}
\delta(TPE) = (\delta u_0) & \cdot \int_{-b}^b (2c_{00} u_0 + 2c_{01} u_1 - \frac{F}{b}) dz \\
& + 2 \int_{-b}^b \left(-b_{11} \frac{d^2 u_1}{dz^2} - b_{12} \frac{d^2 u_2}{dz^2} + c_{01} u_0 + c_{11} u_1 + c_{12} u_2 + \frac{1}{2} d_{11} \frac{dv_1}{dz} \right) (\delta u_1) dz \\
& + 2 \int_{-b}^b \left(-b_{12} \frac{d^2 u_1}{dz^2} - b_{22} \frac{d^2 u_2}{dz^2} + c_{12} u_1 + c_{22} u_2 + \frac{1}{2} d_{21} \frac{dv_1}{dz} + \frac{1}{2} d_{22} \frac{dv_2}{dz} \right) (\delta u_2) dz \\
& + 2 \int_{-b}^b \left(a_{11} v_1 + a_{12} v_2 - \frac{1}{2} d_{11} \frac{du_1}{dz} - \frac{1}{2} d_{21} \frac{du_2}{dz} - e_{11} \frac{d^2 v_1}{dz^2} - e_{12} \frac{d^2 v_2}{dz^2} \right) (\delta v_1) dz
\end{aligned}$$

(equation continued on next page)

$$\begin{aligned}
& + 2 \int_{-b}^b (a_{12}v_1 + a_{22}v_2 - \frac{1}{2} d_{22} \frac{du_2}{dz} - e_{12} \frac{d^2v_1}{dz^2} - e_{22} \frac{d^2v_2}{dz^2}) (\delta v_2) dz \\
& + 2 \left[(b_{11} \frac{du_1}{dz} + b_{12} \frac{du_2}{dz}) (\delta u_1) \right] \Big|_{-b}^b + 2 \left[(b_{12} \frac{du_1}{dz} + b_{22} \frac{du_2}{dz}) (\delta u_2) \right] \Big|_{-b}^b \\
& + \left[(d_{11}u_1 + d_{21}u_2 + 2e_{11} \frac{dv_1}{dz} + 2e_{12} \frac{dv_2}{dz}) (\delta v_1) \right] \Big|_{-b}^b \\
& + \left[(d_{22}u_2 + 2e_{12} \frac{dv_1}{dz} + 2e_{22} \frac{dv_2}{dz}) (\delta v_2) \right] \Big|_{-b}^b \tag{B4}
\end{aligned}$$

Equation (B4) is valid for the case in which there are point attachments at the ends of the trough lines only (fig. 3(a)). If there are wide attachments at the ends of the trough lines, as idealized in figure 3d, it is necessary to drop out the boundary term involving δv_1 , i.e. the term next to the last.

If there are point attachments at the ends of the crest lines (fig. 3(b)) then δv_1 and δv_2 at $z = \pm b$ are not independent. The attachment at the end of a crest line restricts the attachment point against horizontal and vertical movement in the plane of the cross section. The component cross-sectional deformations of figure 4 automatically satisfy the condition of zero vertical movement of this point but not the condition of zero horizontal movement. From figure 4(c) it is seen that the resultant horizontal displacement of the crest plate element is $(v_1 \sin \theta) \cos \theta + v_2 \sin \theta$. The vanishing of this displacement at $z = \pm b$ implies that

$$(v_1 \cos \theta + v_2)_{z = \pm b} = 0 \tag{B5}$$

whence

$$(\delta v_1 \cos \theta + \delta v_2)_{z = \pm b} = 0 \tag{B6}$$

Thus, when there are attachments at the ends of the crest lines, δv_2 in the last term of equation (B4) should be replaced by $-\delta v_1 \cos \theta$. The last two terms of equation (B4) can then be combined, giving the following form of $\delta(TPE)$:

$$\begin{aligned}
(\text{TPE}) = & (\delta u_0) \cdot \int_{-b}^b (\dots) dz + 2 \int_{-b}^b (\dots) (\delta u_1) dz + 2 \int_{-b}^b (\dots) (\delta u_2) dz \\
& + 2 \int_{-b}^b (\dots) (\delta v_1) dz + 2 \int_{-b}^b (\dots) (\delta v_2) dz \\
& + 2 \left[(b_{11} \frac{du_1}{dz} + b_{12} \frac{du_2}{dz}) (\delta u_1) \right] \Big|_{-b}^b + 2 \left[(b_{12} \frac{du_1}{dz} + b_{22} \frac{du_2}{dz}) (\delta u_2) \right] \Big|_{-b}^b \\
& + \left[\left[d_{11} u_1 + d_{21} u_2 + 2e_{11} \frac{dv_1}{dz} + 2e_{12} \frac{dv_2}{dz} \right. \right. \\
& \quad \left. \left. - (d_{22} u_2 + 2e_{12} \frac{dv_1}{dz} + 2e_{22} \frac{dv_2}{dz}) \cos \theta \right] (\delta v_1) \right] \Big|_{-b}^b
\end{aligned} \tag{B7}$$

where the notation (\dots) has been used to indicate terms which are identical to the corresponding terms in equation (B4).

Differential equations.— If the TPE is to be a minimum, $\delta(\text{TPE})$ must vanish for any and all arbitrary variations in $u_0, u_1(z), u_2(z), v_1(z), v_2(z)$, and it then follows from the integral terms in equations (B4) and (B7) that u_0, u_1, u_2, v_1, v_2 must satisfy the following equations:

$$4c_{00} u_0 b + 2c_{01} \int_{-b}^b u_1 dz - 2F = 0 \tag{B8}$$

$$\begin{aligned}
& -b_{11} \frac{d^2 u_1}{dz^2} - b_{12} \frac{d^2 u_2}{dz^2} + c_{01} u_0 + c_{11} u_1 + c_{12} u_2 + \frac{1}{2} d_{11} \frac{dv_1}{dz} = 0 \\
& -b_{12} \frac{d^2 u_1}{dz^2} - b_{22} \frac{d^2 u_2}{dz^2} + c_{12} u_1 + c_{22} u_2 + \frac{1}{2} d_{21} \frac{dv_1}{dz} + \frac{1}{2} d_{22} \frac{dv_2}{dz} = 0 \\
& a_{11} v_1 + a_{12} v_2 - \frac{1}{2} d_{11} \frac{du_1}{dz} - \frac{1}{2} d_{21} \frac{du_2}{dz} - e_{11} \frac{d^2 v_1}{dz^2} - e_{12} \frac{d^2 v_2}{dz^2} = 0 \\
& a_{12} v_1 + a_{22} v_2 - \frac{1}{2} d_{22} \frac{du_2}{dz} - e_{12} \frac{d^2 v_1}{dz^2} - e_{22} \frac{d^2 v_2}{dz^2} = 0
\end{aligned} \tag{B9}$$

Boundary conditions.— The vanishing of the boundary terms in equations (B4) and (B7) requires that the variables satisfy certain conditions at the boundaries ($z = \pm b$). For the case of point attachment at the ends of the trough lines (fig. 3(a)), equation (B4) applies, and the vanishing of the boundary terms in it leads to the following boundary conditions:

$$b_{11} \frac{du_1}{dz} + b_{12} \frac{du_2}{dz} = 0 \quad (B10)$$

$$b_{12} \frac{du_1}{dz} + b_{22} \frac{du_2}{dz} = 0$$

$$d_{11}u_1 + d_{21}u_2 + 2e_{11} \frac{dv_1}{dz} + 2e_{12} \frac{dv_2}{dz} = 0 \quad (B11)$$

$$d_{22}u_2 + 2e_{12} \frac{dv_1}{dz} + 2e_{22} \frac{dv_2}{dz} = 0$$

at $z = \pm b$. For the case of wide attachments at the ends of the trough lines (fig. 3(d)), equation (B4) applies but with next-to-the-last term omitted. As a result, the first of equations (B11) is non-existent, and the condition

$$v_1(\pm b) = 0 \quad (B11')$$

is used in its stead.

For the case in which there are point attachments at the ends of the crest lines as well as the trough lines (fig. 3(b)), equation (B5) constitutes one of the boundary conditions. The remaining boundary conditions, implied by the vanishing of the boundary terms of equation (B7), are equations (B10) again and the following equation in place of (B11):

$$d_{11}u_1 + d_{21}u_2 + 2e_{11} \frac{dv_1}{dz} + 2e_{12} \frac{dv_2}{dz} - (d_{22}u_2 + 2e_{12} \frac{dv_1}{dz} + 2e_{22} \frac{dv_2}{dz}) \cos \theta = 0 \quad (B12)$$

at $z = \pm b$.

Inasmuch as the determinant $b_{11}b_{22} - b_{12}^2$ of equations (B10) is non-vanishing, these equations can be replaced by

$$\frac{du_1}{dz} = 0, \quad \frac{du_2}{dz} = 0 \quad (B13)$$

Physical interpretation of the boundary conditions.— Equations (B10) or (B13), in conjunction with the fact that $du_0/dz = 0$, are readily interpreted to mean that there are no longitudinal normal stresses acting at the corrugation ends.

In order to interpret equations (B11) it is first necessary to replace the system of shear forces and twisting moments at the ends of the corrugation by a statically equivalent system of shear forces alone acting in the middle planes of the individual plate elements. This replacement is shown in figure 9, which is a view of the corrugation as seen from the positive end of the z-axis. Part (a) of figure 9 shows the basic system of shear forces F_1 , F_2 , F_3 and twisting moments T_1 , T_2 , T_3 acting on the ends of the individual plate elements. The twisting moments are related to the deformations, via equations (9) and table 3, as follows:

$$\begin{aligned} T_1 &= \frac{G'J_1}{e} \frac{dv_1}{dz} \\ T_2 &= -\frac{G'J_2}{k} \left(\frac{dv_2}{dz} + \frac{dv_1}{dz} \cos\theta \right) \\ T_3 &= \frac{G'J_3}{f} \left(-2 \frac{dv_1}{dz} \sin^2\theta + 2 \frac{dv_2}{dz} \cos\theta \right) \end{aligned} \quad (B14)$$

The shear forces F_1 , F_2 , F_3 can be expressed in terms of the deformations with the aid of equations (5) and table 2. The result is

$$\begin{aligned} F_1 &= G\gamma_{1et} = Gt(u_1 - u_0) \\ F_2 &= G\gamma_{2kt} = Gt(u_2 - u_1 + k \frac{dv_1}{dz} \sin\theta) \\ F_3 &= G\gamma_{3ft} = Gt(-2u_2 + f \frac{dv_1}{dz} \sin\theta \cos\theta + f \frac{dv_2}{dz} \sin\theta) \end{aligned} \quad (B15)$$

Part (b) of figure 9 is the same as part (a) except that the twisting moments have been represented by pairs of parallel oppositely directed forces acting at the junctions of the plate elements. In part (c) each such force has been replaced by components parallel to the two plate elements forming the junction at which the force acts. In part (d) of figure 9 all the forces

acting as shearing forces along the middle surface of each plate element have been replaced by a single resultant. These resultants are

$$\begin{aligned}\bar{R}_1 &= F_1 + \frac{T_2}{k} \csc\theta - \frac{T_1}{e} \cot\theta \\ \bar{R}_2 &= F_2 + \frac{T_1}{e} \csc\theta - \frac{T_3}{f} \csc\theta \\ \bar{R}_3 &= F_3 + 2 \frac{T_3}{f} \cot\theta - 2 \frac{T_2}{k} \csc\theta\end{aligned}\tag{B16}$$

and they will be called the effective in-plane shears. Expressing T_1 , T_2 , T_3 and F_1 , F_2 , F_3 in terms of the deformations via equations (B14) and (B15) gives

$$\begin{aligned}\bar{R}_2 &= -Gt u_1 + Gt u_2 + (Gt k \sin\theta + \frac{G'J_1}{e^2} \csc\theta + \frac{2G'J_3}{f^2} \sin\theta) \frac{dv_1}{dz} \\ &\quad - (\frac{2G'J_3}{f^2} \cot\theta) \frac{dv_2}{dz}\end{aligned}\tag{B17}$$

$$\begin{aligned}\bar{R}_3 &= -2Gt u_2 + (Gt f \sin\theta \cos\theta - \frac{4G'J_3}{f^2} \sin\theta \cos\theta + \frac{2G'J_2}{k^2} \cot\theta) \frac{dv_1}{dz} \\ &\quad + (Gt f \sin\theta + \frac{4G'J_3}{f^2} \frac{\cos^2\theta}{\sin\theta} + \frac{2G'J_2}{k^2} \csc\theta) \frac{dv_2}{dz}\end{aligned}\tag{B18}$$

For a free end the forces \bar{R}_1 and T_1/e in figure 9d need not be zero. They are the forces furnished by the attachments at the ends of the trough lines. However, the resultants \bar{R}_2 and \bar{R}_3 do have to be zero for a free end. Thus, as far as the forces in the plane of the end cross section are concerned, the conditions for a free end can be written as

$$\bar{R}_2 = 0 \quad \text{and} \quad \bar{R}_3 = 0\tag{B19}$$

or in the form of any two linearly independent linear combinations of these two equations. Choosing the linear combinations

$$\begin{aligned}2\bar{R}_2 \sin\theta + \bar{R}_3 \sin\theta \cos\theta &= 0 \\ \bar{R}_3 \sin\theta &= 0\end{aligned}\tag{B20}$$

one finds, after substituting the expressions for \bar{R}_2 and \bar{R}_3 from equations (B17) and (B18), that these linear combinations are identical to the boundary conditions (B11) obtained by the variational method.

For the case in which there are attachments at the ends of the crest lines, \bar{R}_3 need not be zero inasmuch as the attachment is capable of exerting a force. Only the inclined plate elements are free of effective in-plane shear, i.e. $\bar{R}_2 = 0$. Writing this as

$$2\bar{R}_2 \sin\theta = 0 \quad (B21)$$

and eliminating \bar{R}_2 via equation (B17), it is seen to be exactly equivalent to the boundary condition (B12) obtained for this case by the variational method.

Thus the boundary conditions (B11) and (B12) obtained by the variational method have been shown to be equivalent to the physical requirement of vanishing of the effective in-plane shears \bar{R}_2 and \bar{R}_3 or \bar{R}_2 alone.

APPENDIX C

SOLUTION OF THE EQUATIONS FOR THE BASIC UNKNOWNNS

In this appendix equations (19) will be solved for $u_1(z)$, $u_2(z)$, $v_1(z)$, and $v_2(z)$ in terms of u_0 (subject to the various sets of boundary conditions discussed in connection with equations (19)). Equation (20) will then be used to determine the relationship between the shearing force F and the relative shearing displacement $2u_0$ of one side of the corrugation with respect to the other.

Particular integral. - A particular integral of equations (19) is first sought in the form

$$u_1 = \text{constant}, u_2 = \text{constant}, v_1 = 0, v_2 = 0.$$

For this form of particular integral equations (19) reduce to

$$c_{11}u_1 + c_{12}u_2 = -c_{01}u_0$$

$$c_{12}u_1 + c_{22}u_2 = 0$$

whence

$$\begin{aligned} u_1 &= \zeta_1 u_0, \\ u_2 &= \zeta_2 u_0 \end{aligned} \tag{C1}$$

where

$$\begin{aligned} \zeta_1 &\equiv \frac{-c_{01}c_{22}}{c_{11}c_{22} - c_{12}^2} \\ \zeta_2 &\equiv \frac{c_{01}c_{12}}{c_{11}c_{22} - c_{12}^2} \end{aligned} \tag{C2}$$

Thus a particular solution of equations (19) is

$$\left. \begin{aligned} u_1 &= \zeta_1 u_0 \\ u_2 &= \zeta_2 u_0 \\ v_1 &= 0 \\ v_2 &= 0 \end{aligned} \right\} \tag{C3}$$

Characteristic equation for complementary solution. - To the above must be added a complementary solution, which is the general solution of equations (19) with right sides all zero. Solutions of this homogeneous system will be sought in the following form:

$$\left. \begin{aligned} u_1 &= Ae^{rz} \\ u_2 &= Be^{rz} \\ v_1 &= Ce^{rz} \\ v_2 &= De^{rz} \end{aligned} \right\} \quad (C4)$$

Substituting these assumptions into equations (19) with the right-hand sides all zero leads to the following restrictions on A, B, C, D and r:

$$\begin{bmatrix} b_{11}r^2 - c_{11} & b_{12}r^2 - c_{12} & -\frac{1}{2}d_{11}r & 0 \\ b_{12}r^2 - c_{12} & b_{22}r^2 - c_{22} & -\frac{1}{2}d_{21}r & -\frac{1}{2}d_{22}r \\ -\frac{1}{2}d_{11}r & -\frac{1}{2}d_{21}r & a_{11} - e_{11}r^2 & a_{12} - e_{12}r^2 \\ 0 & -\frac{1}{2}d_{22}r & a_{12} - e_{12}r^2 & a_{22} - e_{22}r^2 \end{bmatrix} \begin{bmatrix} A \\ B \\ C \\ D \end{bmatrix} = \begin{bmatrix} 0 \\ 0 \\ 0 \\ 0 \end{bmatrix} \quad (C5)$$

Thus, for non-trivial solutions of the form of equations (C4), r must satisfy the following characteristic equation:

$$\begin{vmatrix} b_{11}r^2 - c_{11} & b_{12}r^2 - c_{12} & -\frac{1}{2}d_{11}r & 0 \\ b_{12}r^2 - c_{12} & b_{22}r^2 - c_{22} & -\frac{1}{2}d_{21}r & -\frac{1}{2}d_{22}r \\ -\frac{1}{2}d_{11}r & -\frac{1}{2}d_{21}r & a_{11} - e_{11}r^2 & a_{12} - e_{12}r^2 \\ 0 & -\frac{1}{2}d_{22}r & a_{12} - e_{12}r^2 & a_{22} - e_{22}r^2 \end{vmatrix} = 0 \quad (C6)$$

Expanding the determinant, multiplying through by 16 for convenience, and introducing the short-hand notation

$$\begin{aligned}
 \hat{a} &\equiv a_{11}a_{22} - a_{12}^2 & \hat{g} &\equiv 2a_{12}e_{12} - a_{11}e_{22} - a_{22}e_{11} \\
 \hat{b} &\equiv b_{11}b_{22} - b_{12}^2 & \hat{h} &\equiv a_{12}d_{22} - a_{22}d_{21} \\
 \hat{c} &\equiv c_{11}c_{22} - c_{12}^2 & \hat{j} &\equiv a_{11}d_{22} - a_{12}d_{21} \\
 \hat{e} &\equiv e_{11}e_{22} - e_{12}^2 & \hat{k} &\equiv d_{21}e_{22} - d_{22}e_{12} \\
 \hat{f} &\equiv 2b_{12}c_{12} - b_{11}c_{22} - b_{22}c_{11} & \hat{m} &\equiv d_{21}e_{12} - d_{22}e_{11}
 \end{aligned} \tag{C7}$$

one converts equation (C6) to

$$k_0 + k_2 r^2 + k_4 r^4 + k_6 r^6 + k_8 r^8 = 0 \tag{C8}$$

where

$$\begin{aligned}
 k_0 &= 16 \hat{a}\hat{c} \\
 k_2 &= 16(\hat{a}\hat{f} + \hat{c}\hat{g}) + 4 \hat{h}(2 c_{12}d_{11} - c_{11}d_{21}) \\
 &\quad + 4(c_{11}d_{22}\hat{j} + a_{22}c_{22}d_{11}^2) \\
 k_4 &= 16(\hat{a}\hat{b} + \hat{c}\hat{e} + \hat{f}\hat{g}) \\
 &\quad + 4 b_{11}(d_{21}\hat{h} - d_{22}\hat{j}) \\
 &\quad + 4 c_{11}(d_{22}\hat{m} - d_{21}\hat{k}) \\
 &\quad + 8 d_{11}(c_{12}\hat{k} - b_{12}\hat{h}) \\
 &\quad + d_{11}^2(d_{22}^2 - 4 a_{22}b_{22} - 4 c_{22}e_{22}) \\
 k_6 &= 16(\hat{b}\hat{g} + \hat{e}\hat{f}) + 4 \hat{k}(b_{11}d_{21} - 2 b_{12}d_{11}) \\
 &\quad - 4 b_{11}d_{22}\hat{m} + 4 b_{22}d_{11}^2e_{22} \\
 k_8 &= 16 \hat{b}\hat{e}
 \end{aligned} \tag{C9}$$

Reduced form of the characteristic equation. - By substituting into equations (C9) the definitions of \hat{a} , \hat{c} , etc. from equations (C7), and then further eliminating a_{11} , a_{22} , etc. through equations (4), (8), (B2) and (13), and (15), the coefficients k_0 , k_2 , ..., k_8 of the characteristic equation (C8) can eventually be expressed in terms of the elastic constants, the geometrical parameters e , k , f and θ , and the thickness t .

In reducing the characteristic equation in the manner described above it will also be desirable to introduce the dimensionless parameter er in place of r , divide the equation through by E^4 in order to non-dimensionalize the coefficients, and factor out a common factor $(t/e)^4$.

As a result of these steps, the characteristic equation (C8) becomes

$$\begin{aligned} & \left[k_{04} \left(\frac{t}{e} \right)^4 \right] + \left[k_{22} \left(\frac{t}{e} \right)^2 + k_{24} \left(\frac{t}{e} \right)^4 \right] (re)^2 + \left[k_{42} \left(\frac{t}{e} \right)^2 + k_{44} \left(\frac{t}{e} \right)^4 \right] (re)^4 \\ & + \left[k_{60} + k_{62} \left(\frac{t}{e} \right)^2 + k_{64} \left(\frac{t}{e} \right)^4 \right] (re)^6 \\ & + \left[k_{80} + k_{82} \left(\frac{t}{e} \right)^2 + k_{84} \left(\frac{t}{e} \right)^4 \right] (re)^8 = 0 \end{aligned} \quad (C10)$$

where

$$\begin{aligned} k_{04} & \equiv 16 \left(\frac{G}{E} \right)^2 \hat{a}_1 \hat{c}_1 \\ k_{22} & \equiv 4 \left(\frac{G}{E} \right)^3 \left[4 \hat{c}_1 \hat{g}_1 + 2 \hat{h}_1 c_{12}^* d_{11}^* - \hat{h}_1 c_{11}^* d_{21}^* + c_{11}^* d_{22}^* \hat{j}_1 + a_{22}^* c_{22}^* (d_{11}^*)^2 \right] \\ k_{24} & \equiv 16 \left[\frac{E'}{E} \frac{G}{E} \hat{a}_1 \hat{f}_1 + \left(\frac{G}{E} \right)^2 \frac{G'}{E} \hat{c}_1 \hat{g}_2 \right] \\ k_{42} & \equiv 4 \left(\frac{G}{E} \right)^3 \frac{G'}{E} \left[4 \hat{c}_1 \hat{e}_2 + c_{11}^* d_{11}^* \hat{m}_2 - c_{11}^* d_{21}^* \hat{k}_2 + 2 d_{11}^* c_{12}^* \hat{k}_2 - (d_{11}^*)^2 c_{22}^* \hat{e}_{22}^* \right] \\ & + 4 \frac{E'}{E} \left(\frac{G}{E} \right)^2 \left[4 \hat{f}_1 \hat{g}_1 - b_{11}^* d_{22}^* \hat{j}_1 - 2 d_{11}^* b_{12}^* \hat{h}_1 - (d_{11}^*)^2 a_{22}^* b_{22}^* + b_{11}^* d_{21}^* \hat{h}_1 \right] \\ k_{44} & \equiv 16 \left[\left(\frac{G}{E} \right)^2 \left(\frac{G'}{E} \right)^2 \hat{c}_1 \hat{e}_3 + \frac{E'}{E} \frac{G}{E} \frac{G'}{E} \hat{f}_1 \hat{g}_2 \right] \\ k_{60} & \equiv 4 \frac{E'}{E} \left(\frac{G}{E} \right)^3 \left[4 \hat{f}_1 \hat{e}_1 + \hat{k}_1 b_{11}^* d_{21}^* - 2 \hat{k}_1 b_{12}^* d_{11}^* - b_{11}^* d_{22}^* \hat{m}_1 + b_{22}^* (d_{11}^*)^2 \hat{e}_{22}^* \right] \end{aligned}$$

$$\begin{aligned}
k_{62} &\equiv 16 \left(\frac{E'}{E} \right)^2 \frac{G}{E} \hat{b}_1 \hat{g}_1 + 4 \frac{E'}{E} \left(\frac{G}{E} \right)^2 \frac{G'}{E} \left[4 \hat{f}_1 \hat{e}_2 + \hat{k}_2 b_{11}^* d_{21}^* - 2 \hat{k}_2 b_{12}^* d_{11}^* \right. \\
&\quad \left. - b_{11}^* d_{22}^* \hat{m}_2 + b_{22}^* (d_{11}^*)^2 \bar{e}_{22}^* \right] \\
k_{64} &\equiv 16 \left[\left(\frac{E'}{E} \right)^2 \frac{G'}{E} \hat{b}_1 \hat{g}_2 + \frac{E'}{E} \frac{G}{E} \left(\frac{G'}{E} \right)^2 \hat{f}_1 \hat{e}_3 \right] \\
k_{80} &\equiv 16 \left(\frac{E'}{E} \right)^2 \left(\frac{G}{E} \right)^2 \hat{b}_1 \hat{e}_1 \\
k_{82} &\equiv 16 \left(\frac{E'}{E} \right)^2 \frac{G}{E} \frac{G'}{E} \hat{b}_1 \hat{e}_2 \\
k_{84} &\equiv 16 \left(\frac{E'}{E} \right)^2 \left(\frac{G'}{E} \right)^2 \hat{b}_1 \hat{e}_3
\end{aligned}$$

(C11)

with

$$\begin{aligned}
\hat{a}_1 &\equiv a_{11}^* a_{22}^* - (a_{12}^*)^2 \\
\hat{b}_1 &\equiv b_{11}^* b_{22}^* - (b_{12}^*)^2 \\
\hat{c}_1 &\equiv c_{11}^* c_{22}^* - (c_{12}^*)^2 \\
\hat{e}_1 &\equiv e_{11}^{**} e_{22}^{**} - (e_{12}^{**})^2 \\
\hat{e}_2 &\equiv e_{11}^{**} \bar{e}_{22}^* + e_{22}^{**} \bar{e}_{11}^* - 2 e_{12}^{**} \bar{e}_{12}^* \\
\hat{e}_3 &\equiv \bar{e}_{11}^* \bar{e}_{22}^* - (\bar{e}_{12}^*)^2 \\
\hat{f}_1 &\equiv 2 b_{12}^* c_{12}^* - b_{11}^* c_{22}^* - b_{22}^* c_{11}^* \\
\hat{g}_1 &\equiv 2 a_{12}^* e_{12}^{**} - a_{11}^* e_{22}^{**} - a_{22}^* e_{11}^{**} \\
\hat{g}_2 &\equiv 2 a_{12}^* \bar{e}_{12}^* - a_{11}^* \bar{e}_{22}^* - a_{22}^* \bar{e}_{11}^* \\
\hat{h}_1 &\equiv a_{12}^* d_{22}^* - a_{22}^* d_{11}^* \\
\hat{j}_1 &\equiv a_{11}^* d_{22}^* - a_{12}^* d_{21}^* \\
\hat{k}_1 &\equiv e_{22}^{**} d_{21}^* - e_{12}^{**} d_{22}^* \\
\hat{k}_2 &\equiv \bar{e}_{22}^* d_{21}^* - \bar{e}_{12}^* d_{22}^* \\
\hat{m}_1 &\equiv d_{21}^* e_{12}^{**} - d_{22}^* e_{11}^{**} \\
\hat{m}_2 &\equiv d_{21}^* \bar{e}_{12}^* - d_{22}^* \bar{e}_{11}^*
\end{aligned}$$

(C12)

and

$$\begin{aligned}
a_{11}^* &= \frac{1}{12(1-v^2)\beta^2} \left[A_{11} + A_{22} \left(\frac{e}{k} \right)^2 \cos^2 \theta + 4A_{33} \left(\frac{e}{f} \right)^2 \sin^4 \theta - A_{12} \frac{e}{k} \cos \theta \right. \\
&\quad \left. + 2A_{23} \frac{e}{k} \frac{e}{f} \sin^2 \theta \cos \theta - 2A_{13} \frac{e}{f} \sin^2 \theta \right] \\
a_{12}^* &= \frac{1}{12(1-v^2)\beta^2} \left[A_{22} \left(\frac{e}{k} \right)^2 \cos \theta - 4A_{33} \left(\frac{e}{f} \right)^2 \sin^2 \theta \cos \theta - \frac{1}{2} A_{12} \frac{e}{k} \right. \\
&\quad \left. - A_{23} \frac{e}{k} \frac{e}{f} (\cos^2 \theta - \sin^2 \theta) + A_{13} \frac{e}{f} \cos \theta \right] \\
a_{22}^* &= \frac{1}{12(1-v^2)\beta^2} \left[A_{22} \left(\frac{e}{k} \right)^2 + 4A_{33} \left(\frac{e}{f} \right)^2 \cos^2 \theta - 2A_{23} \frac{e}{k} \frac{e}{f} \cos \theta \right] \\
b_{11}^* &= \frac{1}{3} \left(1 + \frac{k}{e} \right) \\
b_{12}^* &= \frac{1}{6} \frac{k}{e} \\
b_{22}^* &= \frac{1}{6} \left(\frac{f}{e} + 2 \frac{k}{e} \right) \\
c_{11}^* &= 1 + \frac{e}{k} \\
c_{12}^* &= -\frac{e}{k} \\
c_{22}^* &= \frac{e}{k} + 2 \frac{e}{f} \\
d_{11}^* &= d_{22}^* = -2 \sin \theta \\
d_{21}^* &= 2 \sin \theta (1 - \cos \theta) \\
e_{11}^{**} &= \sin^2 \theta \left(\frac{k}{e} + \frac{1}{2} \frac{f}{e} \cos^2 \theta \right) \\
e_{12}^{**} &= \frac{1}{2} \frac{f}{e} \sin^2 \theta \cos \theta \\
e_{22}^{**} &= \frac{1}{2} \frac{f}{e} \sin^2 \theta \\
\bar{e}_{11}^* &= \frac{1}{3} \left(1 + \frac{e}{k} \cos^2 \theta + 2 \frac{e}{f} \sin^4 \theta \right) \\
\bar{e}_{12}^* &= \frac{1}{3} \left(\frac{e}{k} \cos \theta - 2 \frac{e}{f} \sin^2 \theta \cos \theta \right) \\
\bar{e}_{22}^* &= \frac{1}{3} \left(\frac{e}{k} + 2 \frac{e}{f} \cos^2 \theta \right)
\end{aligned} \tag{C13}$$

The nature of the roots. - Computations show that in general four of the roots of equation (C10) will be real and four complex. Also, since only even powers of re appear in equation (C10), four of the roots will be the negatives of the other four. Thus, letting

$$R_j \equiv er_j \quad (j = 1, 2, \dots, 8) \quad (C14)$$

denote the eight roots, they can be represented in the following form:

$$\begin{aligned} R_1 &= U + iV \\ R_2 &= U - iV \\ R_3 &= -U + iV \\ R_4 &= -U - iV \\ R_5 &= X \\ R_6 &= -X \\ R_7 &= Y \\ R_8 &= -Y \end{aligned} \quad (C15)$$

where U , V , X and Y are all real and dimensionless. For a given profile and given elastic constants, U , V , X and Y are functions of t/e only.

Series expansions for the roots of the characteristic equation. - When t/e is sufficiently small, it is feasible to expand the roots re of equation (C10) in power series in t/e . The following three kinds of series expansions are postulated:

$$re = q_0 + q_2 \left(\frac{t}{e}\right)^2 + q_4 \left(\frac{t}{e}\right)^4 + \dots \quad (C16)$$

$$re = p_1 \frac{t}{e} + p_3 \left(\frac{t}{e}\right)^3 + p_5 \left(\frac{t}{e}\right)^5 + \dots \quad (C17)$$

$$re = \left(\frac{t}{e}\right)^{1/2} \left[c_0 + c_1 \frac{t}{e} + c_2 \left(\frac{t}{e}\right)^2 + \dots \right] \quad (C18)$$

Substitution shows that all three forms can indeed satisfy equation (C10), provided that the coefficients have the following values:

$$\begin{aligned}
q_0 &= \pm \sqrt{\frac{-k_{60}}{k_{80}}} && \text{(both values generally real)} \\
q_2 &= -\frac{1}{q_0^3} \frac{k_{22} + k_{42}q_0^2 + k_{62}q_0^4 + k_{82}q_0^6}{6k_{60} + 8k_{80}q_0^2} \\
q_4 &= -\frac{\left[k_{04} + (2k_{22} + 4k_{42}q_0^2 + 6k_{62}q_0^4 + 8k_{82}q_0^6)q_0q_2 \right. \\
&\quad \left. + (15k_{60} + 28k_{80}q_0^2)q_0^4q_2^2 \right. \\
&\quad \left. + (k_{24} + k_{44}q_0^2 + k_{64}q_0^4 + k_{84}q_0^6)q_0^2 \right]}{q_0^5(6k_{60} + 8k_{80}q_0^2)}
\end{aligned} \tag{C19}$$

$$\begin{aligned}
p_1 &= \pm \sqrt{\frac{-k_{04}}{k_{22}}} && \text{(both values generally real)} \\
p_3 &= -\frac{p_1}{2k_{22}} \left(k_{24} + k_{42}p_1^2 + k_{60}p_1^4 \right) \\
p_5 &= -\frac{1}{2k_{22}p_1} \left[k_{22}p_3^2 + (2k_{24} + 4k_{42}p_1^2 + 6k_{60}p_1^4)p_1p_3 \right. \\
&\quad \left. + (k_{44} + k_{62}p_1^2 + k_{80}p_1^4)p_1^4 \right]
\end{aligned} \tag{C20}$$

$$\begin{aligned}
c_0 &= \left(-\frac{k_{22}}{k_{60}} \right)^{1/4} = \pm \sqrt[4]{\frac{k_{22}}{k_{60}}} \cdot \frac{\sqrt{2}}{2} (1 \pm i) \\
&\quad \text{(four complex values)} \\
c_1 &= -\frac{k_{04} + k_{42}c_0^4 + k_{80}c_0^8}{c_0(2k_{22} + 6k_{60}c_0^4)} \\
c_2 &= -\frac{k_{22}c_1^2 + k_{24}c_0^2 + 4k_{42}c_0^3c_1 + 15k_{60}c_0^4c_1^2 + k_{62}c_0^6 + 8k_{80}c_0^7c_1}{c_0(2k_{22} + 6k_{60}c_0^4)}
\end{aligned} \tag{C21}$$

Equations (C19) generate two series expansions of the form (C16); equations (C20) generate two more of the form (C17); and equations (C21) give four of the form (C18). Thus series expansions have been obtained for all eight roots of equation (C10). Computations show that both values of q_0 and both values of p_1 are real; thus the two roots of the form (C16) are real, as are the two roots of the form (C17). These four roots correspond to R_5, R_6, R_7 and R_8 of equations (C15). The four values of c_0 are complex, from which it follows that the four roots of the form (C18) are complex, corresponding to R_1, R_2, R_3 and R_4 of equations (C15). It is seen from the series expansions that of the four real roots, two are of the order of $(t/e)^0$, and the other two are of the order of t/e . The four complex roots are of the order of $(t/e)^{1/2}$.

By retaining only the leading term in each of the three series expansions (C16), (C17) and (C18) and (as noted above) identifying R_1, R_2, R_3 and R_4 with the roots yielded by equation (C18), R_5 and R_6 with the roots yielded by equation (C16), and R_7 and R_8 with the roots yielded by equation (C18), the following approximate expressions for the U, V, X and Y of equations (C15) are obtained:

$$\left. \begin{aligned} U &= V \approx \sqrt[4]{\frac{k_{22}}{4k_{60}}} \left(\frac{t}{e}\right)^{1/2} \\ X &\approx \sqrt{\frac{-k_{60}}{k_{80}}} \\ Y &\approx \sqrt{\frac{-k_{04}}{k_{22}}} \left(\frac{t}{e}\right) \end{aligned} \right\} \quad (C22)$$

Relationship of the coefficients A, B, C, D of equations (C4). - Corresponding to any one of the eight roots of the characteristic equation (C10), say er_j ($j = 1, 2, \dots, 8$), there will be a definite relationship between the coefficients A, B, C and D of equations (C4). This relationship is obtained by substituting r_j for r in equations (C5) and solving any three of those equations for three of the coefficients in terms of the fourth. The last three of those equations will be selected for this purpose and rewritten as follows with the intention of solving for B, C and D in terms of A :

$$\begin{bmatrix} b_{22}(er)^2 - c_{22}e^2 & -\frac{1}{2}d_{21}e \cdot (er) & -\frac{1}{2}d_{22}e \cdot (er) \\ -\frac{1}{2}d_{21}e \cdot (er) & a_{11}e^2 - e_{11}(er)^2 & a_{12}e^2 - e_{12}(er)^2 \\ -\frac{1}{2}d_{22}e \cdot (er) & a_{12}e^2 - e_{12}(er)^2 & a_{22}e^2 - e_{22}(er)^2 \end{bmatrix} \begin{bmatrix} B/A \\ C/A \\ D/A \end{bmatrix} = \begin{bmatrix} c_{12}e^2 - b_{12}(er)^2 \\ \frac{1}{2}d_{11}e \cdot (er) \\ 0 \end{bmatrix} \quad (C23)$$

Introducing the definitions of b_{22} , c_{22} , etc. from equations (4), (8), (13), (B2) and (15), substituting $r = r_j$, letting A_j , B_j , C_j , D_j denote the values of A , B , C , D corresponding to $r = r_j$, and introducing the notation defined in equation (C14), namely $R_j \equiv e r_j$, equations (C23) can be rewritten as follows:

$$\begin{bmatrix} L_{11} & L_{12} & L_{13} \\ L_{12} & L_{22} & L_{23} \\ L_{13} & L_{23} & L_{33} \end{bmatrix} \begin{bmatrix} B_j/A_j \\ C_j/A_j \\ D_j/A_j \end{bmatrix} = \begin{bmatrix} \frac{G}{E} c_{12}^* - \frac{E'}{E} b_{12}^* R_j^2 \\ \frac{1}{2} \frac{G}{E} d_{11}^* R_j \\ 0 \end{bmatrix} \quad (C24)$$

where

$$\begin{aligned} L_{11} &\equiv \frac{E'}{E} b_{22}^* R_j^2 - \frac{G}{E} c_{22}^* \\ L_{12} &\equiv -\frac{1}{2} \frac{G}{E} d_{21}^* R_j \\ L_{13} &\equiv -\frac{1}{2} \frac{G}{E} d_{22}^* R_j \\ L_{22} &\equiv a_{11}^* \left(\frac{t}{e}\right)^2 - \left[\frac{G}{E} e_{11}^{**} + \frac{G'}{E} \left(\frac{t}{e}\right)^2 \frac{-}{e_{12}^*} \right] R_j^2 \\ L_{23} &\equiv a_{12}^* \left(\frac{t}{e}\right)^2 - \left[\frac{G}{E} e_{12}^{**} + \frac{G'}{E} \left(\frac{t}{e}\right)^2 \frac{-}{e_{12}^*} \right] R_j^2 \\ L_{33} &\equiv a_{22}^* \left(\frac{t}{e}\right)^2 - \left[\frac{G}{E} e_{22}^{**} + \frac{G'}{E} \left(\frac{t}{e}\right)^2 \frac{-}{e_{22}^*} \right] R_j^2 \end{aligned} \quad (C25)$$

The solution of equations (C24) can be written as

$$\begin{bmatrix} B_j/A_j \\ C_j/A_j \\ D_j/A_j \end{bmatrix} = \begin{bmatrix} \gamma_j^B \\ \gamma_j^C \\ \gamma_j^D \end{bmatrix} \quad (C26)$$

where

$$\begin{bmatrix} \gamma_j^B \\ \gamma_j^C \\ \gamma_j^D \end{bmatrix} = \begin{bmatrix} L_{11} & L_{12} & L_{13} \\ L_{12} & L_{22} & L_{23} \\ L_{13} & L_{23} & L_{33} \end{bmatrix}^{-1} \begin{bmatrix} \frac{G}{E} c_{12}^* - \frac{E'}{E} b_{12}^* R_j^2 \\ \frac{1}{2} \frac{G}{E} d_{11}^* R_j \\ 0 \end{bmatrix} \quad (C27)$$

For computational purposes it may be desirable to be able to anticipate how $\gamma_j^B, \gamma_j^C, \gamma_j^D$ depend on t/e . Earlier, in discussing the series expansions for the roots $R_j \equiv er_j$, it was found that two real roots are of the order of 1, the other two real roots are of the order of t/e , and the four complex roots are of the order of $(t/e)^{1/2}$. Imagining equations (C24) to be solved by Cramer's rule, it becomes evident that: when R_j is of the order of 1, $\gamma_j^B, \gamma_j^C, \gamma_j^D$ are also of the order of 1; when R_j is of the order of t/e , γ_j^B is of the order of 1, but γ_j^C and γ_j^D are of the order of $(t/e)^{-1}$; when R_j is of the order of $(t/e)^{1/2}$, γ_j^B is of the order of 1, and γ_j^C and γ_j^D are of the order of $(t/e)^{-1/2}$.

The nature of $\gamma_j^B, \gamma_j^C, \gamma_j^D$. - From equations (C23) the following things are evident: (a) if r is replaced by its negative, B/A remains unchanged while C/A and D/A merely change sign; (b) if r is replaced by its complex conjugate, $B/A, C/A$, and D/A are changed to their complex conjugates; (c) if r is real, $B/A, C/A$, and D/A are real; and (d) if r is complex, $B/A, C/A$, and D/A are complex. From (a) and (b) and equations (C15) it follows that

$$\begin{array}{lll} \gamma_4^B = \gamma_1^B & \gamma_4^C = -\gamma_1^C & \gamma_4^D = -\gamma_1^D \\ \gamma_3^B = \gamma_2^B & \gamma_3^C = -\gamma_2^C & \gamma_3^D = -\gamma_2^D \\ \gamma_6^B = \gamma_5^B & \gamma_6^C = -\gamma_5^C & \gamma_6^D = -\gamma_5^D \end{array} \quad (C28a)$$

$$\begin{array}{lll} \gamma_8^B = \gamma_7^B & \gamma_8^C = -\gamma_7^C & \gamma_8^D = -\gamma_7^D \end{array}$$

and

$$\begin{array}{lll} \gamma_2^B = \gamma_1^{B*} & \gamma_2^C = \gamma_1^{C*} & \gamma_2^D = \gamma_1^{D*} \\ \gamma_4^B = \gamma_3^{B*} & \gamma_4^C = \gamma_3^{C*} & \gamma_4^D = \gamma_3^{D*} \end{array} \quad (C28b)$$

where the asterisks denote "complex conjugate".

From these deductions and (c) and (d), it follows that the γ_j^B, γ_j^C , and γ_j^D can be represented as follows:

$$\begin{array}{lll}
\gamma_1^B = P^B + iQ^B & \gamma_1^C = P^C + iQ^C & \gamma_1^D = P^D + iQ^D \\
\gamma_2^B = P^B - iQ^B & \gamma_2^C = P^C - iQ^C & \gamma_2^D = P^D - iQ^D \\
\gamma_3^B = P^B - iQ^B & \gamma_3^C = -P^C + iQ^C & \gamma_3^D = -P^D + iQ^D \\
\gamma_4^B = P^B + iQ^B & \gamma_4^C = -P^C - iQ^C & \gamma_4^D = -P^D - iQ^D \\
\gamma_5^B = S^B & \gamma_5^C = S^C & \gamma_5^D = S^D \\
\gamma_6^B = S^B & \gamma_6^C = -S^C & \gamma_6^D = -S^D \\
\gamma_7^B = T^B & \gamma_7^C = T^C & \gamma_7^D = T^D \\
\gamma_8^B = T^B & \gamma_8^C = -T^C & \gamma_8^D = -T^D
\end{array} \tag{C29}$$

where $P^{B,C,D}$, $Q^{B,C,D}$, $S^{B,C,D}$, and $T^{B,C,D}$ are real numbers.

Complementary solution. - At this point eight solutions of the form of equations (C4) have been derived. The complete complementary solution, obtained by adding the eight individual solutions, is

$$\begin{aligned}
u_1 &= \sum_{j=1}^8 A_j \exp\left(\frac{R_j z}{e}\right) \\
u_2 &= \sum_{j=1}^8 A_j \gamma_j^B \exp\left(\frac{R_j z}{e}\right) \\
v_1 &= \sum_{j=1}^8 A_j \gamma_j^C \exp\left(\frac{R_j z}{e}\right) \\
v_2 &= \sum_{j=1}^8 A_j \gamma_j^D \exp\left(\frac{R_j z}{e}\right)
\end{aligned} \tag{C30}$$

Substituting for the R_j their expressions from equations (C15), and for the γ_j^B , γ_j^C , γ_j^D their expressions from equations (C29), one obtains:

$$\begin{aligned}
u_1 = & e^{\frac{Uz}{e}} \left[(A_1 + A_2) \cos \frac{Vz}{e} + i(A_1 - A_2) \sin \frac{Vz}{e} \right] \\
& + e^{-\frac{Uz}{e}} \left[(A_3 + A_4) \cos \frac{Vz}{e} + i(A_3 - A_4) \sin \frac{Vz}{e} \right] \\
& + A_5 e^{\frac{Xz}{e}} + A_6 e^{-\frac{Xz}{e}} + A_7 e^{\frac{Yz}{e}} + A_8 e^{-\frac{Yz}{e}}
\end{aligned}$$

$$\begin{aligned}
u_2 = & e^{\frac{Uz}{e}} \left[\left\{ (A_1 + A_2)P^B + i(A_1 - A_2)Q^B \right\} \cos \frac{Vz}{e} \right. \\
& \left. + \left\{ i(A_1 - A_2)P^B - (A_1 + A_2)Q^B \right\} \sin \frac{Vz}{e} \right] \\
& + e^{-\frac{Uz}{e}} \left[\left\{ (A_3 + A_4)P^B - i(A_3 - A_4)Q^B \right\} \cos \frac{Vz}{e} \right. \\
& \left. + \left\{ i(A_3 - A_4)P^B + (A_3 + A_4)Q^B \right\} \sin \frac{Vz}{e} \right] \\
& + S^B \left(A_5 e^{\frac{Xz}{e}} + A_6 e^{-\frac{Xz}{e}} \right) + T^B \left(A_7 e^{\frac{Yz}{e}} + A_8 e^{-\frac{Yz}{e}} \right)
\end{aligned}$$

$$\begin{aligned}
v_1 = & e^{\frac{Uz}{e}} \left[\left\{ (A_1 + A_2)P^C + i(A_1 - A_2)Q^C \right\} \cos \frac{Vz}{e} \right. \\
& \left. + \left\{ i(A_1 - A_2)P^C - (A_1 + A_2)Q^C \right\} \sin \frac{Vz}{e} \right] \\
& + e^{-\frac{Uz}{e}} \left[\left\{ -(A_3 + A_4)P^C + i(A_3 - A_4)Q^C \right\} \cos \frac{Vz}{e} \right. \\
& \left. + \left\{ -i(A_3 - A_4)P^C - (A_3 + A_4)Q^C \right\} \sin \frac{Vz}{e} \right] \\
& + S^C \left(A_5 e^{\frac{Xz}{e}} - A_6 e^{-\frac{Xz}{e}} \right) + T^C \left(A_7 e^{\frac{Yz}{e}} - A_8 e^{-\frac{Yz}{e}} \right)
\end{aligned}$$

$$\begin{aligned}
v_2 = & e^{\frac{Uz}{e}} \left[\left\{ (A_1 + A_2)P^D + i(A_1 - A_2)Q^D \right\} \cos \frac{Vz}{e} \right. \\
& + \left. \left\{ i(A_1 - A_2)P^D - (A_1 + A_2)Q^D \right\} \sin \frac{Vz}{e} \right] \\
& + e^{-\frac{Uz}{e}} \left[\left\{ -(A_3 + A_4)P^D + i(A_3 - A_4)Q^D \right\} \cos \frac{Vz}{e} \right. \\
& + \left. \left\{ -i(A_3 - A_4)P^D - (A_3 + A_4)Q^D \right\} \sin \frac{Vz}{e} \right] \\
& + S^D \left(A_5 e^{\frac{Xz}{e}} - A_6 e^{-\frac{Xz}{e}} \right) + T^D \left(A_7 e^{\frac{Yz}{e}} - A_8 e^{-\frac{Yz}{e}} \right)
\end{aligned}$$

By expressing the exponential functions in terms of hyperbolic sines and cosines, these results are converted to the following form, in which each term is easily identified as being odd or even in z :

$$\begin{aligned}
u_1 = & \cosh \frac{Uz}{e} \left(\bar{A}_1 \cos \frac{Vz}{e} + \bar{A}_2 \sin \frac{Vz}{e} \right) \\
& + \sinh \frac{Uz}{e} \left(\bar{A}_3 \cos \frac{Vz}{e} + \bar{A}_4 \sin \frac{Vz}{e} \right) \\
& + \bar{A}_5 \cosh \frac{Xz}{e} + \bar{A}_6 \sinh \frac{Xz}{e} + \bar{A}_7 \cosh \frac{Yz}{e} + \bar{A}_8 \sinh \frac{Yz}{e}
\end{aligned} \tag{C31a}$$

$$\begin{aligned}
u_2 = & \cosh \frac{Uz}{e} \left[(\bar{A}_1 P^B + \bar{A}_4 Q^B) \cos \frac{Vz}{e} + (\bar{A}_2 P^B - \bar{A}_3 Q^B) \sin \frac{Vz}{e} \right] \\
& + \sinh \frac{Uz}{e} \left[(\bar{A}_3 P^B + \bar{A}_2 Q^B) \cos \frac{Vz}{e} + (\bar{A}_4 P^B - \bar{A}_1 Q^B) \sin \frac{Vz}{e} \right] \\
& + S^B \left(\bar{A}_5 \cosh \frac{Xz}{e} + \bar{A}_6 \sinh \frac{Xz}{e} \right) \\
& + T^B \left(\bar{A}_7 \cosh \frac{Yz}{e} + \bar{A}_8 \sinh \frac{Yz}{e} \right)
\end{aligned} \tag{C31b}$$

$$\begin{aligned}
v_1 = & \cosh \frac{Uz}{e} \left[(\bar{A}_3 P^C + \bar{A}_4 Q^C) \cos \frac{Vz}{e} + (\bar{A}_4 P^C - \bar{A}_1 Q^C) \sin \frac{Vz}{e} \right] \\
& + \sinh \frac{Uz}{e} \left[(\bar{A}_1 P^C + \bar{A}_4 Q^C) \cos \frac{Vz}{e} + (\bar{A}_2 P^C - \bar{A}_3 Q^C) \sin \frac{Vz}{e} \right] \\
& + S^C \left(\bar{A}_6 \cosh \frac{Xz}{e} + \bar{A}_5 \sinh \frac{Xz}{e} \right) \\
& + T^C \left(\bar{A}_8 \cosh \frac{Yz}{e} + \bar{A}_7 \sinh \frac{Yz}{e} \right)
\end{aligned} \tag{C31c}$$

$$\begin{aligned}
v_2 = & \cosh \frac{Uz}{e} \left[(\bar{A}_3 P^D + \bar{A}_2 Q^D) \cos \frac{Vz}{e} + (\bar{A}_4 P^D - \bar{A}_1 Q^D) \sin \frac{Vz}{e} \right] \\
& + \sinh \frac{Uz}{e} \left[(\bar{A}_1 P^D + \bar{A}_4 Q^D) \cos \frac{Vz}{e} + (\bar{A}_2 P^D - \bar{A}_3 Q^D) \sin \frac{Vz}{e} \right] \\
& + S^D \left(\bar{A}_6 \cosh \frac{Xz}{e} + \bar{A}_5 \sinh \frac{Xz}{e} \right) \\
& + T^D \left(\bar{A}_8 \cosh \frac{Yz}{e} + \bar{A}_7 \sinh \frac{Yz}{e} \right)
\end{aligned} \tag{C31d}$$

where the new arbitrary constants $\bar{A}_1, \bar{A}_2, \dots, \bar{A}_8$ are the following linear combinations of the original arbitrary constants A_1, A_2, \dots, A_8 :

$$\begin{aligned}
\bar{A}_1 & \equiv A_1 + A_2 + A_3 + A_4 \\
\bar{A}_2 & \equiv 1(A_1 - A_2 + A_3 - A_4) \\
\bar{A}_3 & \equiv A_1 + A_2 - A_3 - A_4 \\
\bar{A}_4 & \equiv 1(A_1 - A_2 - A_3 + A_4) \\
\bar{A}_5 & \equiv A_5 + A_6 \\
\bar{A}_6 & \equiv A_5 - A_6 \\
\bar{A}_7 & \equiv A_7 + A_8 \\
\bar{A}_8 & \equiv A_7 - A_8
\end{aligned}$$

On physical grounds, the total (particular plus complementary) solutions for u_1 and u_2 should be even functions of z , while the total solution for v_1 and v_2 should be odd functions of z . The particular solutions, equations (C3), already satisfy this requirement; therefore the complementary solution, equations (C31), must also satisfy it. In order to eliminate from equations (C31) those terms not having the proper parity, it is necessary to set $\bar{A}_2, \bar{A}_3, \bar{A}_6$, and \bar{A}_8 equal to zero.

Complete solution. - Setting four of the constants equal to zero in the complementary solution, as described above, and adding to it the particular solution, equations (C3), there results the following complete solution in terms of four arbitrary constants \bar{A}_1 , \bar{A}_4 , \bar{A}_5 , \bar{A}_7 :

$$\begin{aligned} u_1 = & \zeta_1 u_0 + \bar{A}_1 \cosh \frac{Uz}{e} \cos \frac{Vz}{e} + \bar{A}_4 \sinh \frac{Uz}{e} \sin \frac{Vz}{e} \\ & + \bar{A}_5 \cosh \frac{Xz}{e} + \bar{A}_7 \cosh \frac{Yz}{e} \end{aligned} \quad (C32a)$$

$$\begin{aligned} u_2 = & \zeta_2 u_0 + (\bar{A}_1 P^B + \bar{A}_4 Q^B) \cosh \frac{Uz}{e} \cos \frac{Vz}{e} \\ & + (\bar{A}_4 P^B - \bar{A}_1 Q^B) \sinh \frac{Uz}{e} \sin \frac{Vz}{e} \\ & + \bar{A}_5 S^B \cosh \frac{Xz}{e} + \bar{A}_7 T^B \cosh \frac{Yz}{e} \end{aligned} \quad (C32b)$$

$$\begin{aligned} v_1 = & (\bar{A}_4 P^C - \bar{A}_1 Q^C) \cosh \frac{Uz}{e} \sin \frac{Vz}{e} \\ & + (\bar{A}_1 P^C + \bar{A}_4 Q^C) \sinh \frac{Uz}{e} \cos \frac{Vz}{e} \\ & + \bar{A}_5 S^C \sinh \frac{Xz}{e} + \bar{A}_7 T^C \sinh \frac{Yz}{e} \end{aligned} \quad (C32c)$$

$$\begin{aligned} v_2 = & (\bar{A}_4 P^D - \bar{A}_1 Q^D) \cosh \frac{Uz}{e} \sin \frac{Vz}{e} \\ & + (\bar{A}_1 P^D + \bar{A}_4 Q^D) \sinh \frac{Uz}{e} \cos \frac{Vz}{e} \\ & + \bar{A}_5 S^D \sinh \frac{Xz}{e} + \bar{A}_7 T^D \sinh \frac{Yz}{e} \end{aligned} \quad (C32d)$$

Evaluation of the arbitrary constants through boundary conditions. - The unknown constants \bar{A}_1 , \bar{A}_4 , \bar{A}_5 , and \bar{A}_7 are determined from the boundary conditions, which are: equations (B13) and (B11) in the case of point attachments at the ends of the trough lines only (fig. 3(a)); equations (B13), (B5) and (B12) if there are point attachments at the ends of the crest lines as well (fig. 3(b)); and equations (B13), (B11') and the second of (B11) if there are wide attachments at the ends of the trough lines (fig. 3(d)). Substitution of equations (C32) into these boundary conditions leads to four simultaneous equations for \bar{A}_1 , \bar{A}_4 , \bar{A}_5 and \bar{A}_7 .

For the case of point attachments at the ends of the trough lines only these equations are

$$\begin{bmatrix} N_{11} & N_{12} & N_{13} & N_{14} \\ N_{21} & N_{22} & N_{23} & N_{24} \\ N_{31} & N_{32} & N_{33} & N_{34} \\ N_{41} & N_{42} & N_{43} & N_{44} \end{bmatrix} \begin{bmatrix} \frac{\bar{A}_1}{u_0} \sinh \frac{U_b}{e} \\ \frac{\bar{A}_4}{u_0} \sinh \frac{U_b}{e} \\ \frac{\bar{A}_5}{u_0} \sinh \frac{X_b}{e} \\ \frac{\bar{A}_7}{u_0} \sinh \frac{Y_b}{e} \end{bmatrix} = \begin{bmatrix} 0 \\ 0 \\ N_3 \\ N_4 \end{bmatrix} \quad (C33)$$

where

$$N_{11} = U\widehat{sc} - V\widehat{cs}$$

$$N_{12} = U\widehat{cs} + V\widehat{sc}$$

$$N_{13} = X$$

$$N_{14} = Y$$

$$N_{21} = P^B_{N_{11}} - Q^B_{N_{12}}$$

$$N_{22} = Q^B_{N_{11}} + P^B_{N_{12}}$$

$$N_{23} = S^B_X$$

$$N_{24} = T^B_Y$$

$$N_{31} = \tilde{d}_{11}\widehat{cc} + \tilde{d}_{21}\alpha_1^B + \tilde{e}_{11}\beta_1^C + \tilde{e}_{12}\beta_1^D$$

$$N_{32} = \tilde{d}_{11}\widehat{ss} + \tilde{d}_{21}\alpha_2^B + \tilde{e}_{11}\beta_2^C + \tilde{e}_{12}\beta_2^D$$

$$N_{33} = (\tilde{d}_{11} + \tilde{d}_{21}S^B + \tilde{e}_{11}S^C_X + \tilde{e}_{12}S^D_X) \coth \frac{X_b}{e}$$

$$N_{34} = (\tilde{d}_{11} + \tilde{d}_{21}T^B + \tilde{e}_{11}T^C_Y + \tilde{e}_{12}T^D_Y) \coth \frac{Y_b}{e}$$

$$N_3 = -\zeta_1\tilde{d}_{11} - \zeta_2\tilde{d}_{21}$$

$$N_{41} = \tilde{d}_{11}\alpha_1^B + \tilde{e}_{12}\beta_1^C + \tilde{e}_{22}\beta_1^D$$

$$N_{42} = \tilde{d}_{11}\alpha_2^B + \tilde{e}_{12}\beta_2^C + \tilde{e}_{22}\beta_2^D$$

(Continued on next page)

$$\begin{aligned}
N_{43} &= (\tilde{d}_{11} S^B + \tilde{e}_{12} S^C_X + \tilde{e}_{22} S^D_X) \coth \frac{Xb}{e} \\
N_{44} &= (\tilde{d}_{11} T^B + \tilde{e}_{12} T^C_Y + \tilde{e}_{22} T^D_Y) \coth \frac{Yb}{e} \\
N_4 &= -\tilde{d}_{11} \zeta_2
\end{aligned} \tag{C34}$$

with

$$\begin{aligned}
\widehat{ss} &\equiv \sin \frac{Vb}{e} \\
\widehat{sc} &\equiv \cos \frac{Vb}{e} \\
\widehat{cs} &\equiv \coth \frac{Ub}{e} \sin \frac{Vb}{e} \\
\widehat{cc} &\equiv \coth \frac{Ub}{e} \cos \frac{Vb}{e}
\end{aligned} \tag{C35}$$

$$\begin{aligned}
\alpha_1^B &\equiv P^B_{\widehat{cc}} - Q^B_{\widehat{ss}} \\
\alpha_2^B &\equiv P^B_{\widehat{ss}} + Q^B_{\widehat{cc}} \\
\beta_1^C &\equiv U(P^C_{\widehat{cc}} - Q^C_{\widehat{ss}}) - V(P^C_{\widehat{ss}} + Q^C_{\widehat{cc}}) \\
\beta_2^C &\equiv U(P^C_{\widehat{ss}} + Q^C_{\widehat{cc}}) + V(P^C_{\widehat{cc}} - Q^C_{\widehat{ss}}) \\
\beta_1^D &\equiv U(P^D_{\widehat{cc}} - Q^D_{\widehat{ss}}) - V(P^D_{\widehat{ss}} + Q^D_{\widehat{cc}}) \\
\beta_2^D &\equiv U(P^D_{\widehat{ss}} + Q^D_{\widehat{cc}}) + V(P^D_{\widehat{cc}} - Q^D_{\widehat{ss}})
\end{aligned} \tag{C36}$$

and

$$\begin{aligned}
\tilde{d}_{11} &\equiv -\sin \theta \\
\tilde{d}_{21} &\equiv \sin \theta (1 - \cos \theta) \\
\tilde{e}_{11} &\equiv \sin^2 \theta \left(\frac{k}{e} + \frac{1}{2} \frac{f}{e} \cos^2 \theta \right) + \frac{1}{3} \frac{G'}{G} \left(\frac{t}{e} \right)^2 \left(1 + \frac{e}{k} \cos^2 \theta + 2 \frac{e}{f} \sin^4 \theta \right) \\
\tilde{e}_{12} &\equiv \frac{1}{2} \frac{f}{e} \sin^2 \theta \cos \theta + \frac{1}{3} \frac{G'}{G} \left(\frac{t}{e} \right)^2 \left(\frac{e}{k} \cos \theta - 2 \frac{e}{f} \sin^2 \theta \cos \theta \right) \\
\tilde{e}_{22} &\equiv \frac{1}{2} \frac{f}{e} \sin^2 \theta + \frac{1}{3} \frac{G'}{G} \left(\frac{t}{e} \right)^2 \left(\frac{e}{k} + 2 \frac{e}{f} \cos^2 \theta \right)
\end{aligned} \tag{C37}$$

As is implied in the form of equations (C33), it is usually convenient for computational purposes to regard $\frac{\bar{A}_1}{u_0} \sinh \frac{U_b}{e}$, $\frac{\bar{A}_4}{u_0} \sinh \frac{U_b}{e}$, $\frac{\bar{A}_5}{u_0} \sinh \frac{X_b}{e}$ and $\frac{\bar{A}_7}{u_0} \sinh \frac{Y_b}{e}$ as unknowns, rather than $\frac{\bar{A}_1}{u_0}$, $\frac{\bar{A}_4}{u_0}$, $\frac{\bar{A}_5}{u_0}$, $\frac{\bar{A}_7}{u_0}$.

For the case of point attachments at the ends of the crest lines and the trough lines the simultaneous equations arising from the boundary conditions are

$$\begin{bmatrix} N_{11} & N_{12} & N_{13} & N_{14} \\ N_{21} & N_{22} & N_{23} & N_{24} \\ \bar{N}_{31} & \bar{N}_{32} & \bar{N}_{33} & \bar{N}_{34} \\ \bar{N}_{41} & \bar{N}_{42} & \bar{N}_{43} & \bar{N}_{44} \end{bmatrix} \begin{bmatrix} \frac{\bar{A}_1}{u_0} \sinh \frac{U_b}{e} \\ \frac{\bar{A}_4}{u_0} \sinh \frac{U_b}{e} \\ \frac{\bar{A}_5}{u_0} \sinh \frac{X_b}{e} \\ \frac{\bar{A}_7}{u_0} \sinh \frac{Y_b}{e} \end{bmatrix} = \begin{bmatrix} 0 \\ 0 \\ 0 \\ \bar{N}_4 \end{bmatrix} \quad (C38)$$

where

$$\begin{aligned} \bar{N}_{31} &= (P^{\text{Csc}} - Q^{\text{Ccs}}) \cos \theta + (P^{\text{Dsc}} - Q^{\text{Dcs}}) \\ \bar{N}_{32} &= (P^{\text{Ccs}} + Q^{\text{Csc}}) \cos \theta + (P^{\text{Dcs}} + Q^{\text{Dsc}}) \\ \bar{N}_{33} &= S^{\text{C}} \cos \theta + S^{\text{D}} \\ \bar{N}_{34} &= T^{\text{C}} \cos \theta + T^{\text{D}} \\ \bar{N}_{41} &= N_{31} - N_{41} \cos \theta \\ \bar{N}_{42} &= N_{32} - N_{42} \cos \theta \\ \bar{N}_{43} &= N_{33} - N_{43} \cos \theta \\ \bar{N}_{44} &= N_{34} - N_{44} \cos \theta \\ \bar{N}_4 &= N_3 - N_4 \cos \theta \end{aligned} \quad (C39)$$

Finally, for the case of wide attachments at the ends of the trough lines they are

$$\begin{bmatrix} N_{11} & N_{12} & N_{13} & N_{14} \\ N_{21} & N_{22} & N_{23} & N_{24} \\ \bar{N}_{31} & \bar{N}_{32} & \bar{N}_{33} & \bar{N}_{34} \\ N_{41} & N_{42} & N_{43} & N_{44} \end{bmatrix} \begin{bmatrix} \frac{\bar{A}_1}{u_0} \sinh \frac{U_b}{e} \\ \frac{\bar{A}_4}{u_0} \sinh \frac{U_b}{e} \\ \frac{\bar{A}_5}{u_0} \sinh \frac{X_b}{e} \\ \frac{\bar{A}_7}{u_0} \sinh \frac{Y_b}{e} \end{bmatrix} = \begin{bmatrix} 0 \\ 0 \\ 0 \\ N_4 \end{bmatrix} \quad (C38')$$

where

$$\left. \begin{aligned} \bar{N}_{31} &= P^{\widehat{C}_{sc}} - Q^{\widehat{C}_{cs}} \\ \bar{N}_{32} &= P^{\widehat{C}_{cs}} + Q^{\widehat{C}_{sc}} \\ \bar{N}_{33} &= S^C \\ \bar{N}_{34} &= T^C \end{aligned} \right\} \quad (C39')$$

Relationship between shearing displacement and shearing force. - At this stage the displacement quantities have all been determined in terms of u_0 , and equations (20) and (C32a) can therefore be used to determine the shearing forces F needed to maintain the relative shearing displacement $2u_0$. The resulting relationship, taking into account the definitions of c_{00} and c_{01} (eq. (8)), is

$$\begin{aligned} \frac{F}{2u_0} \cdot \frac{e}{Gtb} &= 1 - \zeta_1 - \frac{e}{b} \left[\left(\frac{\bar{A}_1}{u_0} \sinh \frac{U_b}{e} \right) \frac{U^{\widehat{sc}} + V^{\widehat{cs}}}{U^2 + V^2} \right. \\ &\quad + \left(\frac{\bar{A}_4}{u_0} \sinh \frac{U_b}{e} \right) \frac{U^{\widehat{cs}} - V^{\widehat{sc}}}{U^2 + V^2} \\ &\quad \left. + \left(\frac{\bar{A}_5}{u_0} \sinh \frac{bX}{e} \right) \frac{1}{X} + \left(\frac{\bar{A}_7}{u_0} \sinh \frac{bY}{e} \right) \frac{1}{Y} \right] \end{aligned} \quad (C40)$$

APPENDIX D

SPECIAL CASE: $f = 0$

For the special case $f = 0$ (fig. 10(b)) junction lines ② and ③ coincide and form a line of points of inflection of the cross sections. Along the common junction line the longitudinal displacements must vanish, and the vertical displacement must also vanish. These conditions can be met by setting

$$u_2(z) = 0 \quad (D1)$$

and

$$[v_1(z) \sin \theta] \sin \theta - [v_2(z)] \cos \theta = 0 \quad (D2)$$

The variational form of these equations is

$$\delta u_2 = 0 \quad (D3)$$

$$\delta v_1 = \delta v_2 \cos \theta / \sin^2 \theta \quad (D4)$$

Incorporation of these conditions into equation (B4) gives the following expression for the first variation of the TPE:

$$\begin{aligned} \delta(TPE) = (\delta u_0) \cdot \int_{-b}^b (2c_{00}u_0 + 2c_{01}u_1 - \frac{F}{b}) dz \\ + 2 \int_{-b}^b (-b_{11} \frac{d^2 u_1}{dz^2} + c_{01}u_0 + c_{11}u_1 + \frac{1}{2} d_{11} \frac{dv_2}{dz} \frac{\cos \theta}{\sin^2 \theta}) (\delta u_1) dz \\ + 2 \int_{-b}^b [(a_{11} \frac{\cos^2 \theta}{\sin^4 \theta} + 2a_{12} \frac{\cos \theta}{\sin^2 \theta} + a_{22}) v_2 - \frac{1}{2} d_{11} \frac{du_1}{dz} \frac{\cos \theta}{\sin^2 \theta} \\ - (e_{11}'' \frac{\cos^2 \theta}{\sin^4 \theta} + 2e_{12}'' \frac{\cos \theta}{\sin^2 \theta} + e_{22}'') \frac{d^2 v_2}{dz^2}] (\delta v_2) dz \end{aligned}$$

(equation continued on next page)

$$\begin{aligned}
& + (2b_{11} \frac{du_1}{dz} \delta u_1) \Big|_{-b}^b \\
& + [d_{11} u_1 \frac{\cos \theta}{\sin^2 \theta} + 2(e''_{11} \frac{\cos^2 \theta}{\sin^4 \theta} + 2e''_{12} \frac{\cos \theta}{\sin^2 \theta} + e''_{22}) \frac{dv_2}{dz}] (\delta v_2) \Big|_{-b}^b
\end{aligned} \tag{D5}$$

where

$$\begin{aligned}
e''_{11} &= Gt \sin^2 \theta (k + \frac{f}{2} \cos^2 \theta) + G' (\frac{J_1}{e^2} + \frac{J_2}{k^2} \cos^2 \theta) \\
e''_{22} &= \frac{1}{2} Gtf \sin^2 \theta + G' \frac{J_2}{k^2} \\
e''_{12} &= \frac{1}{2} Gtf \sin^2 \theta \cos \theta + G' \frac{J_2}{k^2} \cos \theta
\end{aligned} \tag{D6}$$

So far the vanishing of f has not been incorporated into equation (D5). In order to incorporate this condition into the terms arising from strain energy of middle-surface shearing, f may simply be allowed to approach zero in equations (D6). However, the strain energy of frame bending cannot be obtained correctly by letting f approach zero in the equations for a_{11} , a_{12} and a_{22} — equations (A12), (A10) and (A8). The reason is that with condition (D2) imposed to prevent vertical displacements of junctions ② and ③, allowing f to then approach zero will lead to a clamping (zero rotation) condition at the vertex formed by junctions ② and ③ as they meet, rather than to the condition of free rotation corresponding to the point of inflection (zero moment) which must exist at this junction. In order to obtain correctly the zero moment condition existing at the vertex, f must be allowed to approach infinity, rather than zero, in those terms of equation (D5) which arise from strain energy of frame bending, namely a_{11} , a_{12} and a_{22} . Doing this, one obtains the following limiting values of a_{11} , a_{12} and a_{22} for use in equation (D5):

$$\begin{aligned}
a_{11} &\rightarrow \frac{D}{\beta^2 e^3} [\tilde{A}_{11} + \tilde{A}_{22} (\frac{e}{k})^2 \cos^2 \theta - \tilde{A}_{12} \frac{e}{k} \cos \theta] \equiv \tilde{a}_{11} \\
a_{12} &\rightarrow \frac{D}{\beta^2 e^3} [\tilde{A}_{22} (\frac{e}{k})^2 \cos \theta - \frac{1}{2} \tilde{A}_{12} \frac{e}{k}] \equiv \tilde{a}_{12} \\
a_{22} &\rightarrow \frac{D}{\beta^2 e^3} [\tilde{A}_{22} (\frac{e}{k})^2] \equiv \tilde{a}_{22}
\end{aligned} \tag{D7}$$

where

$$\tilde{\beta} \equiv 4(3 + \alpha) \frac{e}{k} + 12 \left(\frac{e}{k}\right)^2 \quad (D8a)$$

$$\begin{aligned} \tilde{A}_{11} &\equiv 768 \alpha^2 \left(\frac{e}{k}\right)^2 + 144(15\alpha^2 + 2\alpha + 3) \left(\frac{e}{k}\right)^3 + 432(3\alpha^2 + 1) \left(\frac{e}{k}\right)^4 \\ \tilde{A}_{22} &\equiv 48(\alpha + 3)^2 \left(\frac{e}{k}\right)^3 + 144(\alpha^2 + 3) \left(\frac{e}{k}\right)^4 \end{aligned} \quad (D8b)$$

$$\tilde{A}_{12} \equiv -288(3\alpha^2 + 2\alpha + 3) \left(\frac{e}{k}\right)^3 - 864(\alpha^2 + 1) \left(\frac{e}{k}\right)^4$$

Incorporating the above limiting values of a_{11} , a_{12} and a_{22} into equation (D5) and letting f approach zero in equations (D6) leads to the following expression for $\delta(TPE)$:

$$\begin{aligned} \delta(TPE) &= (\delta u_0) \cdot \int_{-b}^b (2c_{00}u_0 + 2c_{01}u_1 - \frac{F}{b}) dz \\ &+ 2 \int_{-b}^b (-b_{11} \frac{d^2 u_1}{dz^2} + c_{01}u_0 + c_{11}u_1 + \frac{1}{2} d_{11} \frac{dv_2}{dz} \frac{\cos\theta}{\sin^2\theta}) (\delta u_1) dz \\ &+ 2 \int_{-b}^b [(\tilde{a}_{11} \frac{\cos^2\theta}{\sin^4\theta} + 2\tilde{a}_{12} \frac{\cos\theta}{\sin^2\theta} + \tilde{a}_{22}) v_2 - \frac{1}{2} d_{11} \frac{du_1}{dz} \frac{\cos\theta}{\sin^2\theta} \\ &\quad - (\tilde{e}'_{11} \frac{\cos^2\theta}{\sin^4\theta} + 2\tilde{e}'_{12} \frac{\cos\theta}{\sin^2\theta} + \tilde{e}'_{22}) \frac{d^2 v_2}{dz^2}] (\delta v_2) dz \\ &+ (2b_{11} \frac{du_1}{dz} \delta u_1) \Big|_{-b}^b \\ &+ \left[d_{11}u_1 \frac{\cos\theta}{\sin^2\theta} + 2(\tilde{e}'_{11} \frac{\cos^2\theta}{\sin^4\theta} + 2\tilde{e}'_{12} \frac{\cos\theta}{\sin^2\theta} + \tilde{e}'_{22}) \frac{dv_2}{dz} \right] (\delta v_2) \Big|_{-b}^b \end{aligned} \quad (D9)$$

where

$$\begin{aligned}\tilde{e}_{11}' &= G k \sin^2 \theta + G' \left(\frac{J_1}{2} + \frac{J_2}{k^2} \cos^2 \theta \right) \\ \tilde{e}_{22}' &= G' \frac{J_2}{k^2} \\ \tilde{e}_{12}' &= G' \frac{J_2}{k^2} \cos \theta\end{aligned}\tag{D10}$$

Differential equations and boundary conditions.— From the vanishing of the $\delta(TPE)$, equation (D9), the following conditions are obtained, analogous to equations (B8) through (B11):

$$4c_{00}u_0^b + 2c_{01} \int_{-b}^b u_1 dz - 2F = 0\tag{D11}$$

$$-b_{11} \frac{d^2 u_1}{dz^2} + c_{01}u_0 + c_{11}u_1 + \frac{1}{2} d_{11} \frac{\cos \theta}{\sin^2 \theta} \frac{dv_2}{dz} = 0\tag{D12}$$

$$a_{22}' v_2 - \frac{1}{2} d_{11} \frac{\cos \theta}{\sin^2 \theta} \frac{du_1}{dz} - e_{22}' \frac{d^2 v_2}{dz^2} = 0$$

$$\left(\frac{du_1}{dz} \right)_{z = \pm b} = 0\tag{D13}$$

$$\left(d_{11}u_1 \frac{\cos \theta}{\sin^2 \theta} + 2e_{22}' \frac{dv_2}{dz} \right)_{z = \pm b} = 0\tag{D14}$$

where

$$\begin{aligned}a_{22}' &\equiv \tilde{a}_{11} \frac{\cos^2 \theta}{\sin^4 \theta} + 2\tilde{a}_{12} \frac{\cos \theta}{\sin^2 \theta} + \tilde{a}_{22} \\ e_{22}' &\equiv \tilde{e}_{11} \frac{\cos^2 \theta}{\sin^4 \theta} + 2\tilde{e}_{12} \frac{\cos \theta}{\sin^2 \theta} + \tilde{e}_{22}\end{aligned}\tag{D15}$$

The above equations apply to the case of point attachments at the ends of the trough lines only (fig. 3(a)). For the case in which there are also point attachments at the ends of the crest lines (fig. 3(b)), equation (D14) must be replaced by

$$v_2(\pm b) = 0 \quad (D16)$$

This replacement must be made also for the case in which there are wide attachments at the ends of the trough lines (fig. 3(d)).

Solution of the differential equations.— Equations (D12) have the particular solution

$$\begin{aligned} u_1 &= -\frac{c_{01}}{c_{11}} u_0 \\ v_2 &= 0 \end{aligned} \quad (D17)$$

To this must be added the complementary solution, which is the solution of the homogeneous system obtained by omitting the term $c_{01} u_0$ from the first of equations (D12). As in the general case, solutions of the homogeneous system will be sought in the form

$$\begin{aligned} u_1 &= \tilde{A}' e^{\tilde{r}z} \\ v_2 &= \tilde{D}' e^{\tilde{r}z} \end{aligned} \quad (D18)$$

Substitution of this assumption into equations (D12) with the u_0 term omitted leads to the following conditions on \tilde{A}' , \tilde{D}' and \tilde{r} :

$$\begin{bmatrix} b_{11}\tilde{r}^2 - c_{11} & -\frac{1}{2}d_{11}\frac{\cos\theta}{\sin^2\theta}\tilde{r} \\ -\frac{1}{2}d_{11}\frac{\cos\theta}{\sin^2\theta}\tilde{r} & a'_{22} - e'_{22}\tilde{r}^2 \end{bmatrix} \begin{bmatrix} \tilde{A}' \\ \tilde{D}' \end{bmatrix} = \begin{bmatrix} 0 \\ 0 \end{bmatrix} \quad (D19)$$

which leads to the following characteristic equation for \tilde{r} :

$$\begin{vmatrix} b_{11}\tilde{r}^2 - c_{11} & -\frac{1}{2}d_{11}\frac{\cos\theta}{\sin^2\theta}\tilde{r} \\ -\frac{1}{2}d_{11}\frac{\cos\theta}{\sin^2\theta}\tilde{r} & a'_{22} - e'_{22}\tilde{r}^2 \end{vmatrix} = 0 \quad (D20)$$

or

$$[\tilde{k}_{02}(\frac{t}{e})^2] + [\tilde{k}_{20} + \tilde{k}_{22}(\frac{t}{e})^2] \tilde{R}^2 + [\tilde{k}_{40} + \tilde{k}_{42}(\frac{t}{e})^2] \tilde{R}^4 = 0 \quad (D21)$$

where

$$\tilde{R} \equiv e\tilde{r} \quad (D22)$$

$$\begin{aligned} \tilde{k}_{02} &= -\frac{G}{E} (1 + \frac{e}{k}) \tilde{a}_{22}^* \\ \tilde{k}_{20} &= (\frac{G}{E})^2 \frac{k}{e} \cot^2 \theta \\ \tilde{k}_{22} &= \frac{1}{3} \frac{E}{E} (1 + \frac{k}{e}) \tilde{a}_{22}^* + \frac{G}{E} (1 + \frac{e}{k}) \tilde{e}_{22}^* \\ \tilde{k}_{40} &= -\frac{1}{3} \frac{G}{E} \frac{E}{E} (1 + \frac{k}{e}) \frac{k}{e} \cot^2 \theta \\ \tilde{k}_{42} &= -\frac{1}{3} \frac{E}{E} (1 + \frac{k}{e}) \tilde{e}_{22}^* \end{aligned} \quad (D23)$$

with

$$\begin{aligned} \tilde{a}_{22}^* &\equiv \frac{1}{12(1-\nu^2) \tilde{\beta}^2 \sin^4 \theta} [\tilde{A}_{11} \cos^2 \theta - \tilde{A}_{12} \frac{e}{k} \cos \theta + \tilde{A}_{22} (\frac{e}{k})^2] \\ \tilde{e}_{22}^* &\equiv \frac{1}{3} \frac{G}{E} \cdot \frac{\cos^2 \theta + \frac{e}{k}}{\sin^4 \theta} \end{aligned} \quad (D24)$$

Equation (D21) will have four roots for \tilde{R} , two of them being the negatives of the other two. For any geometries of interest the roots will all be real. Denoted by \tilde{R}_1 , \tilde{R}_2 , \tilde{R}_3 and \tilde{R}_4 , they can be represented as

$$\begin{aligned} \tilde{R}_1 &= \tilde{X} \\ \tilde{R}_2 &= -\tilde{X} \\ \tilde{R}_3 &= \tilde{Y} \\ \tilde{R}_4 &= -\tilde{Y} \end{aligned} \quad (D25)$$

where \tilde{X} and \tilde{Y} are real members.

The following series expansions for \tilde{X} and \tilde{Y} are readily obtained:

$$\begin{aligned}\tilde{X} &= \tilde{q}_0 + \tilde{q}_2 \left(\frac{t}{e}\right)^2 + \tilde{q}_4 \left(\frac{t}{e}\right)^4 + \dots \\ \tilde{Y} &= \tilde{p}_1 \frac{t}{e} + \tilde{p}_3 \left(\frac{t}{e}\right)^3 + \tilde{p}_5 \left(\frac{t}{e}\right)^5 + \dots\end{aligned}\quad (D26)$$

where

$$\begin{aligned}\tilde{q}_0 &= +\sqrt{-\tilde{k}_{20}/\tilde{k}_{40}} \quad (\text{real}) \\ \tilde{q}_2 &= -\frac{\tilde{k}_{02} + \tilde{k}_{22} \tilde{q}_0^2 + \tilde{k}_{42} \tilde{q}_0^4}{2 \tilde{q}_0 \tilde{k}_{20} + 4 \tilde{q}_0^3 \tilde{k}_{40}} \\ \tilde{q}_4 &= -\frac{\tilde{k}_{20} \tilde{q}_2^2 + 2 \tilde{k}_{22} \tilde{q}_0 \tilde{q}_2 + 6 \tilde{k}_{40} \tilde{q}_0^2 \tilde{q}_2^2 + 4 \tilde{k}_{42} \tilde{q}_0^3 \tilde{q}_2}{2 \tilde{q}_0 \tilde{k}_{20} + 4 \tilde{q}_0^3 \tilde{k}_{40}} \\ &\dots\end{aligned}\quad (D27)$$

$$\begin{aligned}\tilde{p}_1 &= +\sqrt{-\tilde{k}_{02}/\tilde{k}_{20}} \quad (\text{real}) \\ \tilde{p}_3 &= -\frac{\tilde{k}_{22} \tilde{p}_1 + \tilde{k}_{40} \tilde{p}_1^3}{2 \tilde{k}_{20}} \\ \tilde{p}_5 &= -\frac{\tilde{k}_{20} \tilde{p}_3^2 + 2 \tilde{k}_{22} \tilde{p}_1 \tilde{p}_3 + 4 \tilde{k}_{40} \tilde{p}_1^2 \tilde{p}_3 + \tilde{k}_{42} \tilde{p}_1^4}{2 \tilde{k}_{20} \tilde{p}_1} \\ &\dots\end{aligned}\quad (D28)$$

Corresponding to any root $\tilde{R} = \tilde{R}_j$ there is a relationship between \tilde{A}' and \tilde{D}' which can be obtained by substituting $\tilde{r} = \tilde{r}_j = \tilde{R}_j/e$ into the first of equations (D19). Letting \tilde{A}'_j and \tilde{D}'_j denote the values of \tilde{A}' and \tilde{D}' associated with $\tilde{R} = \tilde{R}_j$, this relationship can be written as

$$\frac{\tilde{D}'_j}{\tilde{A}'_j} = \tilde{\gamma}_j \quad (D29)$$

where

$$\tilde{\gamma}_j \equiv \left[\frac{1}{\tilde{R}_j} \left(1 + \frac{e}{k}\right) - \frac{1}{3} \tilde{R}_j \frac{E}{G} \left(1 + \frac{k}{e}\right) \right] \tan \theta \quad (D30)$$

Taking into account equations (D25), it follows that

$$\begin{aligned}\tilde{\gamma}_1 &= -\tilde{\gamma}_2 = \left[\frac{1}{\tilde{x}} \left(1 + \frac{e}{k} \right) - \frac{\tilde{x}}{3} \frac{E'}{G} \left(1 + \frac{k}{e} \right) \right] \tan \theta \\ \tilde{\gamma}_3 &= -\tilde{\gamma}_4 = \left[\frac{1}{\tilde{y}} \left(1 + \frac{e}{k} \right) - \frac{\tilde{y}}{3} \frac{E'}{G} \left(1 + \frac{k}{e} \right) \right] \tan \theta\end{aligned}\quad (D31)$$

Summation of the four solutions of the form of equations (D18) leads to the following complete complementary solution:

$$\begin{aligned}u_1 &= \tilde{A}_1 e^{\frac{\tilde{x}z}{e}} + \tilde{A}_2 e^{-\frac{\tilde{x}z}{e}} + \tilde{A}_3 e^{\frac{\tilde{y}z}{e}} + \tilde{A}_4 e^{-\frac{\tilde{y}z}{e}} \\ v_2 &= \tilde{\gamma}_1 \left(\tilde{A}_1 e^{\frac{\tilde{x}z}{e}} - \tilde{A}_2 e^{-\frac{\tilde{x}z}{e}} \right) + \tilde{\gamma}_3 \left(\tilde{A}_3 e^{\frac{\tilde{y}z}{e}} - \tilde{A}_4 e^{-\frac{\tilde{y}z}{e}} \right)\end{aligned}\quad (D32)$$

Expressing the exponential functions in terms of hyperbolic functions, discarding the terms which do not have the proper symmetry (in the case of u_2) or antisymmetry (in the case of v_2) with respect to z , and adding the particular solution, equations (D17), one obtains the following complete solution for the displacements $u_1(z)$ and $v_2(z)$:

$$\begin{aligned}u_1 &= -\frac{c_{01}}{c_{11}} u_0 + \bar{A}_1 \cosh \frac{\tilde{x}z}{e} + \bar{A}_3 \cosh \frac{\tilde{y}z}{e} \\ v_2 &= \tilde{\gamma}_1 \bar{A}_1 \sinh \frac{\tilde{x}z}{e} + \tilde{\gamma}_3 \bar{A}_3 \sinh \frac{\tilde{y}z}{e}\end{aligned}\quad (D33)$$

where \bar{A}_1 and \bar{A}_3 are new arbitrary constants, to be determined from the boundary conditions, and $-c_{01}/c_{11}$ equals $(1 + \frac{e}{k})^{-1}$, in accordance with equations (8).

Evaluation of the arbitrary constants.— For the case of point attachments at the ends of the trough lines only (fig. 3(a)), the boundary conditions are equations (D13) and (D14). Substitution of (D33) into those equations leads to the following equations defining \bar{A}_1 and \bar{A}_3 :

$$\begin{bmatrix} P_{11} & P_{12} \\ P_{21} & P_{22} \end{bmatrix} \begin{bmatrix} \frac{\bar{A}_1}{u_0} \sinh \frac{\tilde{x}b}{e} \\ \frac{\bar{A}_3}{u_0} \sinh \frac{\tilde{y}b}{e} \end{bmatrix} = \begin{bmatrix} 0 \\ P_2 \end{bmatrix} \quad (D34)$$

where

$$\begin{aligned} P_{11} &= \tilde{x} \\ P_{12} &= \tilde{y} \\ P_{21} &= \left[- (1 - \tilde{\gamma}_1 \tilde{x} \frac{k}{e} \cot \theta) \cot \theta \right. \\ &\quad \left. + \frac{1}{3} \left(\frac{t}{e} \right)^2 \frac{G'}{G} \tilde{\gamma}_1 \tilde{x} \left(\frac{e}{k} + \cos^2 \theta \right) \csc^4 \theta \right] \coth \frac{\tilde{x}b}{e} \\ P_{22} &= \left[- (1 - \tilde{\gamma}_3 \tilde{y} \frac{k}{e} \cot \theta) \cot \theta \right. \\ &\quad \left. + \frac{1}{3} \left(\frac{t}{e} \right)^2 \frac{G'}{G} \tilde{\gamma}_3 \tilde{y} \left(\frac{e}{k} + \cos^2 \theta \right) \csc^4 \theta \right] \coth \frac{\tilde{y}b}{e} \\ P_2 &= \frac{\cot \theta}{1 + \frac{e}{k}} \end{aligned} \quad (D35)$$

For the other two kinds of end attachment (figs. 3(b) and 3(d)), equation (D16) replaces (D14) as a boundary condition. This results in

$$\bar{A}_1 = \bar{A}_3 = 0 \quad (D36)$$

which makes the particular solution (D17) also the complete solution and implies that the corrugation sheet is in a state of uniform shear like that obtainable by continuous attachment. This case therefore requires no further analysis, and the remainder of this appendix will pertain only to the case of point attachments at the ends of the trough lines (fig. 3(a)).

Relationship between F and u_0 .— With $u_1(z)$ now known in terms of u_0 , equation (D11) yields the following relationship between shearing force F and relative shearing displacement $2u_0$ of the sides of the corrugation:

$$\frac{F}{2u_0} = \frac{Gtb}{e} \tilde{\psi} \quad (D37)$$

where

$$\tilde{\psi} = 1 - \frac{1}{1 + \frac{e}{k}} - \left(\frac{\bar{A}_1}{u_0} \sinh \frac{\tilde{X}b}{e} \right) \frac{e}{\tilde{X}b} - \left(\frac{\bar{A}_3}{u_0} \sinh \frac{\tilde{Y}b}{e} \right) \frac{e}{\tilde{Y}b} \quad (D38)$$

As in the general case, relative shear stiffnesses and an effective shear modulus can be defined. Equations (37) through (46) of the body of the paper still apply with f set equal to zero and ψ replaced by $\tilde{\psi}$.

Stresses.— The longitudinal normal stresses are

$$\sigma_{\textcircled{1}} = E \frac{du_1}{dz} \quad (D39)$$

at junction $\textcircled{1}$ and zero at the other junctions. Eliminating u_1 through equation (D33) gives

$$\frac{\sigma_{\textcircled{1}} e}{E u_0} = \frac{\bar{A}_1}{u_0} \tilde{X} \sinh \frac{\tilde{X}z}{e} + \frac{\bar{A}_3}{u_0} \tilde{Y} \sinh \frac{\tilde{Y}z}{e} \quad (D40)$$

The middle-surface shearing stresses, obtained with the aid of table 2 and equations (D33), are given in dimensionless form as follows:

$$\frac{\tau_{01} e}{G u_0} = - \frac{1}{1 + \frac{k}{e}} + \frac{\bar{A}_1}{u_0} \cosh \frac{\tilde{X}z}{e} + \frac{\bar{A}_3}{u_0} \cosh \frac{\tilde{Y}z}{e} \quad (D41a)$$

$$\frac{\tau_{12} e}{G u_0} = - \frac{1}{1 + \frac{k}{e}} + \frac{\bar{A}_1}{u_0} (\tilde{\gamma}_1 \tilde{X} \cot \theta - \frac{e}{k}) \cosh \frac{\tilde{X}z}{e} + \frac{\bar{A}_3}{u_0} (\tilde{\gamma}_3 \tilde{Y} \cot \theta - \frac{e}{k}) \cosh \frac{\tilde{Y}z}{e} \quad (D41b)$$

where the subscripts 01 and 12 refer to plate elements 01 and 12 respectively.

From the rates of twist in table 3 and the displacement equations (D33) the following equations are obtained for the extreme-fiber shearing stresses due to torsion, in plate elements 01 and 12 respectively:

$$\frac{\tau'_{01} e}{G u_0} = \frac{t}{e} \frac{\cos \theta}{\sin^2 \theta} W(z) \quad (D42)$$

$$\frac{\tau'_{12} e}{G u_0} = -\frac{t}{k} \frac{1}{\sin^2 \theta} W(z)$$

where

$$W(z) \equiv \left(\frac{\bar{A}_1}{u_0} \sinh \frac{\tilde{X}b}{e} \right) \frac{\tilde{\gamma}_1 \tilde{X} \cosh \frac{\tilde{X}z}{e}}{\sinh \frac{\tilde{X}b}{e}} + \left(\frac{\bar{A}_3}{u_0} \sinh \frac{\tilde{Y}b}{e} \right) \frac{\tilde{\gamma}_3 \tilde{Y} \cosh \frac{\tilde{Y}z}{e}}{\sinh \frac{\tilde{Y}b}{e}} \quad (D43)$$

The frame bending moments and associated extreme-fiber bending stresses will be zero at junctions (2) and (3) because in this special case these junctions meet to form a line of inflection points. The frame bending moments at junctions (0) and (1) can be obtained by first introducing condition (D2) into table A1, writing equations (A1) for M_{01} and M_{12} , and then letting $f \rightarrow \infty$ (not zero), as discussed earlier. The associated extreme-fiber stresses $\sigma'_{(0)}$ and $\sigma'_{(1)}$ are obtained by multiplying the bending moments by $6/t^2$. In this way the following results are obtained:

$$\frac{\sigma'_{(0)} e}{E u_0} = \frac{\alpha}{1 - \nu^2} \frac{t}{k} \frac{12 \cos \theta}{\beta \sin^2 \theta} \left(1 + \frac{e}{k} \right) \left(2 + \frac{e}{k} \right) \left(\frac{v_2}{u_0} \right) \quad (D44)$$

$$\frac{\sigma'_{(1)} e}{E u_0} = -\frac{6}{1 - \nu^2} \frac{t}{k} \frac{1}{\beta \sin^2 \theta} \left[3(1 + \alpha) \frac{e}{k} \cos \theta + (3 + \alpha) \left(\frac{e}{k} \right)^2 \right] \left(\frac{v_2}{u_0} \right)$$

in which, $\sigma'_{(0)}$ and $\sigma'_{(1)}$ are positive for compression in the upper fibers, tension in the lower fibers.

APPENDIX E

SPECIAL CASE: $e = 0$

For the special case $e = 0$ (fig. 10(c)) the plate elements at the troughs are of zero width, with the result that the two adjacent sloping plate elements meet to form a vertex along the trough line.

This special case can be obtained from the general case by first imposing along junction (1) the same displacement conditions as exist along junction (0), namely

$$u_1(z) = u_0 \quad (E1)$$

$$v_1(z) = 0 \quad (E2)$$

The condition

$$e \rightarrow 0 \quad (E3)$$

is then imposed to simulate the condition of clamping (zero rotation) along the trough lines; or the condition

$$e \rightarrow \infty \quad (E4)$$

in order to simulate a hinged attachment (free rotation) along the trough lines.

Applying the above procedure to equation (B4), the latter becomes

$$\begin{aligned} \delta(TPE) = & (\delta u_0) \cdot \int_{-b}^b \left(-\frac{F}{b} + 2\bar{c}_{00} u_0 + 2c_{12} u_2 \right) dz \\ & + 2 \int_{-b}^b \left(-b_{22} \frac{d^2 u_2}{dz^2} + c_{12} u_0 + c_{22} u_2 + \frac{1}{2} d_{22} \frac{dv_2}{dz} \right) (\delta u_2) dz \\ & + 2 \int_{-b}^b \left(\bar{a}_{22} v_2 - \frac{1}{2} d_{22} \frac{du_2}{dz} - e_{22} \frac{d^2 v_2}{dz^2} \right) (\delta v_2) dz \\ & + \left[2 b_{22} \frac{du_2}{dz} (\delta u_2) \right] \bigg|_{-b}^b + \left[\left(d_{22} u_2 + 2 e_{22} \frac{dv_2}{dz} \right) (\delta v_2) \right] \bigg|_{-b}^b \end{aligned} \quad (E5)$$

where

$$\bar{c}_{00} = Gt/k \quad (E6)$$

and \bar{a}_{22} has the following two different values, depending on whether the trough lines are prevented from rotating (condition (E3)) or free to rotate (condition (E4)):

$$\bar{a}_{22} = \frac{E}{2(1-\nu^2)} \left(\frac{t}{k}\right)^3 \left[\frac{1 + 6 \frac{k}{f} + 12 \left(\frac{k}{f}\right)^2 \cos\theta + 8 \left(\frac{k}{f}\right)^3 \cos^2\theta}{2 + 3 \frac{k}{f}} \right] \quad (E7a)$$

for rotation along trough lines prevented;

$$\bar{a}_{22} = \frac{E}{2(1-\nu^2)} \left(\frac{t}{k}\right)^3 \left[\frac{\frac{k}{f} \left(1 + 2 \frac{k}{f} \cos\theta\right)}{1 + 2 \frac{k}{f}} \right] \quad (E7b)$$

for freedom of rotation along the trough lines.

From the vanishing of $\delta(\text{TPE})$, equation (E5), the following equations governing u_2 and v_2 are obtained:

$$-2F + 4 \bar{c}_{00} u_0 b + 2 c_{12} \int_{-b}^b u_2 dz = 0 \quad (E8)$$

$$\left. \begin{aligned} -b_{22} \frac{d^2 u_2}{dz^2} + c_{12} u_0 + c_{22} u_2 + \frac{1}{2} d_{22} \frac{dv_2}{dz} &= 0 \\ \bar{a}_{22} v_2 - \frac{1}{2} d_{22} \frac{du_2}{dz} - e_{22} \frac{d^2 v_2}{dz^2} &= 0 \end{aligned} \right\} \quad (E9)$$

$$\left(\frac{du_2}{dz} \right)_{z = \pm b} = 0 \quad (E10)$$

$$\left(d_{22} u_2 + 2 e_{22} \frac{dv_2}{dz} \right)_{z = \pm b} = 0 \quad (E11)$$

The above development is for the case of attachments at the ends of the trough lines only (figs. 3(a) and 3(d)). With $e = 0$ the presence of additional attachments at the ends of the crest lines (fig. 3(b)) is tantamount to continuous attachment, within the framework of the present type of analysis. (A similar phenomenon was observed in appendix D for the case $f = 0$.)

Solution of the differential equations.— Equations (E9) have the particular solution

$$u_2 = -\frac{c_{12}}{c_{22}} u_0 \quad (\text{E12})$$

$$v_2 = 0$$

The terms of the complementary solution will be assumed in the form

$$\begin{aligned} u_2 &= \hat{A} e^{\hat{r}z} \\ v_2 &= \hat{D} e^{\hat{r}z} \end{aligned} \quad (\text{E13})$$

Substitution of these expressions into equations (E9) with the u_0 term omitted leads to the following conditions on \hat{A} , \hat{D} and \hat{r} :

$$\begin{bmatrix} b_{22} \hat{r}^2 - c_{22} & -\frac{1}{2} d_{22} \hat{r} \\ -\frac{1}{2} d_{22} \hat{r} & \bar{a}_{22} - e_{22} \hat{r}^2 \end{bmatrix} \begin{bmatrix} \hat{A} \\ \hat{D} \end{bmatrix} = \begin{bmatrix} 0 \\ 0 \end{bmatrix} \quad (\text{E14})$$

from which arises the following characteristic equation for \hat{r} :

$$\begin{vmatrix} b_{22} \hat{r}^2 - c_{22} & -\frac{1}{2} d_{22} \hat{r} \\ -\frac{1}{2} d_{22} \hat{r} & \bar{a}_{22} - e_{22} \hat{r}^2 \end{vmatrix} = 0 \quad (\text{E15})$$

or

$$\hat{k}_{02} \left(\frac{t}{k}\right)^2 + \left[\hat{k}_{20} + \hat{k}_{22} \left(\frac{t}{k}\right)^2 \right] \hat{R}^2 + \left[\hat{k}_{40} + \hat{k}_{42} \left(\frac{t}{k}\right)^2 \right] \hat{R}^4 = 0 \quad (\text{E16})$$

where

$$\hat{R} \equiv k\hat{r} \quad (\text{E17})$$

and

$$\begin{aligned}
 \hat{k}_{02} &= -\frac{G}{E} \left(1 + 2 \frac{k}{f}\right) \bar{a}_{22}^* \\
 \hat{k}_{20} &= \frac{1}{2} \left(\frac{G}{E}\right)^2 \frac{f}{k} \sin^2 \theta \\
 \hat{k}_{22} &= \frac{1}{6} \frac{E'}{E} \left(2 + \frac{f}{k}\right) \bar{a}_{22}^* + \frac{1}{3} \frac{G}{E} \frac{G'}{E} \left(1 + 2 \frac{k}{f}\right) \left(1 + 2 \frac{k}{f} \cos^2 \theta\right) \\
 \hat{k}_{40} &= -\frac{1}{12} \frac{E'}{E} \frac{G}{E} \left(2 + \frac{f}{k}\right) \frac{f}{k} \sin^2 \theta \\
 \hat{k}_{42} &= -\frac{1}{18} \frac{E'}{E} \frac{G'}{E} \left(2 + \frac{f}{k}\right) \left(1 + 2 \frac{k}{f} \cos^2 \theta\right)
 \end{aligned} \tag{E18}$$

with

$$\bar{a}_{22}^* \equiv \frac{1 + 6 \frac{k}{f} + 12 \left(\frac{k}{f}\right)^2 \cos \theta + 8 \left(\frac{k}{f}\right)^3 \cos^2 \theta}{2(1-\nu^2) \left(2 + 3 \frac{k}{f}\right)} \tag{E19a}$$

for the case in which the trough lines are clamped, or

$$\bar{a}_{22}^* \equiv \frac{\frac{k}{f} \left(1 + 2 \frac{k}{f} \cos \theta\right)^2}{2(1-\nu^2) \left(1 + 2 \frac{k}{f}\right)} \tag{E19b}$$

for the case in which the trough lines are free to rotate.

Equation (E16) will have four real roots, \hat{R}_1 , \hat{R}_2 , \hat{R}_3 and \hat{R}_4 , representable in the following form:

$$\hat{R}_1 = \hat{X}, \quad \hat{R}_2 = -\hat{X}, \quad \hat{R}_3 = \hat{Y}, \quad \hat{R}_4 = -\hat{Y} \tag{E20}$$

where \hat{X} and \hat{Y} are real numbers. Series expansions may be used, if desired, for the evaluation of \hat{X} and \hat{Y} . These expansions are

$$\begin{aligned}
 \hat{X} &= \hat{q}_0 + \hat{q}_2 \left(\frac{t}{k}\right)^2 + \hat{q}_4 \left(\frac{t}{k}\right)^4 + \dots \\
 \hat{Y} &= \hat{p}_1 \frac{t}{k} + \hat{p}_3 \left(\frac{t}{k}\right)^3 + \hat{p}_5 \left(\frac{t}{k}\right)^5 + \dots
 \end{aligned} \tag{E21}$$

where $\hat{q}_0, \hat{q}_2, \dots$ and $\hat{p}_1, \hat{p}_3, \dots$ are defined by equations (D27) and (D28) with all tildes (\sim) replaced by circumflex accents (\wedge).

Letting \hat{A}_j and \hat{D}_j denote the values of \hat{A} and \hat{D} associated with the root $\hat{R} = \hat{R}_j$, the relationship between them can be obtained from the first of equations (E14). It is

$$\frac{\hat{D}_j}{\hat{A}_j} = \hat{\gamma}_j \quad (\text{E22})$$

where

$$\hat{\gamma}_j = \left[\frac{1}{\hat{R}_j} \left(1 + 2 \frac{k}{f} \right) - \frac{1}{6} \hat{R}_j \frac{E'}{G} \left(2 + \frac{f}{k} \right) \right] \frac{1}{\sin \theta} \quad (\text{E23})$$

Taking into account equations (E20), it follows that

$$\begin{aligned} \hat{\gamma}_1 &= -\hat{\gamma}_2 = \left[\frac{1}{\hat{X}} \left(1 + 2 \frac{k}{f} \right) - \frac{1}{6} \hat{X} \frac{E'}{G} \left(2 + \frac{f}{k} \right) \right] \frac{1}{\sin \theta} \\ \hat{\gamma}_3 &= -\hat{\gamma}_4 = \left[\frac{1}{\hat{Y}} \left(1 + 2 \frac{k}{f} \right) - \frac{1}{6} \hat{Y} \frac{E'}{G} \left(2 + \frac{f}{k} \right) \right] \frac{1}{\sin \theta} \end{aligned} \quad (\text{E24})$$

Summing the four solutions of the form of equations (E13), adding the particular solution, equations (E12), and taking into account the fact that u_2 must be even in z , u_2 odd in z , one arrives at the following complete solution of the differential equations (E9):

$$\begin{aligned} u_2 &= -\frac{c_{12}}{c_{22}} u_0 + A_1^* \cosh \frac{\hat{X}z}{k} + A_3^* \cosh \frac{\hat{Y}z}{k} \\ v_2 &= \hat{\gamma}_1 A_1^* \sinh \frac{\hat{X}z}{k} + \hat{\gamma}_3 A_3^* \sinh \frac{\hat{Y}z}{k} \end{aligned} \quad (\text{E25})$$

where A_1^*, A_3^* are arbitrary constants to be evaluated from the boundary conditions, and $-c_{12}/c_{22}$ equals $(1 + 2 \frac{k}{f})^{-1}$, in accordance with equations (8).

Evaluation of the arbitrary constants.— The boundary conditions (E10) and (E11) lead to the following equations defining A_1^* and A_3^* :

$$\begin{bmatrix} Q_{11} & Q_{12} \\ Q_{21} & Q_{22} \end{bmatrix} \begin{bmatrix} \frac{A_1^*}{u_0} \sinh \frac{\hat{X}b}{k} \\ \frac{A_3^*}{u_0} \sinh \frac{\hat{Y}b}{k} \end{bmatrix} = \begin{bmatrix} 0 \\ Q_2 \end{bmatrix} \quad (E26)$$

where

$$\begin{aligned} Q_{11} &= \hat{X} \\ Q_{12} &= \hat{Y} \\ Q_{21} &= \left[(-2 \sin \theta + \hat{\gamma}_1 \hat{X} \frac{f}{k} \sin^2 \theta) + \frac{2}{3} \left(\frac{t}{k} \right)^2 \frac{G'}{G} \hat{\gamma}_1 \hat{X} (1 + 2 \frac{k}{f} \cos^2 \theta) \right] \coth \frac{\hat{X}b}{k} \\ Q_{22} &= \left[(-2 \sin \theta + \hat{\gamma}_3 \hat{Y} \frac{f}{k} \sin^2 \theta) + \frac{2}{3} \left(\frac{t}{k} \right)^2 \frac{G'}{G} \hat{\gamma}_3 \hat{Y} (1 + 2 \frac{k}{f} \cos^2 \theta) \right] \coth \frac{\hat{Y}b}{k} \\ Q_2 &= \frac{2 \sin \theta}{1 + 2 \frac{k}{f}} \end{aligned} \quad (E27)$$

Relationship between F and u_0 .— With $u_2(z)$ now known in terms of u_0 , equation (E8) yields the following relationship between the shearing force F and the relative shearing displacement $2u_0$:

$$\frac{F}{2u_0} = \frac{Gtb}{k} \hat{\psi} \quad (E28)$$

where

$$\begin{aligned} \hat{\psi} &= 1 - \frac{1}{1 + 2 \frac{k}{f}} - \left(\frac{A_1^*}{u_0} \sinh \frac{\hat{X}b}{k} \right) \frac{k}{\hat{X}b} \\ &\quad - \left(\frac{A_3^*}{u_0} \sinh \frac{\hat{Y}b}{k} \right) \frac{k}{\hat{Y}b} \end{aligned} \quad (E29)$$

The ratio Ω of the shearing stiffness (E28) to that of the same corrugation with continuous end attachment producing uniform middle-surface shear strain throughout the sheet is given by

$$\Omega = \left(1 + \frac{1}{2} \frac{f}{k} \right) \hat{\psi} \quad (E30)$$

On the other hand, the ratio Ω' of the shearing stiffness (E28) to that of a uniformly sheared flat plate of thickness t , length $2b$, and width p is

$$\Omega' = (\cos\theta + \frac{1}{2} \frac{f}{k}) \hat{\psi} \quad (E31)$$

Defining an effective shear modulus G_{eff} as the ratio of the average shear stress $F/2bt$ to the average shear strain $2u_0/p$, it is easily seen that

$$G_{\text{eff}} = G \Omega' \quad (E32)$$

Stresses.— The longitudinal normal stresses $\sigma_{\text{②}}$ along junction ②, obtained from the strains du_2/dz , are given in dimensionless form by

$$\frac{\sigma_{\text{②}}^k}{E' u_0} = \frac{A_1^*}{u_0} \hat{X} \sinh \frac{\hat{X}z}{k} + \frac{A_3^*}{u_0} \hat{Y} \sinh \frac{\hat{Y}z}{k} \quad (E33)$$

The dimensionless middle-surface shearing stresses, as obtained from table 2 and equations (E25), are given by

$$\frac{\tau_{12}^k}{G u_0} = \frac{u_2(z)}{u_0} - 1 \quad (E34)$$

$$\frac{\tau_{23}^k}{G u_0} = -2 \frac{k}{f} \frac{u_2(z)}{u_0} + \sin\theta \cdot (\hat{\gamma}_1 \hat{X} \hat{A}_1^* \cosh \frac{\hat{X}z}{k} + \hat{\gamma}_3 \hat{Y} \hat{A}_3^* \cosh \frac{\hat{Y}z}{k})$$

From the rates of twist in table 3 and equations (E25) the following equations are obtained for the extreme-fiber shearing stresses τ'_{12} , τ'_{23} due to twisting of the plate elements 12 and 23 respectively:

$$\frac{\tau'_{12}^k}{G' u_0} = - \frac{t}{k} \bar{W}(z) \quad (E35)$$

$$\frac{\tau'_{23}^k}{G' u_0} = 2 \frac{t}{f} \cos\theta \bar{W}(z)$$

where

$$\bar{W}(z) = \hat{\gamma}_1 \hat{X} \hat{A}_1^* \cosh \frac{\hat{X}z}{k} + \hat{\gamma}_3 \hat{Y} \hat{A}_3^* \cosh \frac{\hat{Y}z}{k} \quad (E36)$$

The frame bending moments at junctions ① and ② can be obtained by introducing condition (E2) into table A1, then writing equations (A1) for M_{12} and M_{23} , and then letting $e \rightarrow 0$ if the trough lines are restrained against rotation or $e \rightarrow \infty$ if they are free to rotate. The resulting bending moments are then multiplied by $6/t^2$ to obtain the associated extreme-fiber bending stresses σ'_1 and σ'_2 . The results are as follows:

$$\begin{aligned} \frac{\sigma'_1 k}{E u_0} &= \frac{3}{1 - \nu^2} \frac{t}{k} \left[\frac{1 - 2 \cos \theta}{2 + 3 \frac{k}{f}} - 1 \right] \frac{v_2(z)}{u_0} \\ \frac{\sigma'_2 k}{E u_0} &= \frac{3}{1 - \nu^2} \frac{t}{f} \left[\frac{3 - 6 \left(\frac{k}{f}\right)^2 \cos \theta}{2 + 3 \frac{k}{f}} + 2 \frac{k}{f} \cos \theta \right] \frac{v_2(z)}{u_0} \end{aligned} \quad (E37)$$

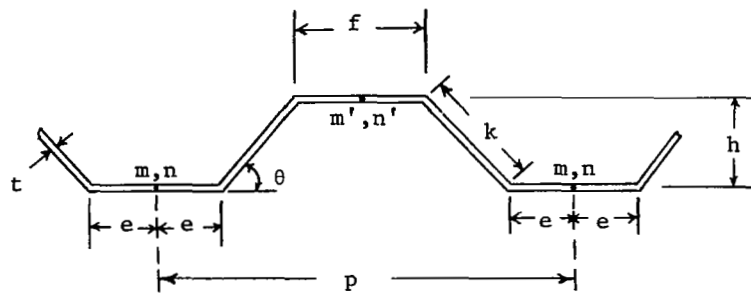
when the trough lines are restrained against rotating; and

$$\begin{aligned} \frac{\sigma'_1 k}{E u_0} &= 0 \\ \frac{\sigma'_2 k}{E u_0} &= \frac{3}{1 - \nu^2} \frac{t}{f} \frac{1 + 2 \frac{k}{f} \cos \theta}{1 + 2 \frac{k}{f}} \frac{v_2(z)}{u_0} \end{aligned} \quad (E38)$$

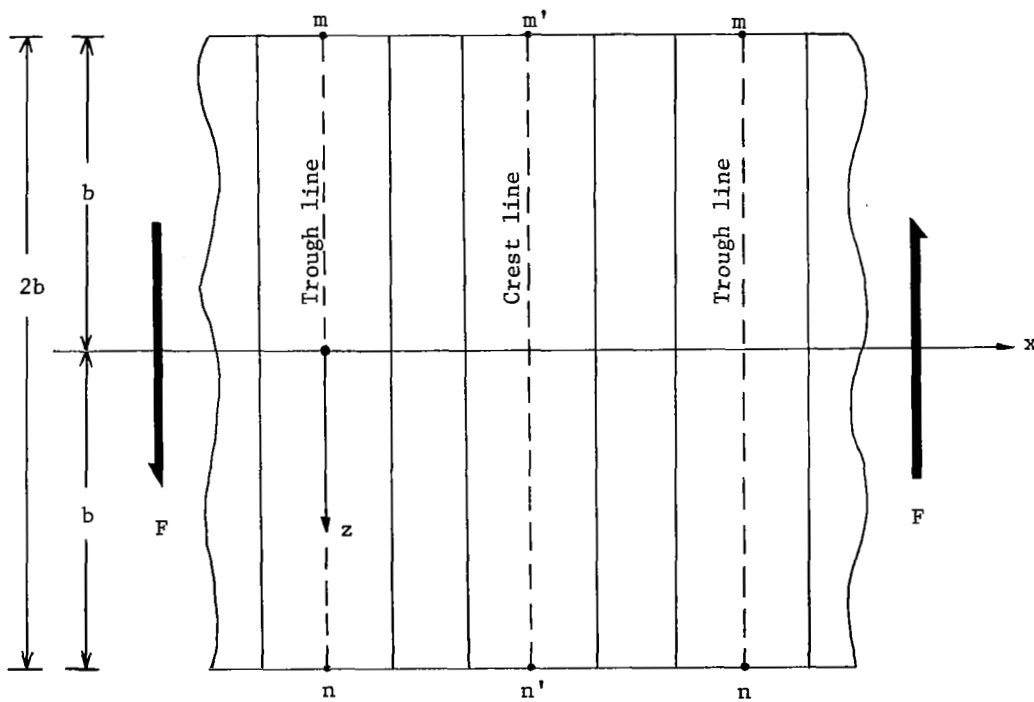
when the trough lines are free to rotate.

REFERENCES

1. Bryan, E.R.: and El-Dakhakhni, W.M.: Shear Flexibility and Strength of Corrugated Decks. J. of the Structural Division, Proc. ASCE, vol. 94, no. ST 11, Nov. 1968, pp. 2549-2580.
2. Bryan, E.R.; and Jackson, P.: The Shear Behavior of Corrugated Steel Sheeting. In "Thin Walled Steel Structures: their design and use in buildings," K.C. Rokey and H.V. Hill, eds., Crosby Lockwood(London), Gordon and Breach (New York), 1969 (Proceedings of a symposium held in Sept. 1967).
3. Houbolt, J.C.; and Stowell, E.Z.: Critical Stress of Plate Columns. NACA TN 2163, 1950.
4. Argyris, J.H.; and Kelsey, S.: Energy Theorems and Structural Analysis. Butterworths (London), 1960.
5. Timoshenko, S.P.; and Goodier, J.N.: Theory of Elasticity. Second ed., McGraw-Hill Book Co., Inc., 1951, p. 273.
6. McKenzie, K.I.: The Shear Stiffness of a Corrugated Web. R. & M. No. 3342, British A.R.C., 1963.
7. Falkenburg, J.C.: Shear Flexibility and Strength of Corrugated Decks. (Discussion of reference 1.) J. of the Structural Division, Proc. ASCE, vol. 95, no. ST 6, June 1969, pp. 1382-1386.

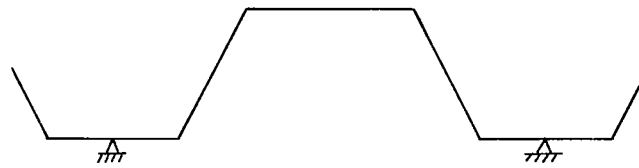


(a) Cross section

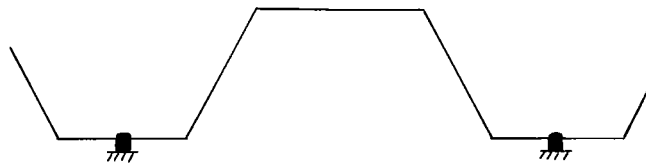


(b) Plan view

Figure 1. - Configuration of trapezoidally corrugated plate considered in the present analysis.



(a) Complete freedom of rotation

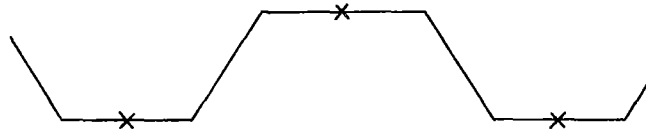


(b) Clamping

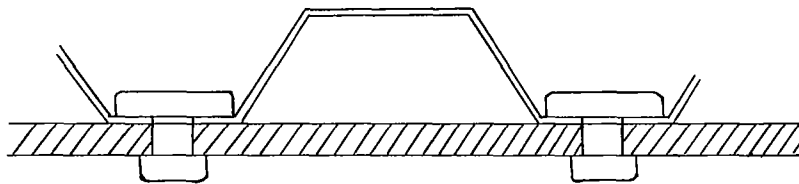
Figure 2. - Types of external restraint against rotation considered along the trough lines.



(a) Point attachment at the ends of the trough lines.



(b) Point attachment at the ends of the trough lines and crest lines.



(c) Wide attachment at ends of trough lines only.



(d) Idealization of (c) used in the analysis: Point attachments at the ends of the trough lines, and point attachments permitting longitudinal sliding at the junctions of the trough plate elements and the inclined plate elements.

Figure 3. - Types of attachment considered at the ends of the corrugations.

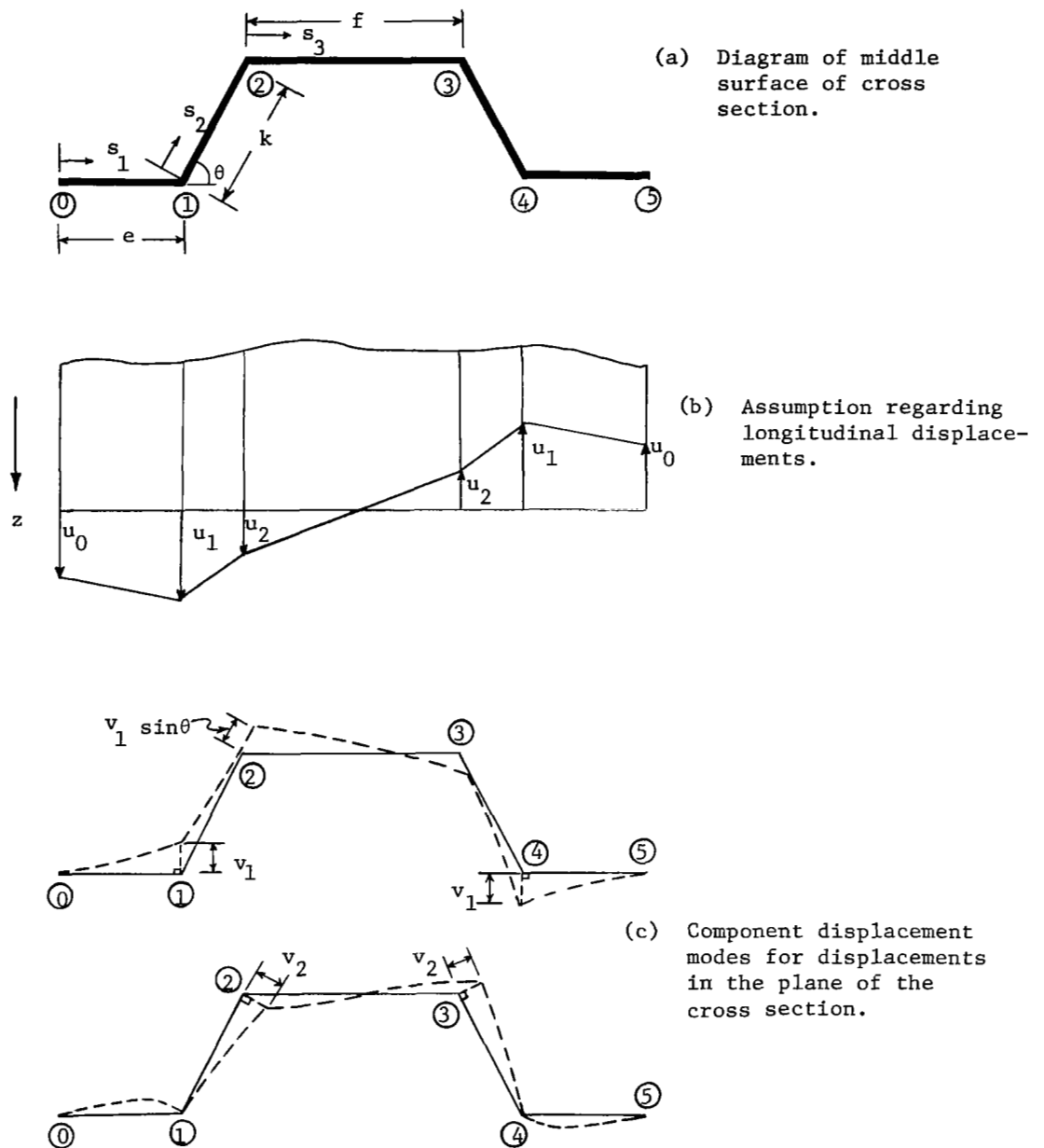


Figure 4. - Diagrammatic representation of assumptions regarding displacements.

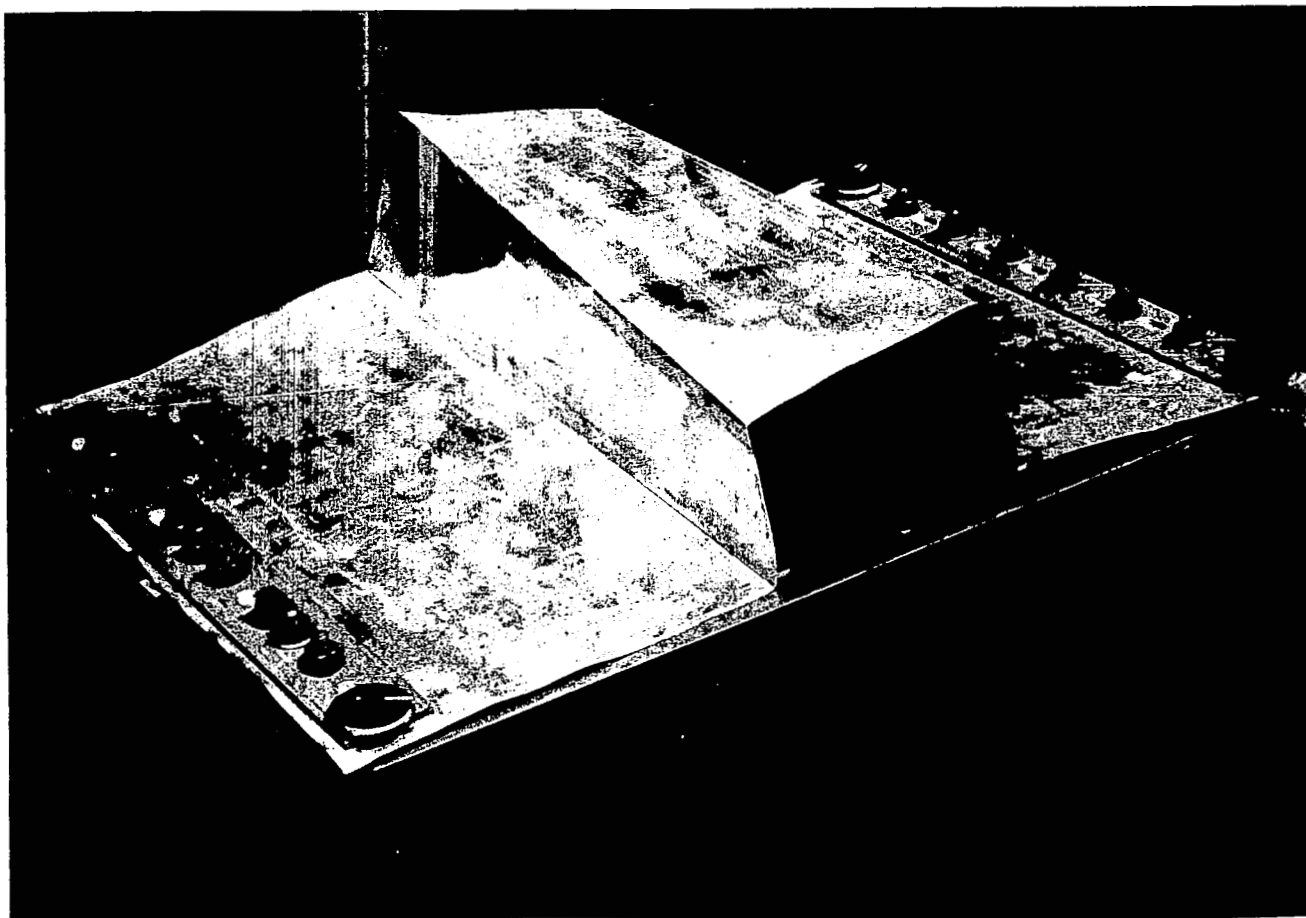


Figure 5. - Photograph showing flexural deformations during shearing of a single corrugation (from ref. 1).

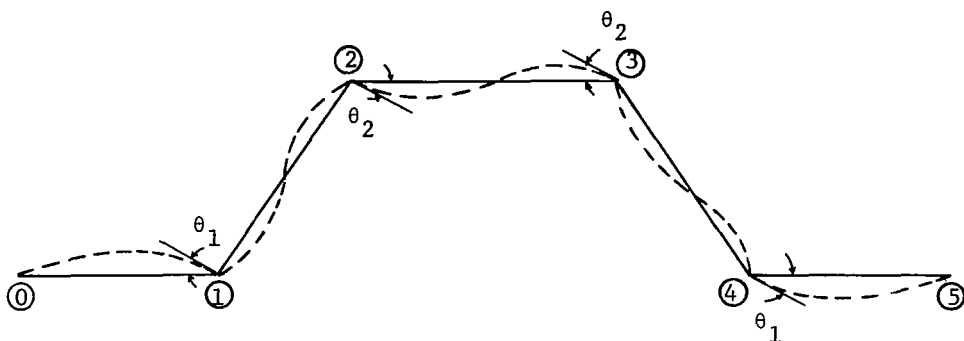


Figure 6. - Sign convention for joint rotations assumed in the analysis for strain energy of frame bending.

$$\begin{aligned}
 M_L = \alpha \cdot \frac{6D}{L} \frac{\Delta}{L} & \left\{ \begin{array}{l} \begin{array}{l} \text{Diagram 1: Clamped left end, deflection } \Delta \text{ at right end.} \\ M_L = \frac{6D}{L} \frac{\Delta}{L}, \quad M_R = \frac{6D}{L} \frac{\Delta}{L} \end{array} \\ \begin{array}{l} \text{Diagram 2: Hinged left end, deflection } \Delta \text{ at right end.} \\ M_L = 0, \quad M_R = \frac{3D}{L} \frac{\Delta}{L} \end{array} \end{array} \right\} M_R = \frac{3(1+\alpha)D}{L} \frac{\Delta}{L} \\
 \\
 M_L = \alpha \cdot \frac{2D}{L} \theta & \left\{ \begin{array}{l} \begin{array}{l} \text{Diagram 3: Clamped left end, rotation } \theta \text{ at right end.} \\ M_L = \frac{2D}{L} \theta, \quad M_R = \frac{4D}{L} \theta \end{array} \\ \begin{array}{l} \text{Diagram 4: Hinged left end, rotation } \theta \text{ at right end.} \\ M_L = 0, \quad M_R = \frac{3D}{L} \theta \end{array} \end{array} \right\} M_R = \frac{(3+\alpha)D}{L} \theta
 \end{aligned}$$

$\overbrace{\hspace{10em}}^{\hspace{10em}} L \hspace{10em}$

Figure 7. - End moments M_L and M_R due to deflection Δ or rotation θ of the right end of a uniform beam with left end either clamped or hinged. (D = flexural stiffness, $\alpha = 0$ if left end is hinged, $\alpha = 1$ if left end is clamped)

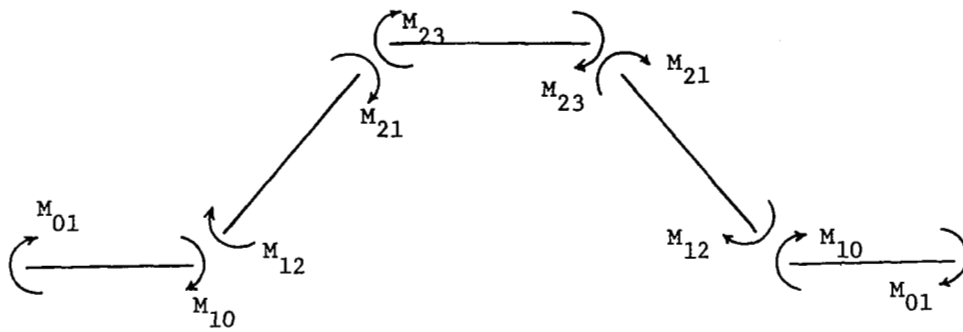
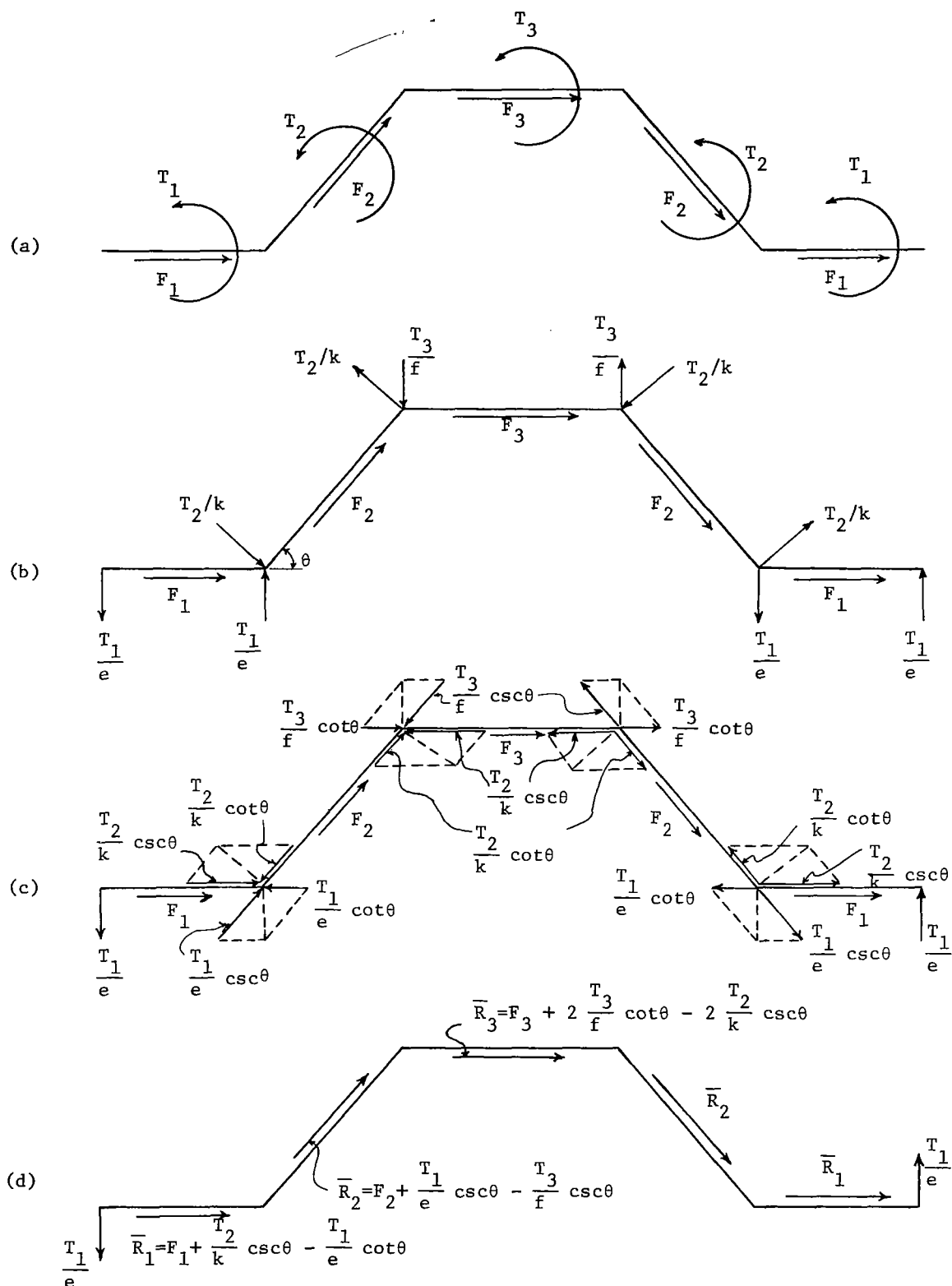
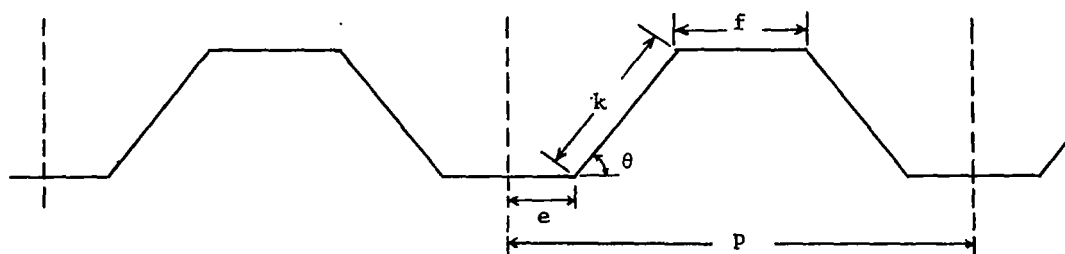
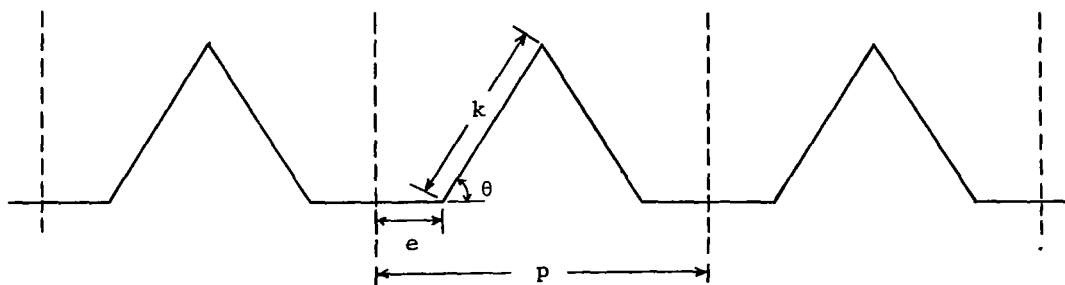


Figure 8. - Notation for end moments in the frame elements.

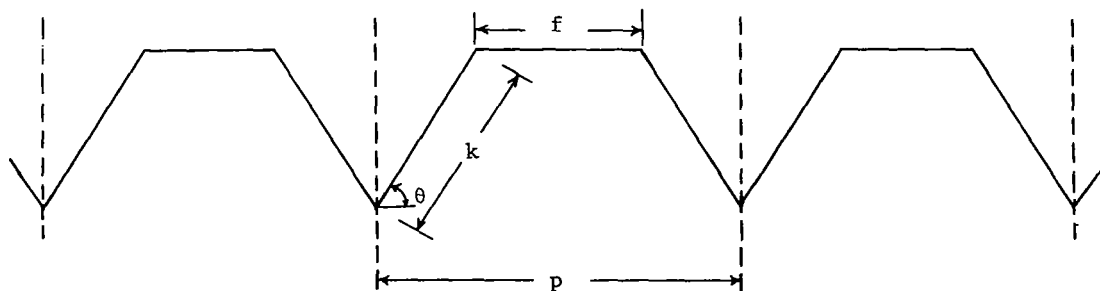




(a) General case

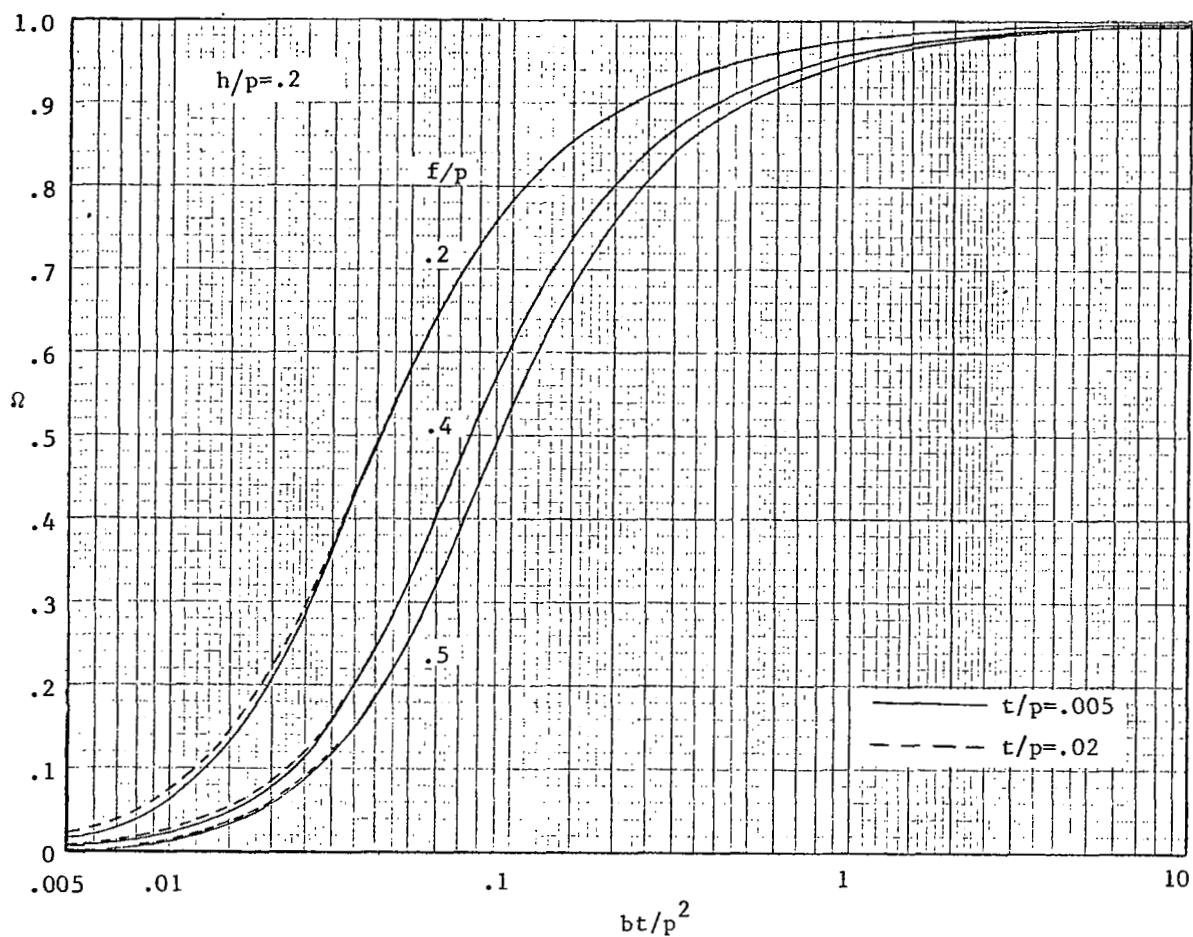


(b) Special case $f = 0$



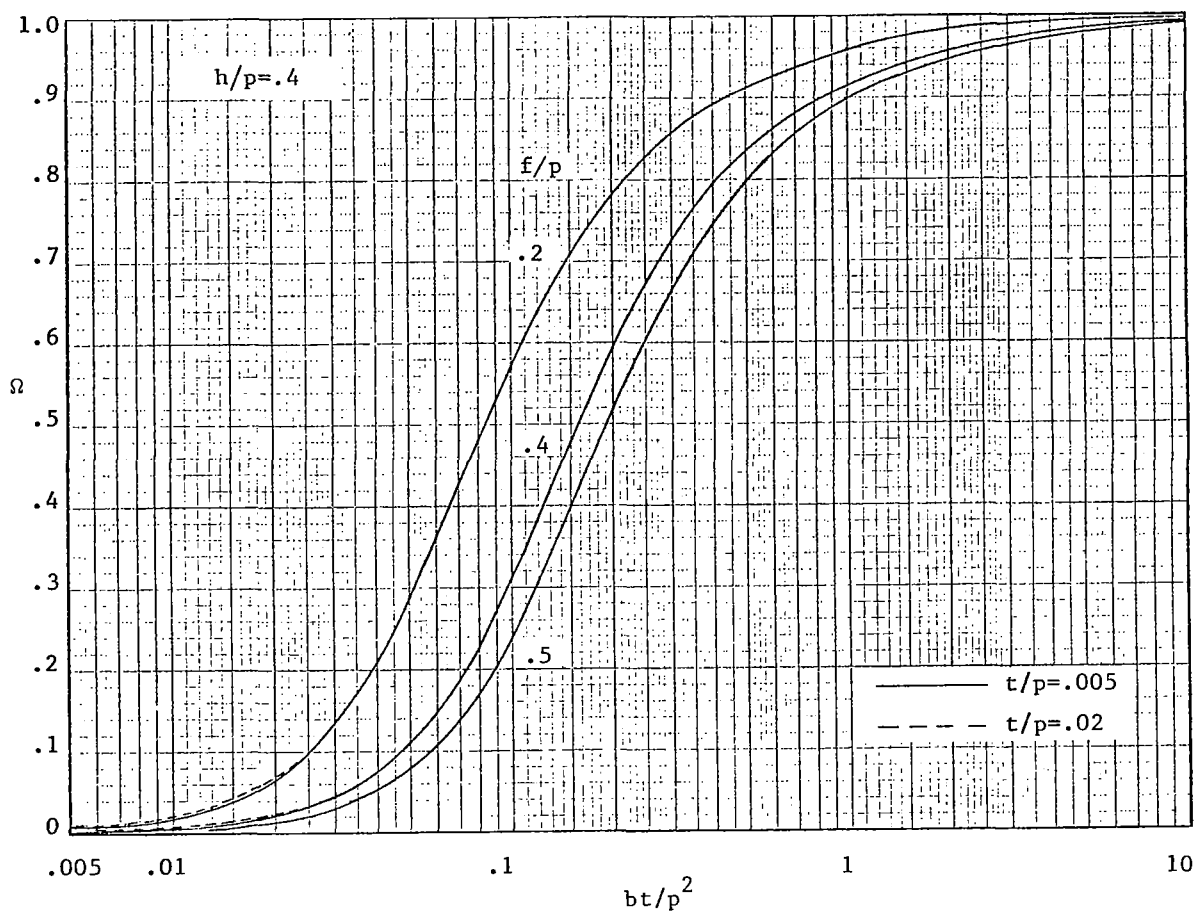
(c) Special case $e = 0$

Figure 10. - General and special cross-sectional geometries considered in the analyses.



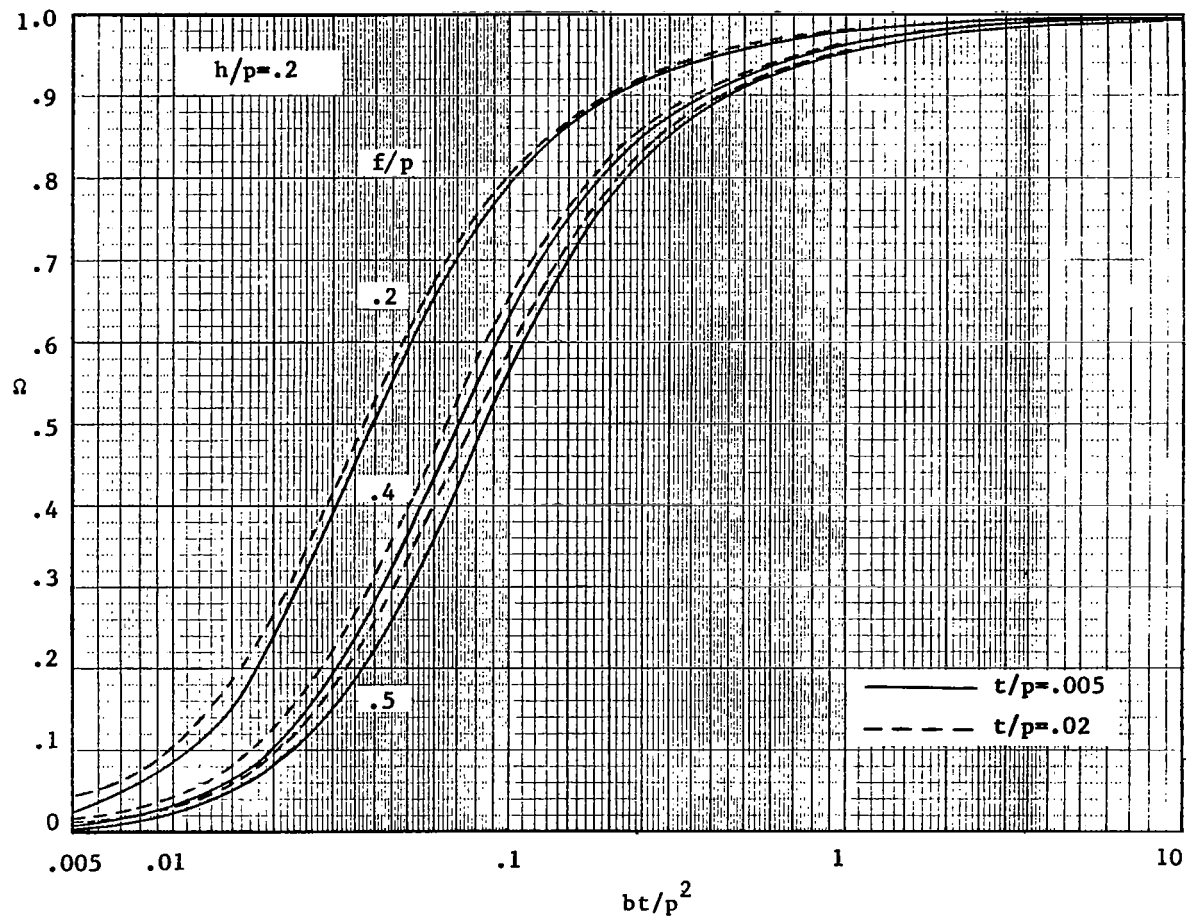
(a) $h/p = .2$

Figure 11.- Relative shear stiffness for the case of point attachments at the ends of the trough lines.



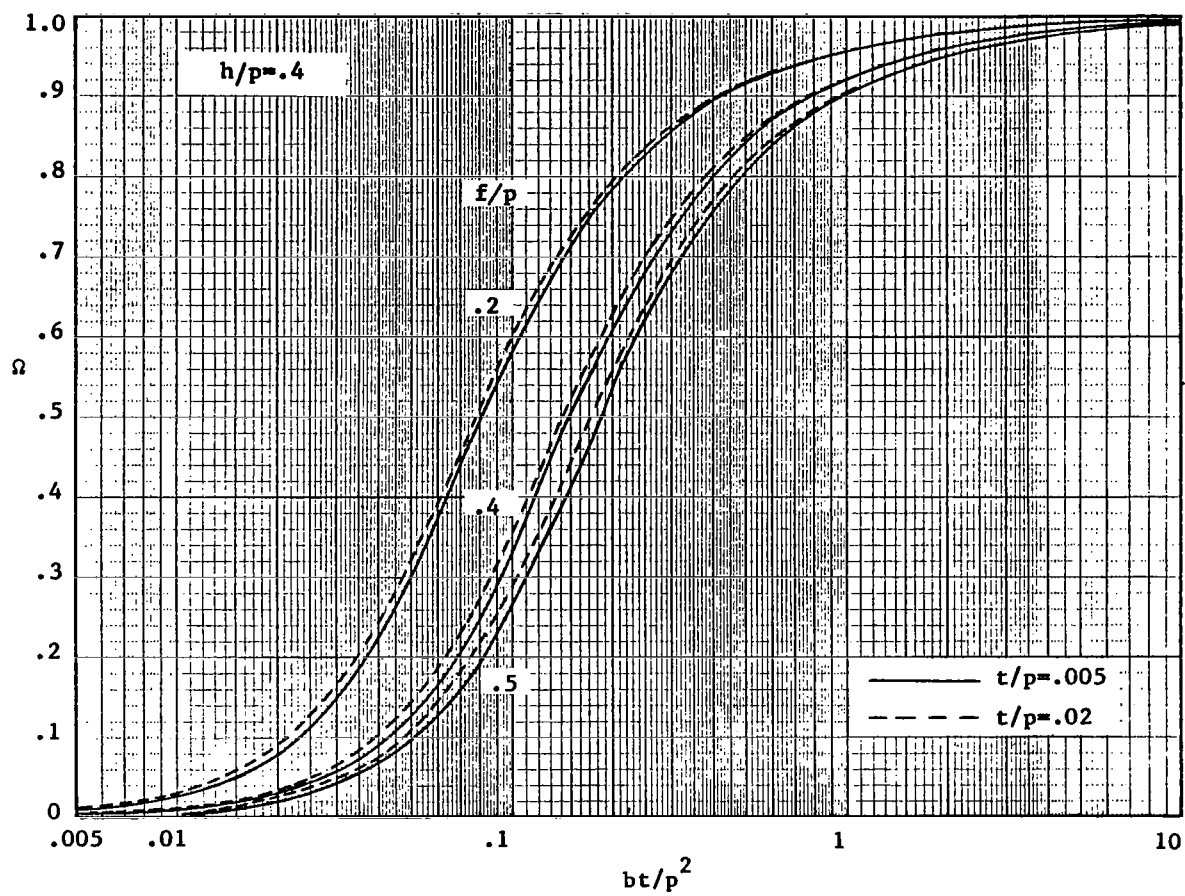
(b) $h/p = .4$

Figure 11.- Concluded.



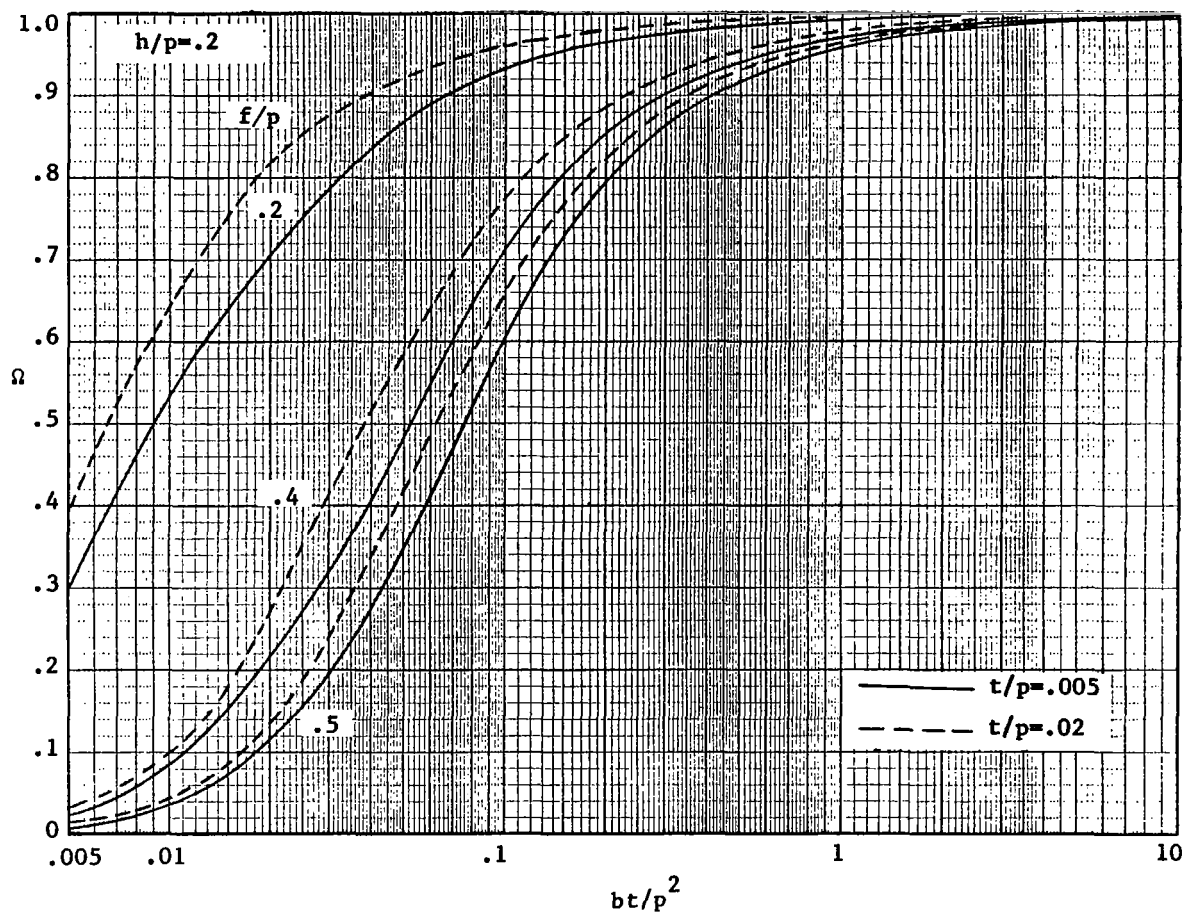
(a) $h/p = .2$

Figure 12.- Relative shear stiffness for the case of point attachments at the ends of both the trough lines and the crest lines.



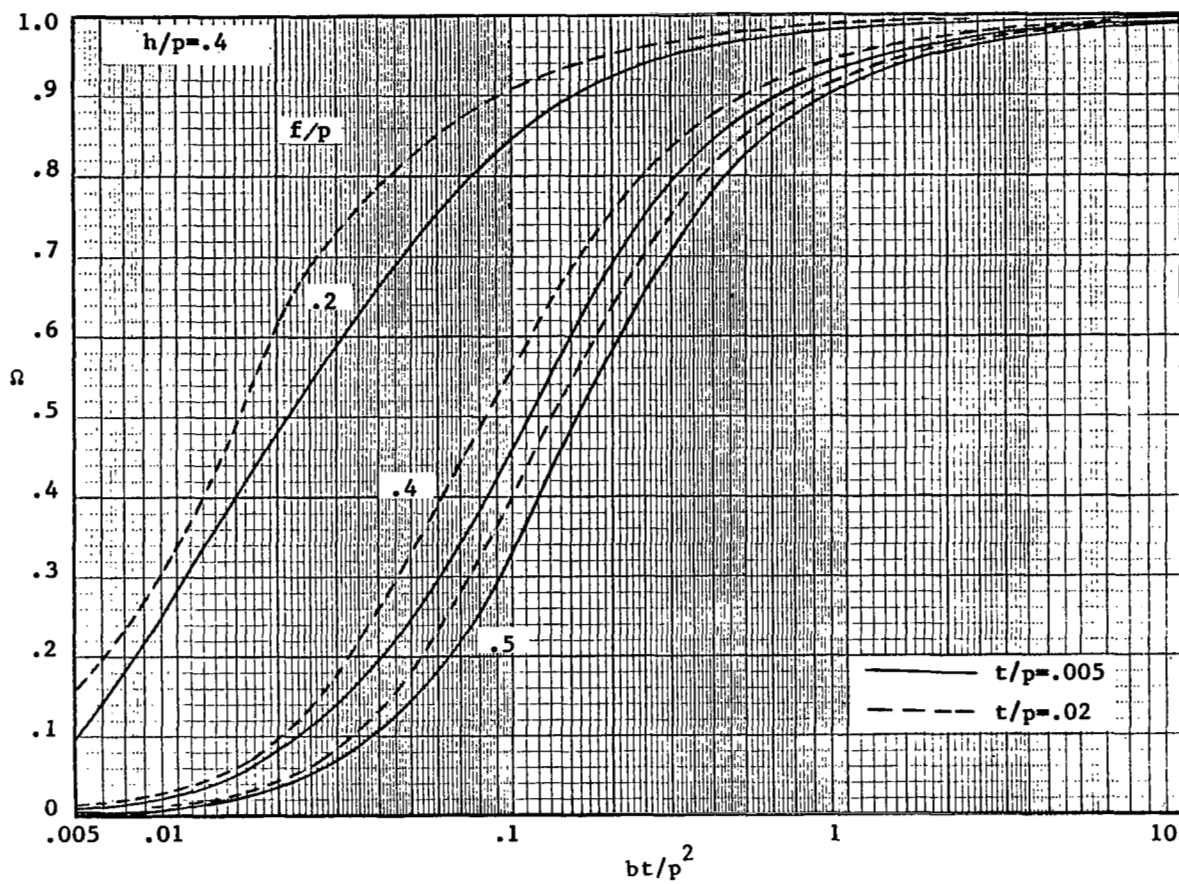
(b) $h/p = 0.4$

Figure 12.- Concluded.



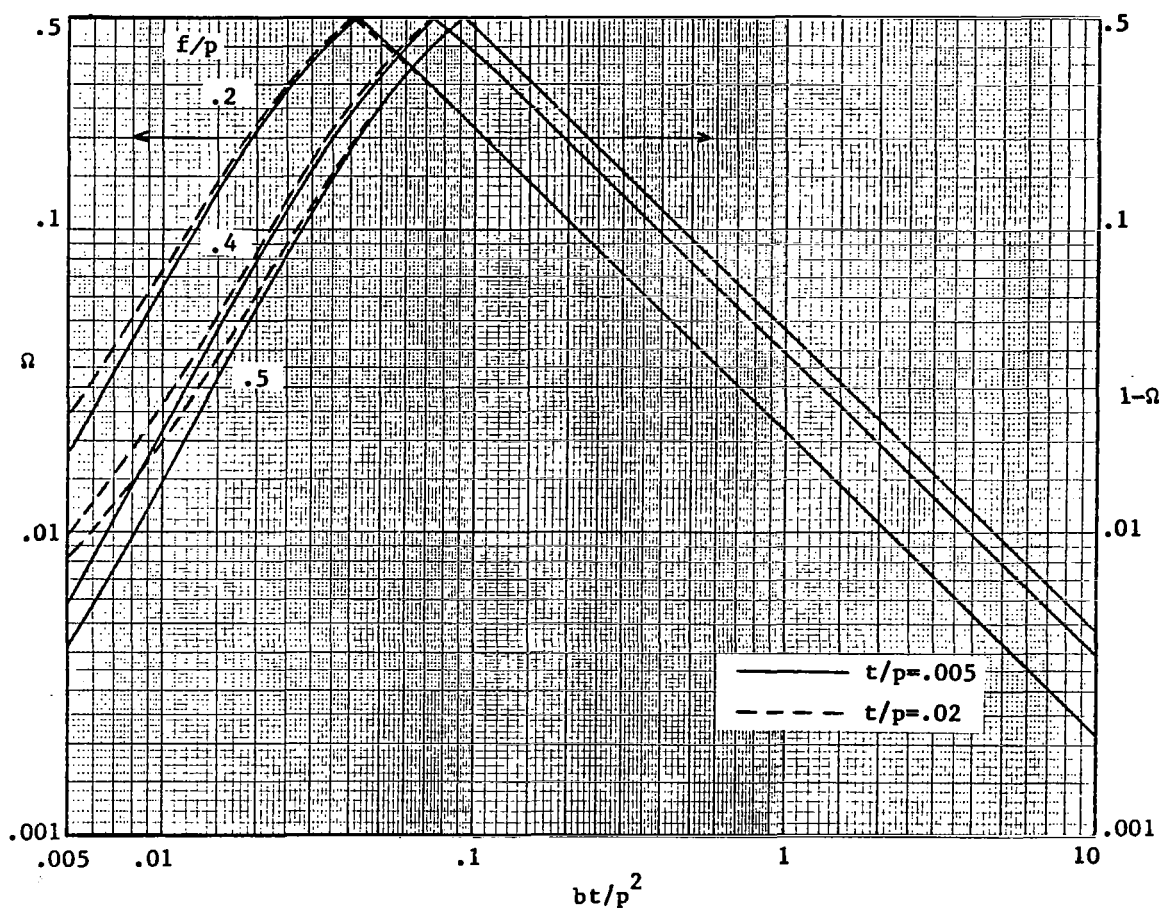
(a) $h/p = 0.2$

Figure 13.- Relative shear stiffness for the case of wide attachments at the ends of the trough lines.



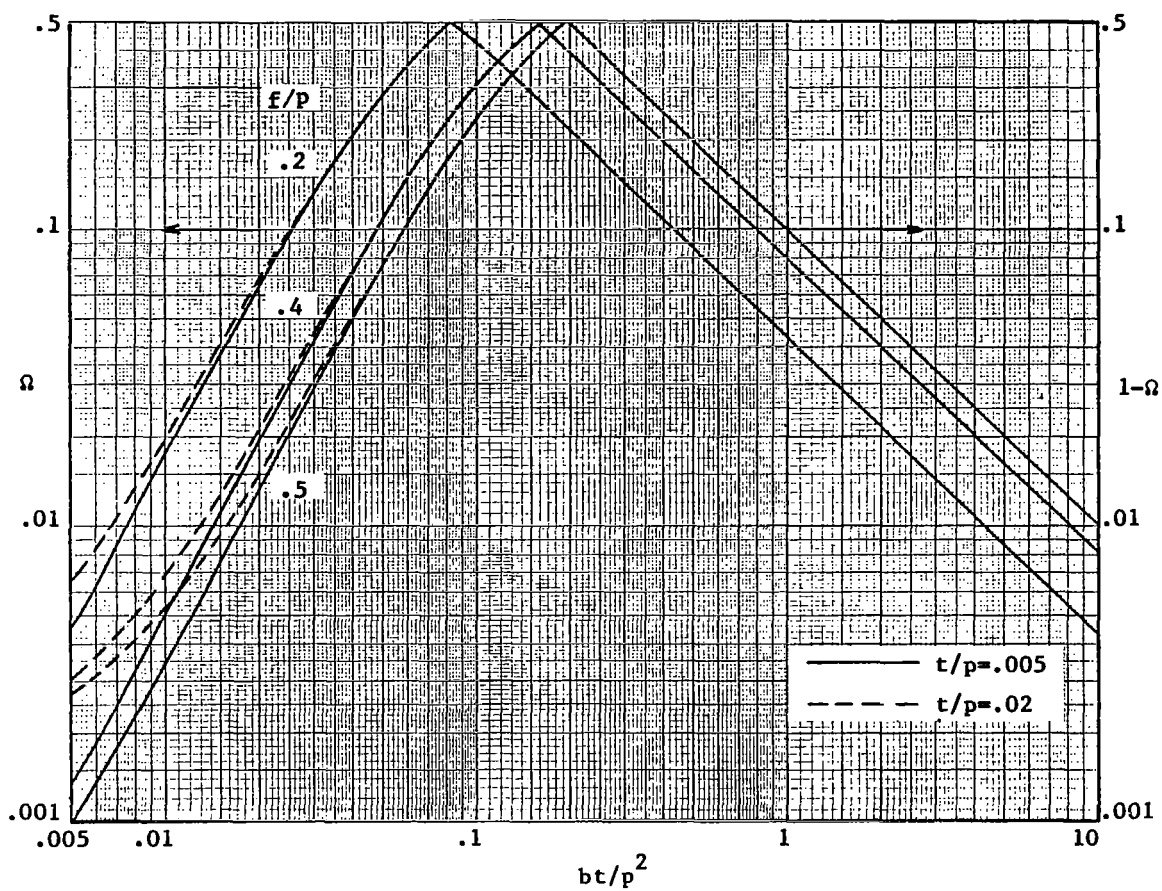
(b) $h/p = .4$

Figure 13.- Concluded.



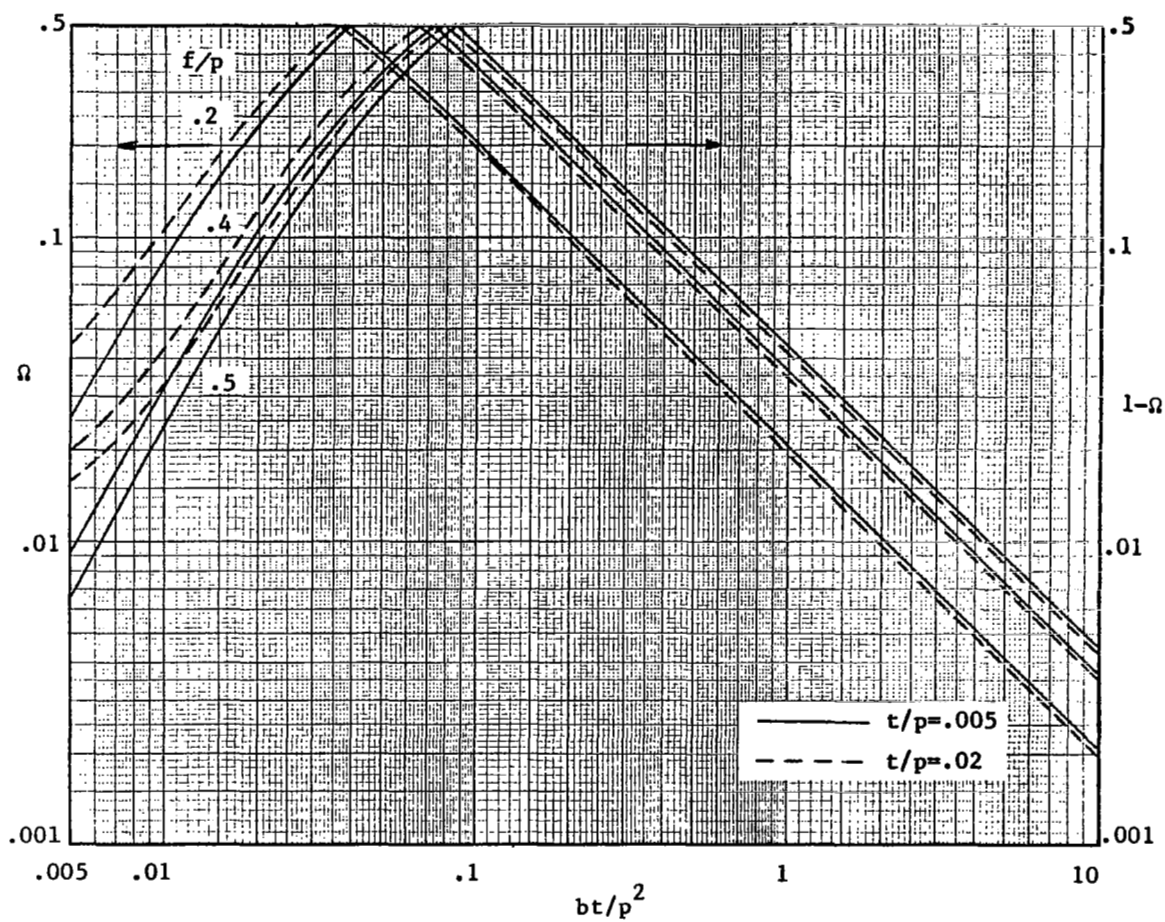
(a) $h/p = .2$

Figure 14.- Re-plot of the data of figure 11.



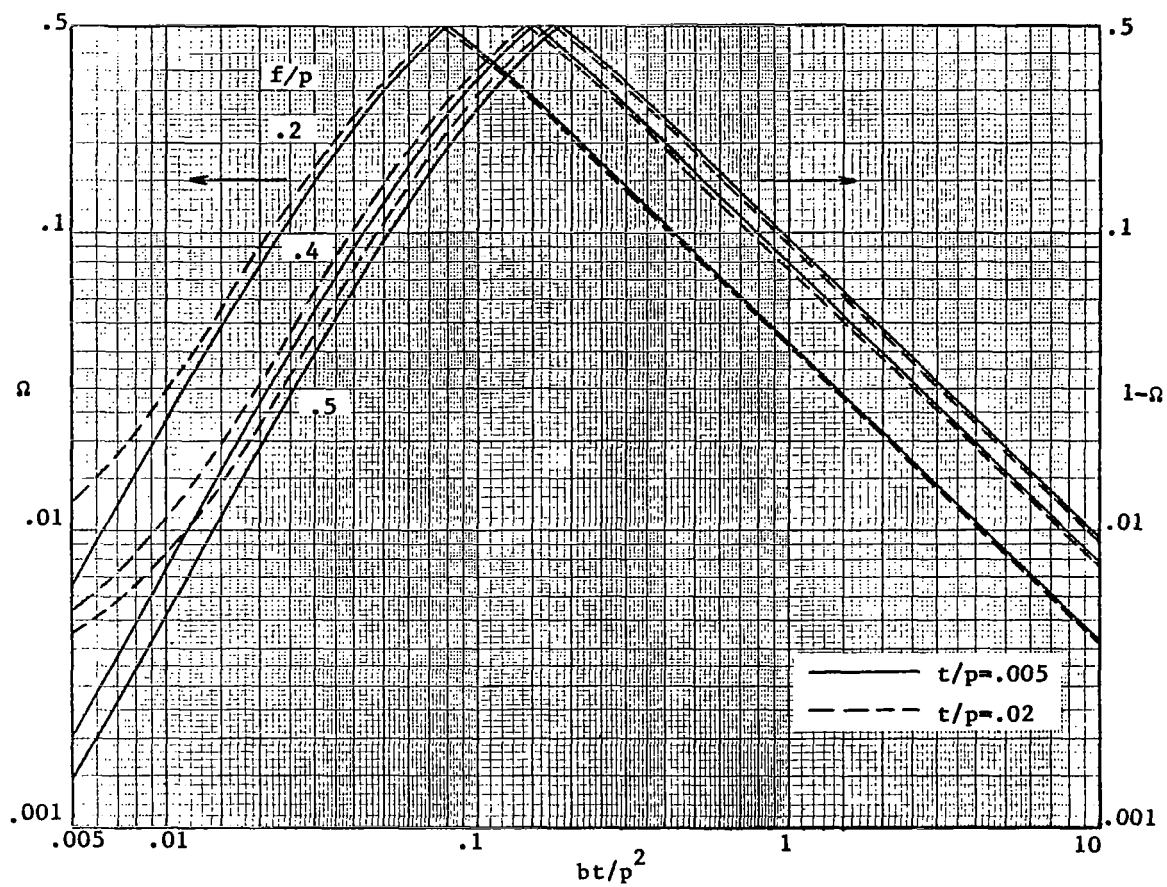
(b) $h/p = .4$

Figure 14.- Concluded.



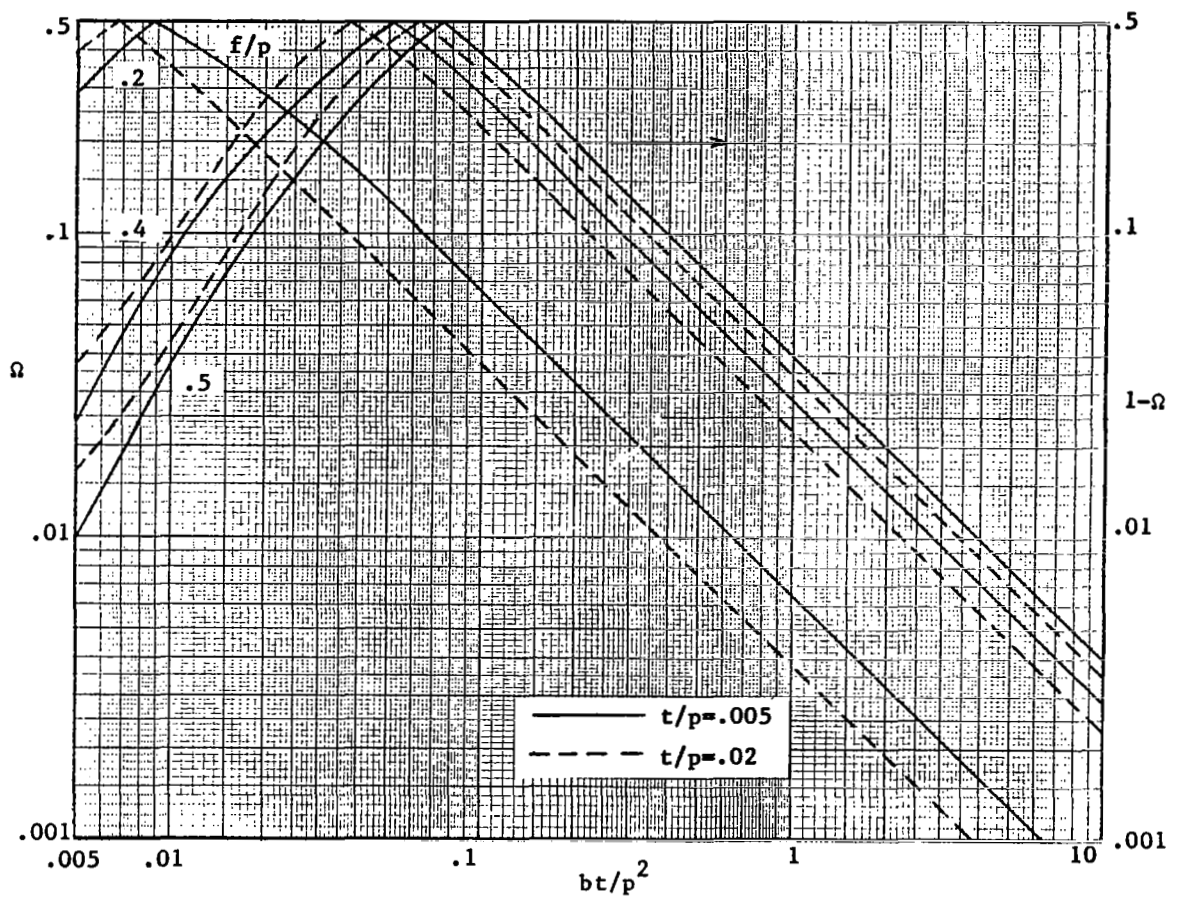
(a) $h/p = 0.2$

Figure 15.- Re-plot of the data of figure 12.



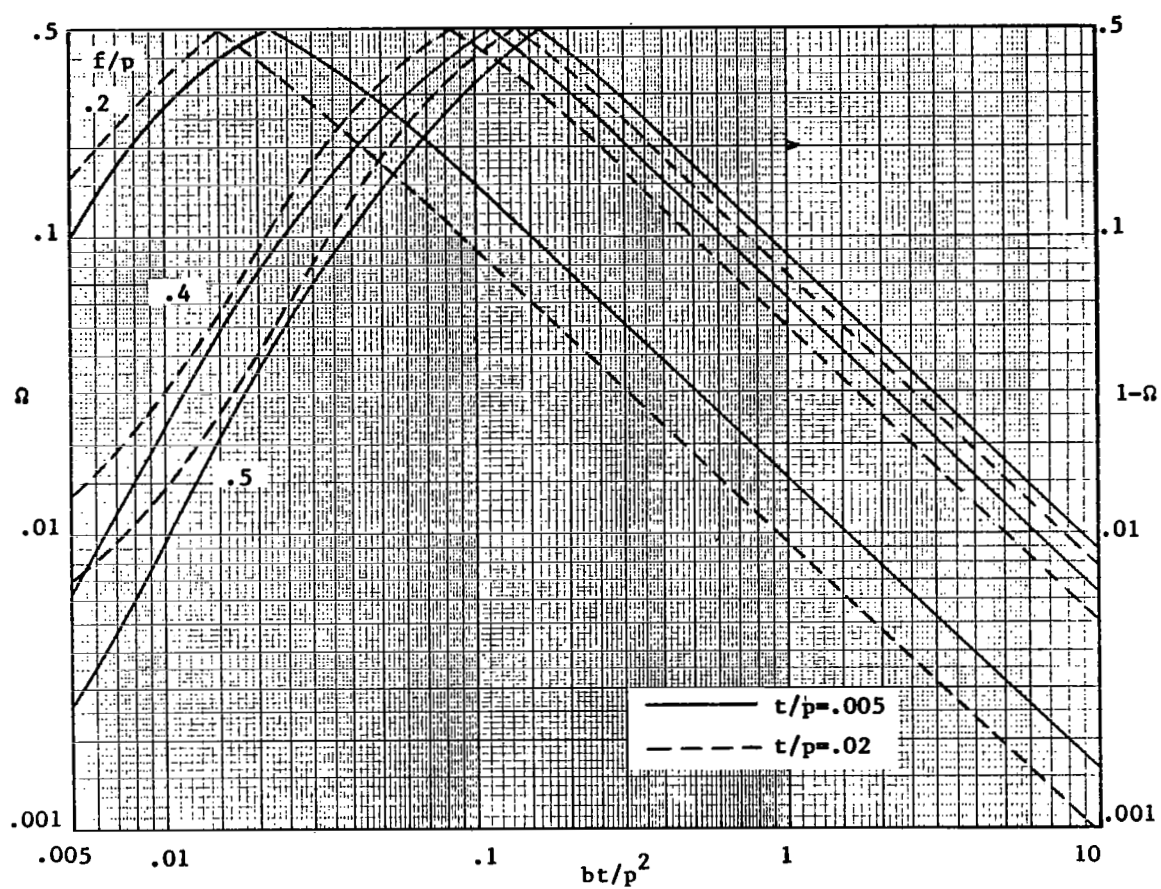
(b) $h/p = .4$

Figure 15.- Concluded.



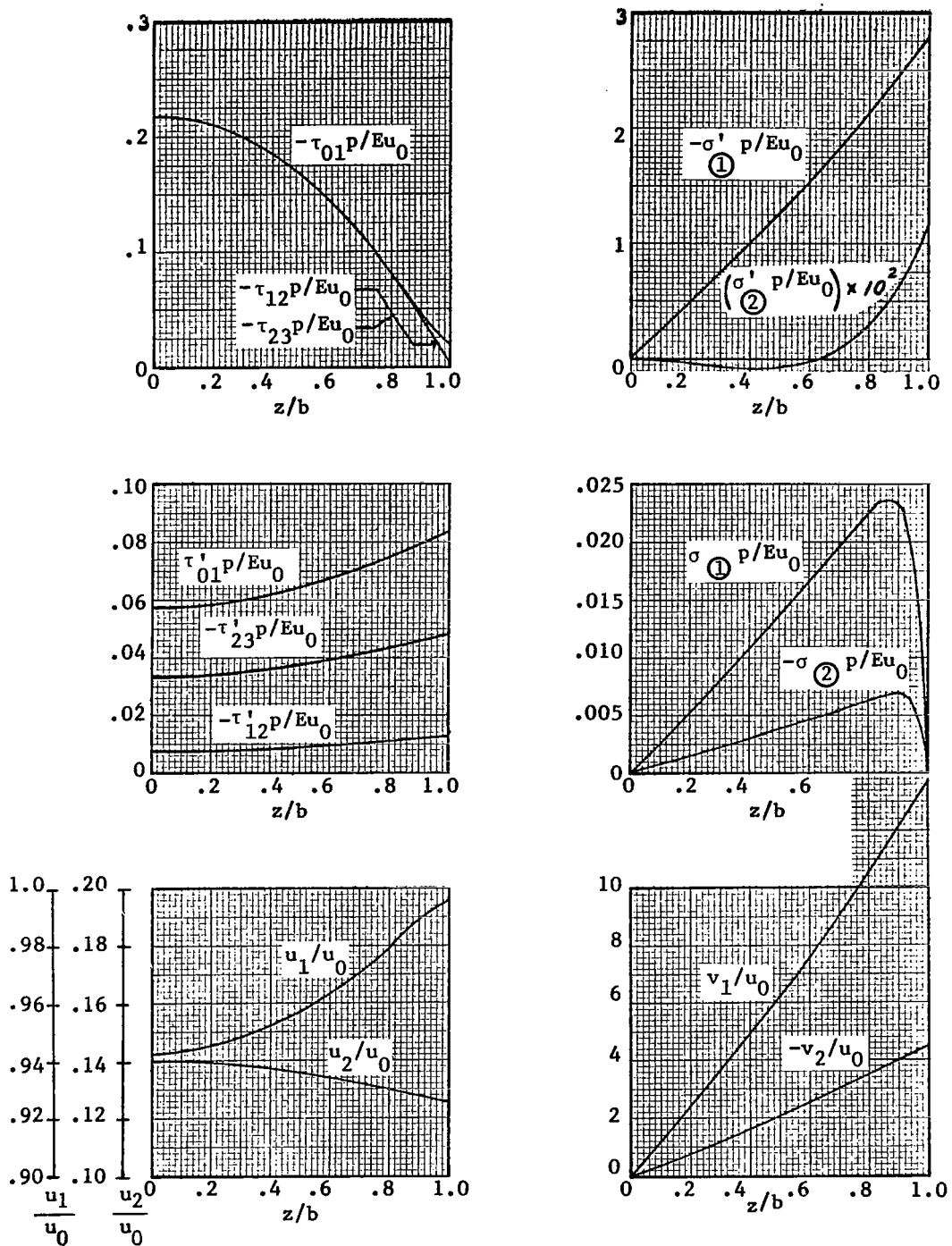
(a) $h/p = .2$

Figure 16.- Re-plot of the data of figure 13.



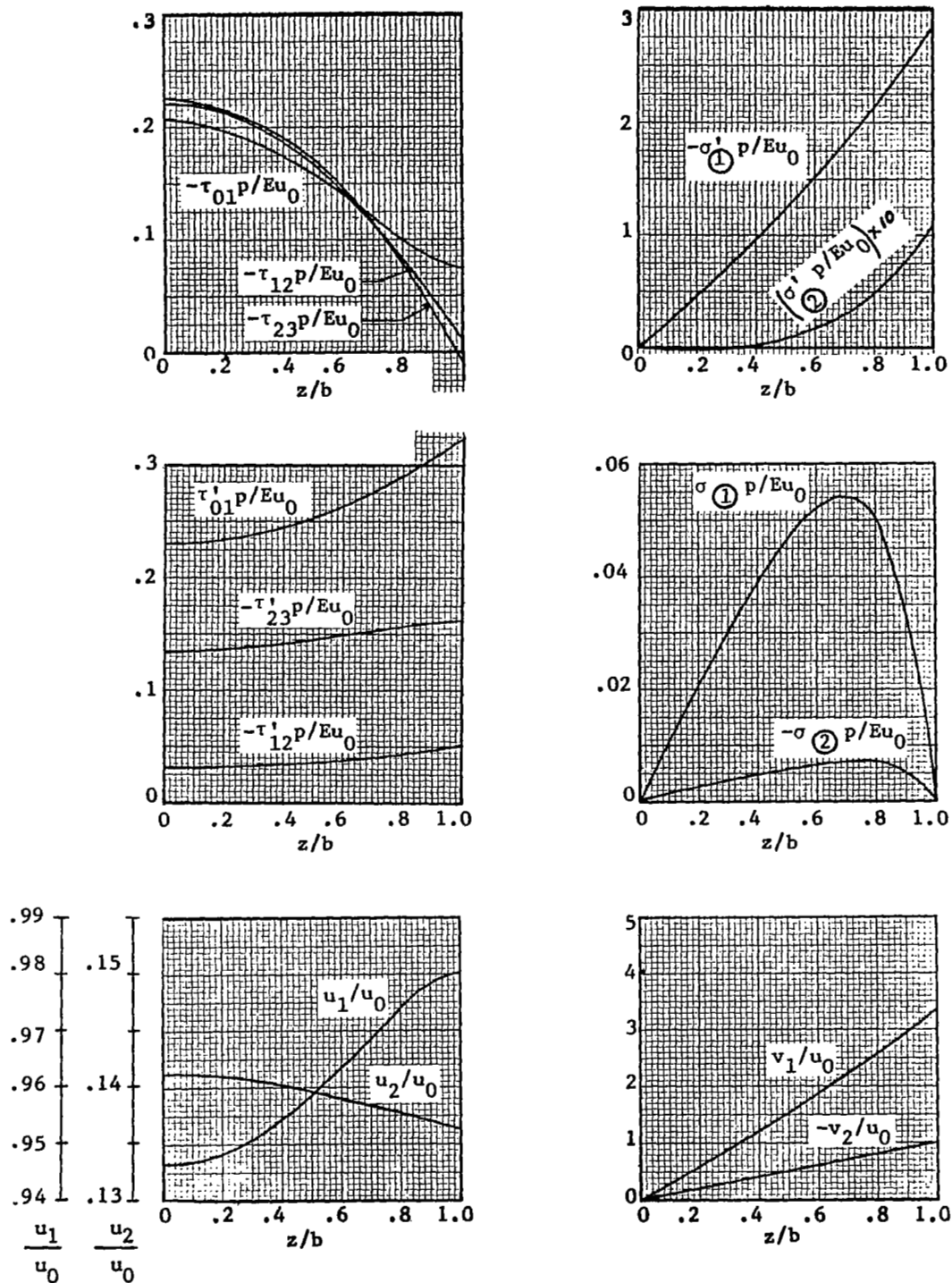
(b) $h/p = .4$

Figure 16.- Concluded.



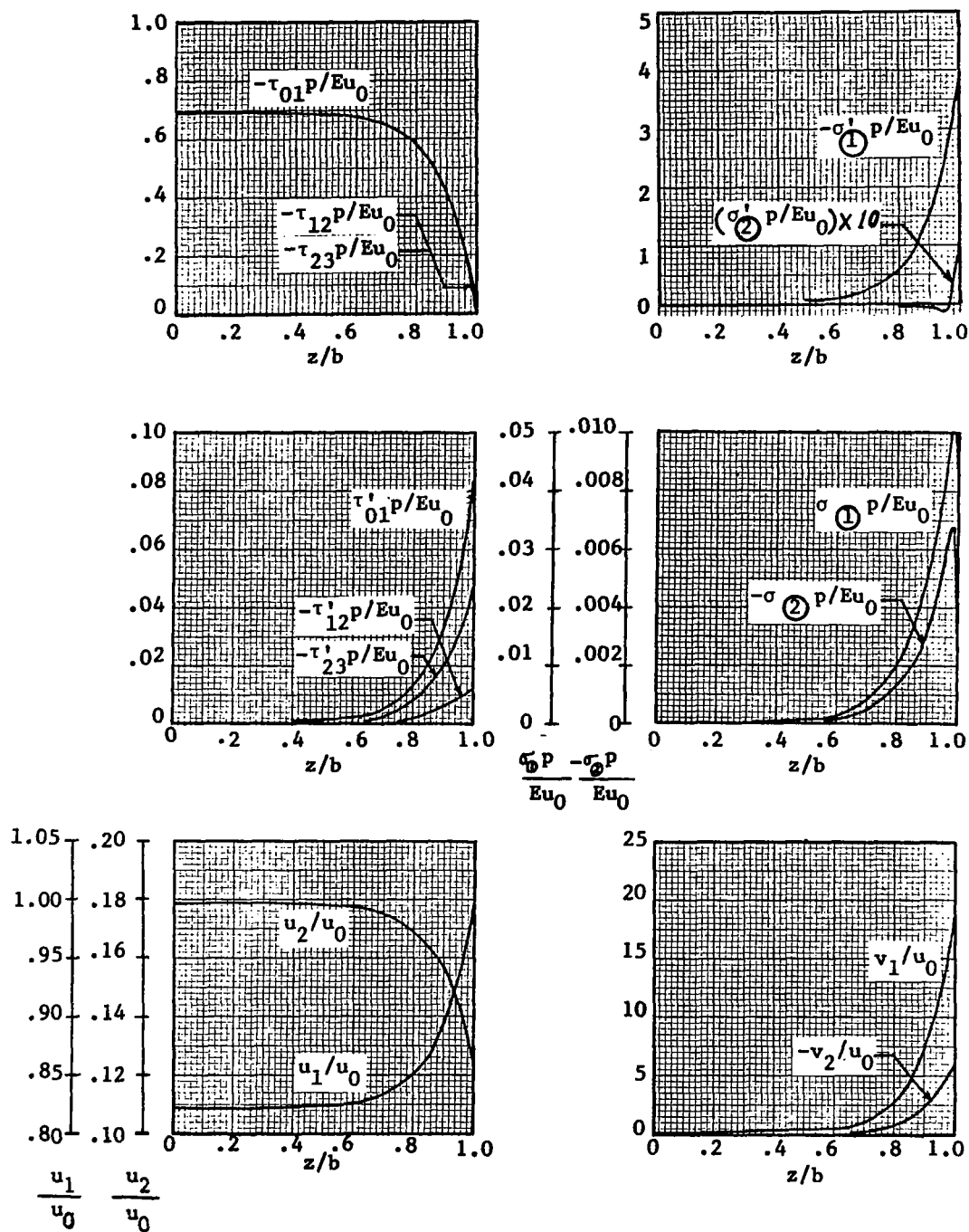
(a) $h/p=f/p=.2$, $bt/p^2=.02$, $t/p=.005$ ($2b/p=8$)

Figure 17.- Stresses and displacements for the case of point attachments at the ends of the trough lines.



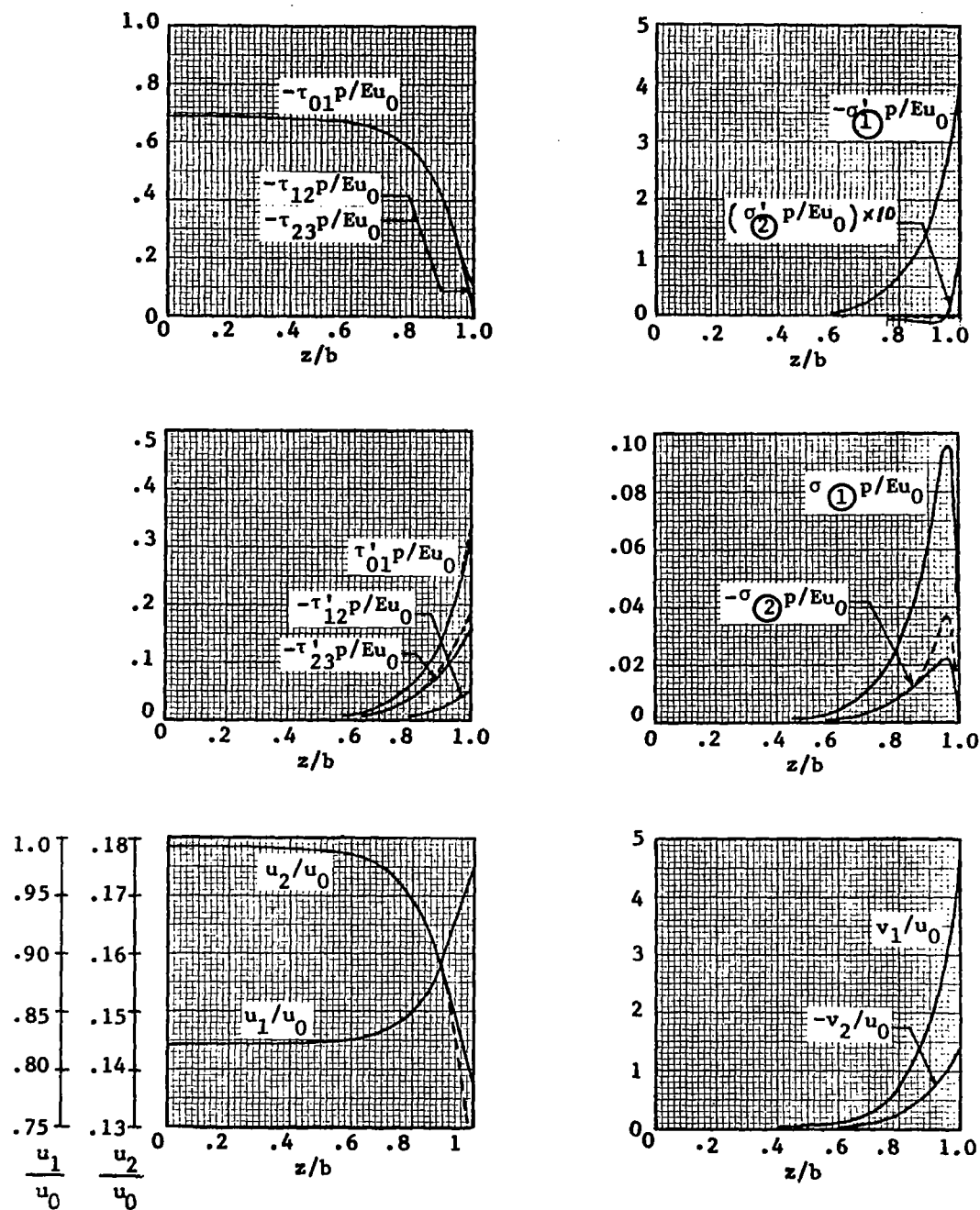
(b) $h/p=f/p=.2$, $bt/p^2=.02$, $t/p=.02$ ($2b/p=2$)

Figure 17.- Continued.



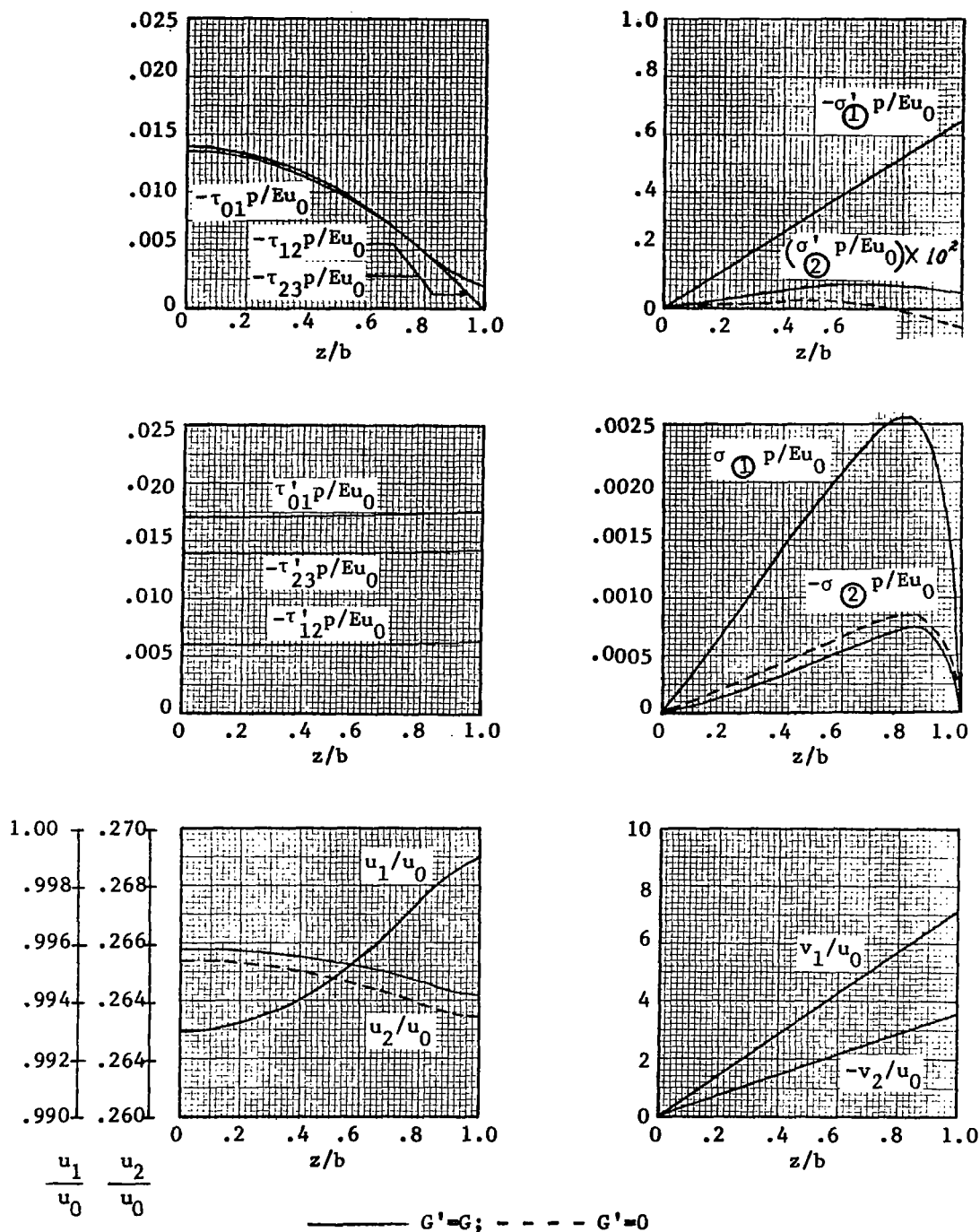
(c) $h/p=f/p=.2$, $bt/p^2=.2$, $t/p=.005$ ($2b/p=80$)

Figure 17.- Continued.



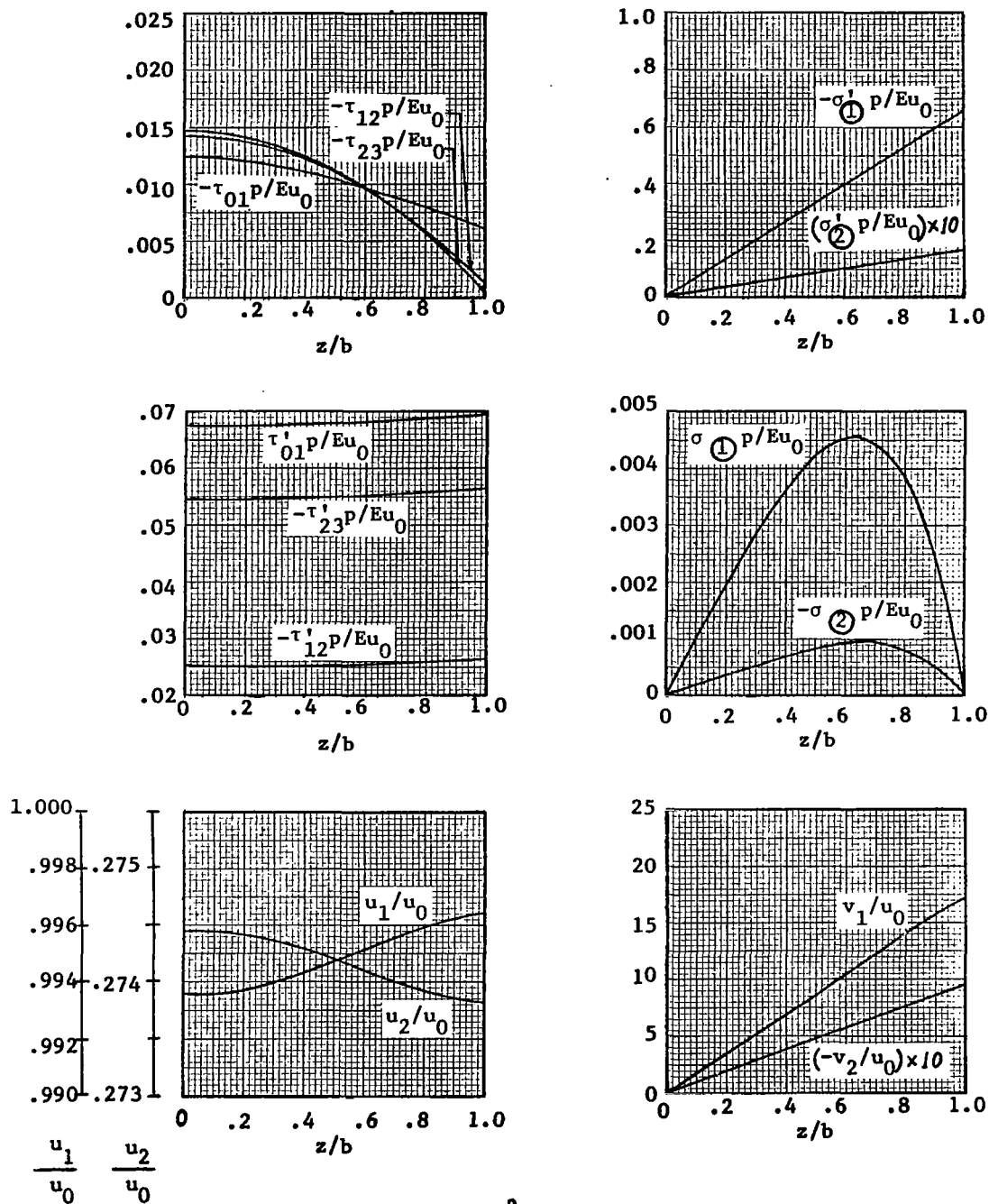
(d) $h/p = f/p = .2$, $bt/p^2 = .2$, $t/p = .02$ ($2b/p = 20$)

Figure 17.- Continued.



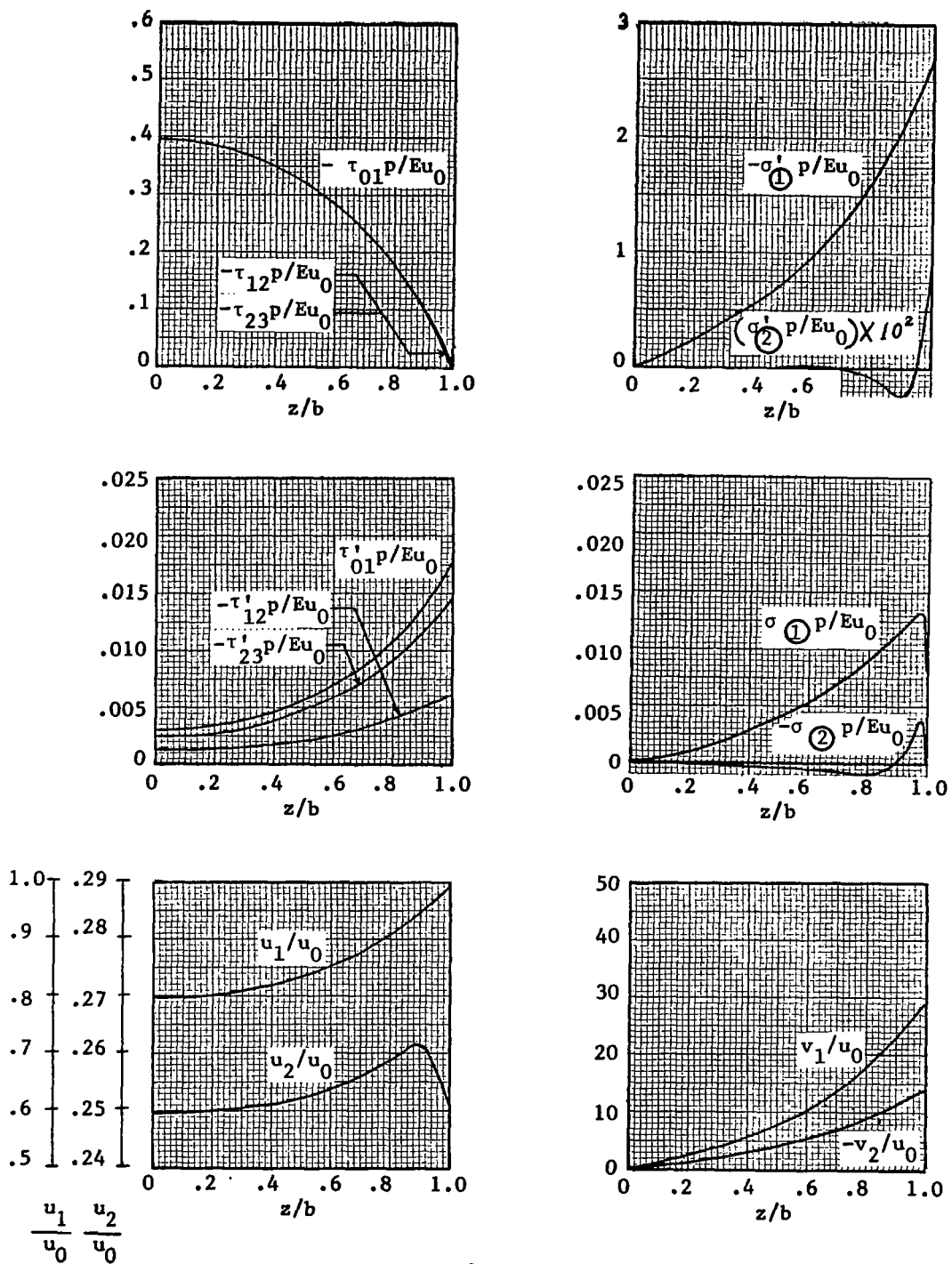
(e) $h/p=f/p=.4$, $bt/p^2=.02$, $t/p=.005$ ($2b/p=8$)

Figure 17.- Continued.



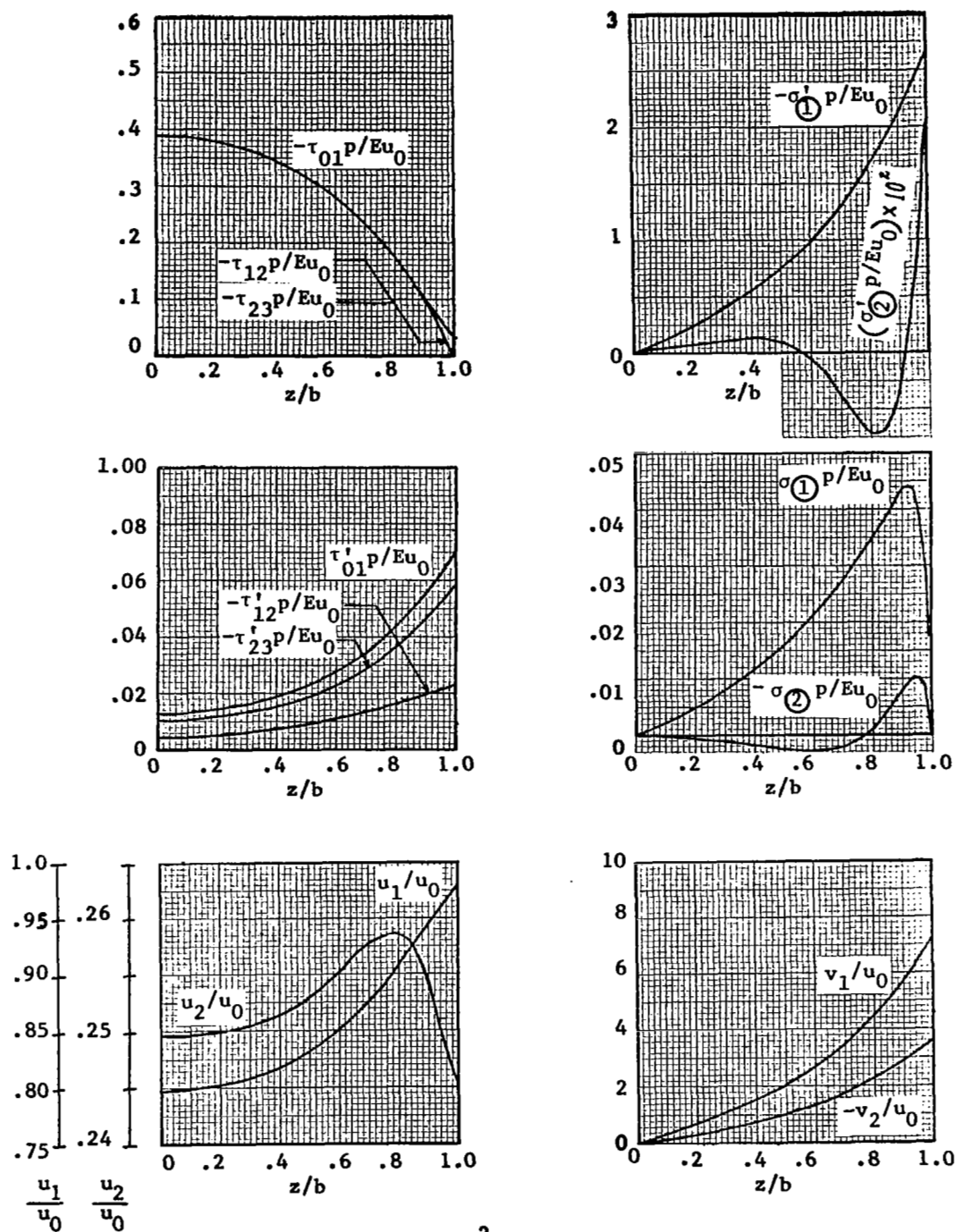
(f) $h/p=f/p=.4$, $bt/p^2=.02$, $t/p=.02$ ($2b/p=2$)

Figure 17.- Continued.



(g) $h/p=f/p=.4$, $bt/p^2=.2$, $t/p=.005$ ($2b/p=80$)

Figure 17.- Continued.



(h) $h/p=f/p=.4$, $bt/p^2=.2$, $t/p=.02$ ($2b/p=20$)

Figure 17.- Concluded.

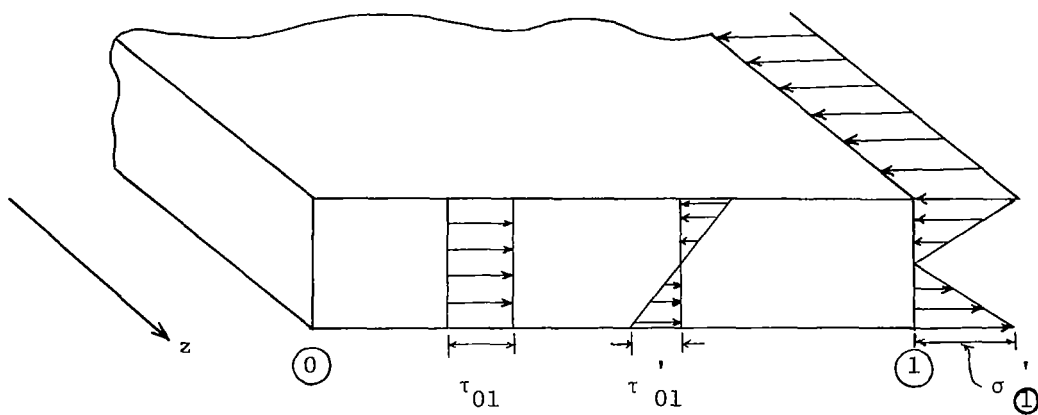
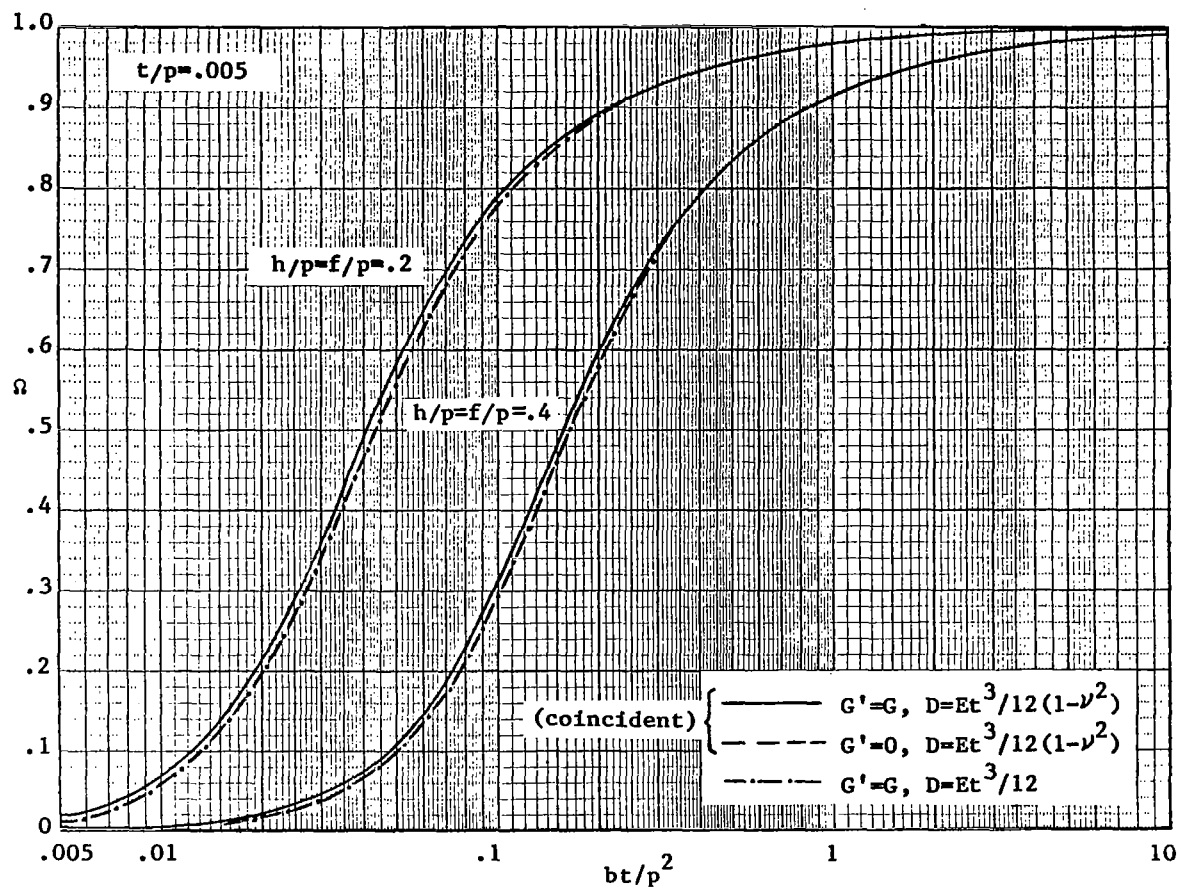
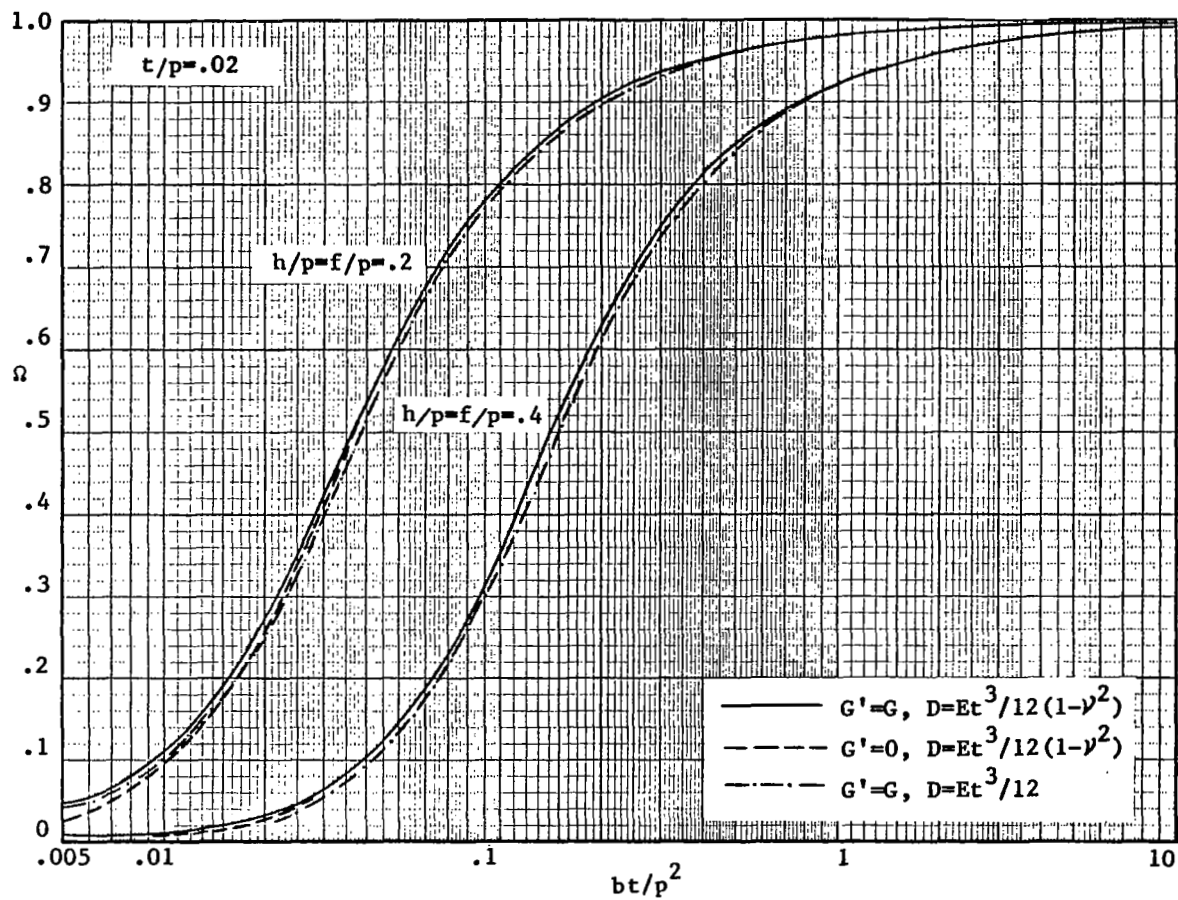


Figure 18. - Sign convention for τ_{01} , τ'_{01} and σ'_1 .



(a) $t/p = 0.005$

Figure 19.- Study of the effect of G' and D on the shearing stiffness.



(b) $t/p = 0.02$
Figure 19.- Concluded.

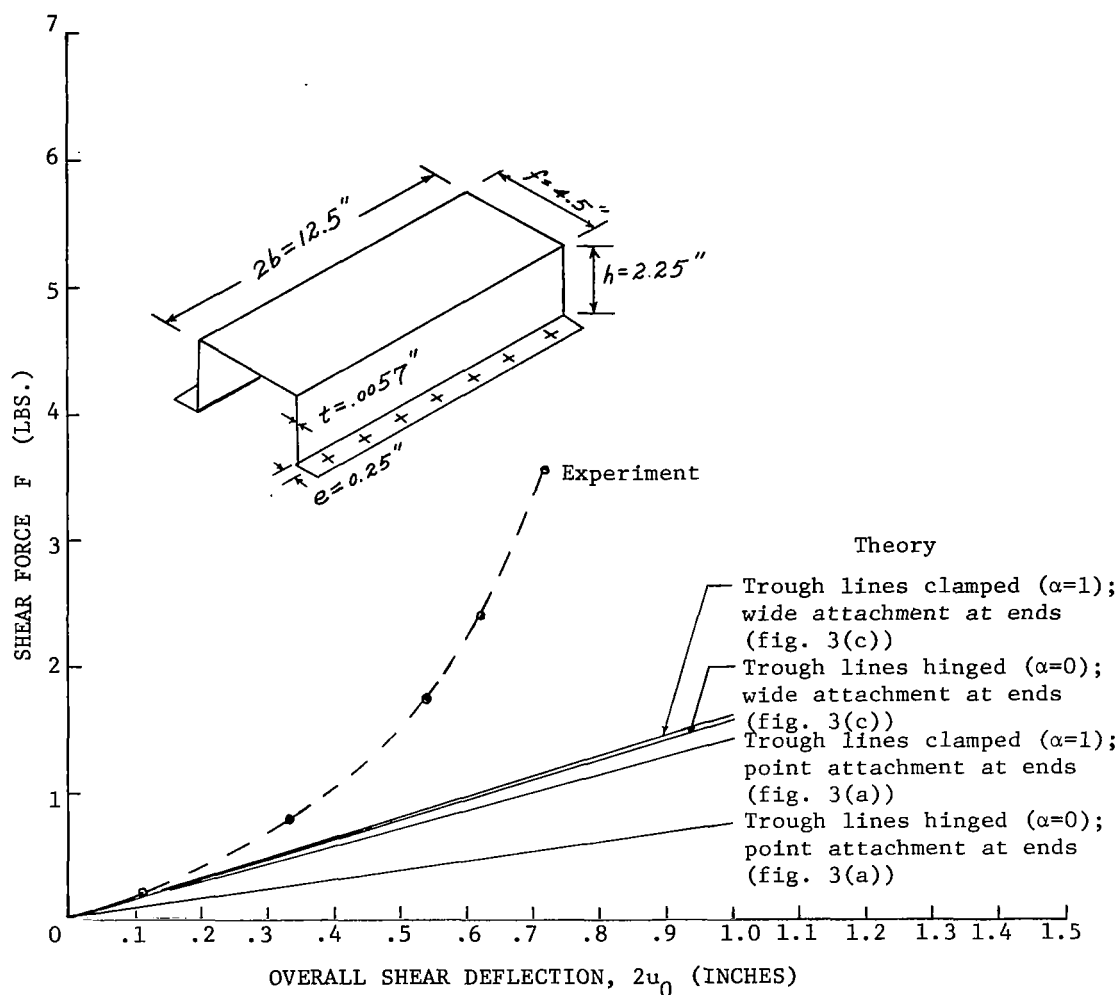


Figure 20. - Comparison present theory (solid lines) with experiment of reference 2 (dashed curve).